Hochschule für Angewandte Wissenschaften Hamburg
Hamburg University of Applied Sciences

Master thesis

Wei Chong Ong

Analytical structural analysis and verification of a composite rotor blade section

Fakultät Technik und Informatik
Department Maschinenbau und Produktion

Faculty of Engineering and Computer Science
Department of Mechanical Engineering and Production Management

Wei Chong Ong

Analytical structural analysis and verification of a composite rotor blade section

Master thesis submitted as part of the master's examination

in the degree program Computational Methods in Mechanical Engineering
at the Department of Mechanical Engineering & Production
of Faculty of Engineering & Computer Science
Hochschule für Angewandte Wissenschaften Hamburg

in cooperation with:

TÜV NORD EnSys GmbH & Co.KG
Department Wind Energy, Rotor blade team
Große Bahnstraße 31,
22525 Hamburg

First examiner: Prof. Dr.-Ing. Georgi Kolarov
Second examiner: José Carlos Román Abadias

Submission date:10.12.2019

Zusammenfassung

Name des Studierenden

Wei Chong Ong

Thema der Masterthesis

Analytical structural analysis and verification of a composite rotor blade

Stichworte

Rotorblatt, Windkraftanlage, Laminat, strukturelle Eigenschafte, klassische Laminattheorie, Analyse der Laminatfestigkeit, Beulanalyse, Klebeanalyse

Kurzzusammenfassung

Rotorblatt von Windkraftanlage hat eine komplexe Form und besteht aus vielen Schichten von Laminaten mit unterschiedlichen Materialeigenschaften. Die strukturellen Eigenschaften des Rotorblatts, wie z. B. die Steifigkeiten, müssen im Voraus bekannt sein, um eine Strukturanalyse durchführen zu können. In diesem Artikel wird ein analytisches Modell vorgestellt, mit dem diese strukturellen Eigenschaften auf einfache und schnelle Weise, die auf der klassischen Laminattheorie basierend, berechnet werden können. Der Code ermöglicht einen generellen Schichtaufbau der Lagen und ist für den Querschnitt mit einer oder zwei Stege geeignet. Es beginnt mit der Diskretisierung des Querschnitts in mehrere Elemente. Jedes Element hat einen Knoten in seiner neutralen Ebene. Die Steifigkeiten jedes Elements werden in Form von ABD-Matrizen bestimmt. Die Steifigkeiten des Querschnitts sind die Summe der Steifigkeiten jedes Elements. Dann wird der Schwerpunkt des Querschnitts erhalten. Durch Aufbringen der Biegemomente für die extremen Lastfälle werden die axialen Dehnungen für alle Knoten am Profilabschnitt berechnet. Darüber hinaus werden die Schubflüsse für jede Kante des Elements durch Aufbringen von Schubkräften als die Eingabe für das Werkzeug bestimmt. Trotz der Einfachheit der Methode zeigen die Ergebnisse eine gute Übereinstimmung mit den FEM-Ergebnissen. Letztendlich wird ein Strukturanalysemodell für die Analyse der Laminatfestigkeit, Beul- und Klebeanalyse unter extremen Belastungen entwickelt, um die Festigkeit des Rotorblatts zu überprüfen. Die Analysewerkzeuge weisen mehrere Einschränkungen auf, da sie nur für einen Querschnitt des Rotorblatts geeignet sind. Die Weiterentwicklung der Werkzeuge ist für eine genauere Beulanalyse sowie die Durchführung einer Ermüdungsanalyse erforderlich.

Abstract

Name of Student

Wei Chong Ong

Title of the paper

Analytical structural analysis and verification of a composite rotor blade

Keywords

Wind turbine blade, laminate, structural properties, classical lamination theory, laminate strength analysis, buckling analysis, bonding analysis

Abstract

Wind turbine blade has a complex shape and consists of many layers of laminates with dissimilar material properties. The structural properties of the blade such as stiffnesses need be known in advance, in order to carry out structural analysis. This paper presents an analytical model to calculate these structural properties in a simple and fast way based on classical lamination theory. The code allows for a general layup of composite laminates and is suitable for cross section with one or two shear webs. It starts with discretization of the cross section into several elements. Each element has a node at its neutral plane. The stiffnesses of each element is determined in the form of ABD-Matrices. The stiffnesses of the cross section is the summation of the stiffnesses of each element. Then, the elastic center of the cross section is obtained. By applying bending moments for the extreme load cases, the axial strains for all nodes at the profile section are calculated. In addition, the shear loads are determined for each edge of the element by applying shear forces as inputs for the tool. Despite the simplicity of the method, the results show a good agreement with FEM results. In the end, structural analysis model for laminate strength analysis, buckling and bonding analysis under extreme loads is developed for the verification of the strength of the rotor blade. The analytical tools have several limitations as it is only suitable for one cross section of the blade. Further development of the tools is needed for more accurate buckling analysis as well as implementation of fatigue analysis.

Acknowledgements

I would like to take this opportunity to express my gratitude to all the people who supported me throughout this project. Firstly, I would like to thank TÜV NORD EnSys GmbH & Co. KG for giving me this great opportunity to work on this project.

I am profoundly grateful to my supervisor, José Carlos Román Abadias for his continued support and her constant input that shaped up my project. He was always willing to take time out of his busy schedule to give me some valuable advice and suggestions whenever I encountered technical and practical difficulties.

Furthermore, heartfelt thanks go to my team leader Michael Lange for trusting me and providing helpful ideas for further development of the project. My research would have been impossible without the aid and support of my supervising professor Prof. Dr.-Ing. Georgi Kolarov, especially in the field of finite element method. Their valuable insights and directions gave me needful guidance to complete the research.

Table of Contents

List of figures

List of tables

List of abbreviation

a	Distance from main girder leading edge to shear web leading edge (Suction side)
b	Main girder width (Suction side)
c	Distance from main girder leading edge to shear web leading edge (Pressure side)
CLT	Classical Lamination Theory
d	Main girder width (Pressure side)
e	Distance from tail girder trailing edge to trailing edge (Suction side)
EC	Elastic center
f	Tail girder width (Suction side)
FBE	Flat back edge
g	Distance from tail girder trailing edge to trailing edge (Pressure side)
h	Tail girder width (Pressure side)
LE	Leading edge
$MGLE$	Main girder leading edge
$MGTE$	Main girder trailing edge
SC	Shear center
$SWLE$	Shear web leading edge
$SWTE$	Shear web trailing edge
TE	Trailing edge
$TGLE$	Tail girder leading edge
$TGTE$	Tail girder trailing edge

List of symbols

Symbol	Description	Units
$[\bar{Q}]$	Stiffness matrix layer axes (x,y)	$\frac{N}{mm^2}$
$[\bar{S}]$	Compliance matrix layer axes (x,y)	$\frac{mm^2}{N}$
$\frac{1}{\rho_x}$	Curvature of the blade x/y axis	$\frac{1}{mm}$
$\frac{1}{\rho_y}$	Curvature of the blade x/y axis	$\frac{N}{mm}$
$[A]$	Extensional stiffness matrix	$\frac{N}{mm}$
$[B]$	Coupling stiffness matrix	N
$[D]$	Bending stiffness matrix	Nmm
E_w	Effective E-Modulus for isotropic buckling condition	$\frac{N}{mm^2}$
F_ξ	Axial force of the wall of the cross section	N
N_ξ	Axial force per unit length of the wall of the cross section	$\frac{1}{mm}$
$[Q]$	Stiffness matrix orthotropic axes (1,2)	$\frac{N}{mm^2}$
Q_x	Shear force in the X_R axis direction	N
Q_y	Shear force in the Y_R axis direction	N
M_x	Edgewise bending moment about X_R axis	Nmm
M_y	Flapwise bending moment about X_R axis	Nmm
$R_\perp$	Strength in transverse fiber direction	$\frac{N}{mm^2}$
$R_{\perp\parallel}$	Shear strength	$\frac{N}{mm^2}$
R_d	Design values of the component resistances	
R_k	Characteristic value	-
S_G	Buckling criteria	-
S_d	Design values of the actions	-
b_k	Width of the kth element in the wall of the cross section	mm
$f_{E,FF}$	Stress exposure for fiber failure	-
$f_{E,IFF}$	Stress exposure for inter-fiber failure	-
k_σ	Buckling coefficient for critical stress	-

p_{cr}	Critical buckling axial load	$\frac{N}{mm}$
q^c	Constant shear flow	$\frac{N}{mm}$
q_{cr}	Critical buckling shear load	$\frac{N}{mm}$
q^{op}	Shear flow of the open section	$\frac{N}{mm}$
u_y	Maximum deflection of the blade in x direction	mm
u_y	Maximum deflection of the blade in y direction	mm
$[\alpha]$	Extensional compliance matrices	$\frac{mm}{N}$
α_k	Angle from reference Y_R-axis to η-axis	^{o}
α_ω	Effective length-to-width ratio	-
$[\beta]$	Coupling compliance matrices	$\frac{1}{N}$
β_ω	Effective width-to-length ratio	-
γ_{Mx}	Partial safety factor for the material	-
$\gamma_{\xi\eta}$	Shear strain of the wall of the cross section	-
$[\delta]$	Bending compliance matrices	$\frac{1}{Nmm}$
σ_1	Stress in fiber direction	$\frac{N}{mm^2}$
σ_2	Stress in transverse fiber direction	$\frac{N}{mm^2}$
σ_{cr}	Critical buckling axial stress	$\frac{N}{mm^2}$
τ_{21}	Shear stress	$\frac{N}{mm^2}$
τ_{Bond}	Shear stress in the bonded joints	$\frac{N}{mm^2}$
τ_{cr}	Critical buckling shear stress	$\frac{N}{mm^2}$
ϵ_ξ	Axial strain of the wall of the cross section	-
ϑ_p	Angle from reference axis to principal axis	^{o}
Ω	Curvature parameter	mm
EI_{max}	Maximum bending stiffness about principal axis	Nmm^2
EI_{min}	Minimum bending stiffness about principal axis	Nmm^2
EI_{xx}	Bending stiffness about X_R axis	Nmm^2
EI_{xy}	Coupled bending stiffness about X_R and Y_R axes	Nmm^2

EI_{yy}	Bending stiffness about Y_R axis	Nmm^2
EA	Axial stiffness of the cross section	N
L	Length of the blade	mm
P	Cross-sectional stiffness matrix	-
k	Buckling coefficient for critical load	-
r	Shell radius	mm
η	Stiffness parameter	-
ν	Poisson's ratio	-

1 Introduction

This chapter describes briefly the development of wind turbine as well as the challenges to find designs and material for large size wind turbine blades. Afterwards, the current tool is discussed. Lastly, the scope of work is presented.

1.1 Motivation

As the topic of climate change is getting more attention nowadays, renewable energy has become the major sectors that are playing a pivotal role in trying to find a right balance between growing energy demands and making it as less harmful to environment as possible. Wind power has some of the lowest environmental impacts of any source of electricity generation. Unlike conventional sources, wind power significantly reduces carbon emissions, saves billions of gallons of water a year, and cuts pollution. Therefore, wind energy plays an important role in achieving global sustainability targets with a transition to renewables.

Out of the many components of a wind turbine, the blade is the most important component to produce electricity from wind. The bigger the radius of the rotor blades, the more wind the blades can use to turn into torque that drives the electrical generators in the hub. More torque means more power. Increasing the diameter means that not only more power can be extracted, but it can be done so more efficiently. Creating more power in one turbine means less energy is lost as it is moved into the transmission system, and from there into the electrical generator. The economies of scale provide an overwhelming push for wind energy companies to develop larger rotor blades. One of the largest wind turbine designs in the world, General Electric's offshore 12 MW Haliade-X, has 107m blades and a total height of 260m. The combination of a bigger rotor, longer blades and higher capacity factor makes Haliade-X less sensitive to wind speed variations, increasing predictability and the ability to generate more power at low wind speeds. Figure 1 shows the evolution of the wind turbine, where the most visible advance is the scale of the wind turbines, presented by Bloomberg New Energy Finance.

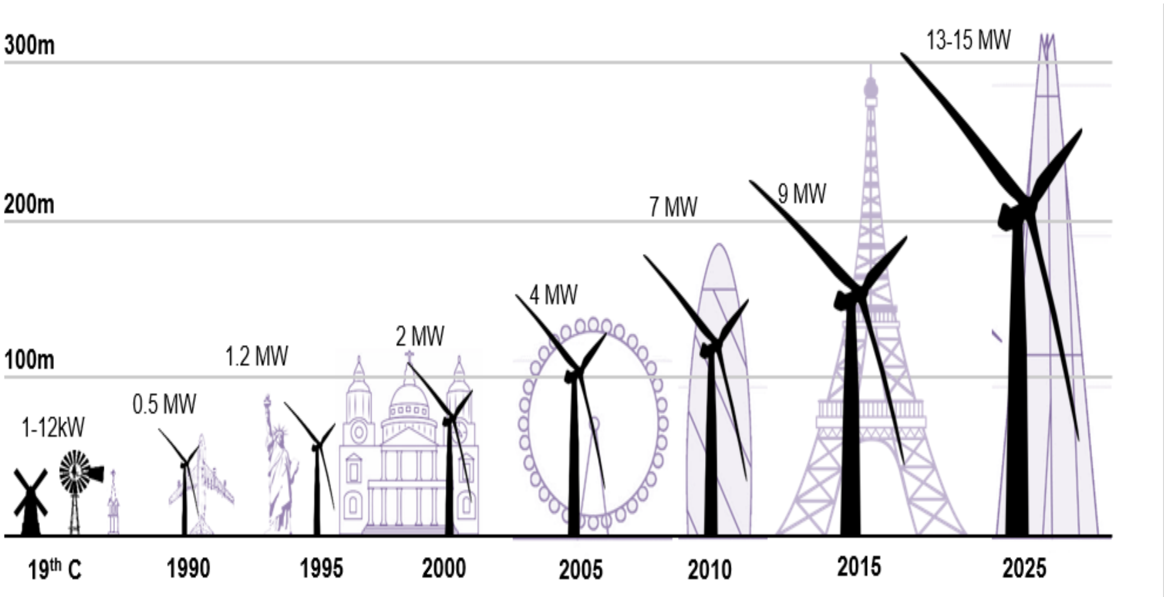

Figure 1: Evolution of wind turbine heights and output; [1] Various; Bloomberg New Energy Finance

However, the quest for bigger and taller turbines comes with its fair share of engineering challenges. Longer blades are more flexible than shorter ones, which can create vibration. If not controlled, this vibration affects performance and reduces the life of the blades and anything they are attached to, such as the gearbox or generator. Materials and manufacturing techniques are constantly being refined to create longer, and longer-lasting, turbine blades. In order to determine the effects of vibrations and loads on the blade to ensure safety, structural analysis has to be performed during the design. For the structural dynamics and aero-elasticity analysis of the complex composite blade, the cross-sectional properties need to be calculated. The calculation is complex due to orthotropic material properties, non-uniform distribution of different materials and the complex shape of the blade.

Finite-element techniques, despite their capability for accurate stress and displacement analysis, cannot yield these properties directly. One must rely on computationally complex post-processing of force-displacement data [1] and it is time and resource consuming and suitable to only a limited extent for rapid development. For this reason, there is a great interest in using analytical methods that not only can be incorporated into the highly iterative development process, but also can be used as verification method for the FEM results.

1.2 Current tool

Modern wind turbine blades generally are made of thin-walled shells with composite materials. However, due to the intrinsic nature of composite materials and the complexity of blade structural topologies, it is quite challenging to obtain the cross-sectional properties of a wind turbine blade. As already mentioned, various methods have been proposed for calculating the cross-sectional properties of wind turbine blades, ranging from complicated finite-element techniques and 3D laminate theories to the simple two-dimensional (2D) lamination theory. Due to the objective of this thesis, an overview of the known tools is given. Article [2] contains a comprehensive summary of some tools for calculating these stiffnesses.

3D finite-element techniques using brick element is the most accurate method to calculate stress and displacement. However, in order to extract the cross-sectional properties, a complicated post-processing of force-displacement data is needed. BPE is one such post-processing tool, which is developed by Sandia National Laboratories and Global Energy Concepts. BPE is a module of NuMAD (Numerical Manufacturing And Design). BPE applies a series of unit loads at the blade tip and transfers the displacement results of the 3D finite-element model of the blade to a series of MATLAB routines, which extract the stiffness matrices for the equivalent beam elements. However, there are several challenges of this approach. Firstly, application of loads must be performed carefully to minimize the boundary layer effects. Additionally, the cross-sectional properties estimated by BPE are sensitive to the length of the blade segment, which one chooses to perform the finite-element analysis. Changing the length of the blade segment may even result in a singular stiffness matrix under some extreme situations [3].

The second variation is based on the 2D finite-element discretization of the cross-section. Because the thickness of walls is usually small when compared with the chord length of the wind turbine blades, it is possible to use a two-dimensional (2D) FEA model based on laminated shell elements to simplify the analysis. This simplified 2D model, in comparison to the 3D FEA using brick elements, will dramatically reduce the required total number of degrees of freedom needed for modelling wind turbine blades to less than two orders of magnitude in comparison to using 3D brick elements [2]. The cross-sectional analysis tool, VABS (Variational Asymptotic Beam Sectional analysis), calculates the cross-sectional properties using the input files containing material and geometry properties of the individual layers. The generation of VABS input files is very tedious because a realistic rotor blade is made of hundreds of composite layers. It requires a separate pre-processor called PreVABS. Nevertheless, this method represents a good compromise between quality of results and computational speed and is therefore commonly used in the development of rotor blades.

Besides the time-consuming problem of a FEM model, the lack of generality of the results is another typical FEM problem. Although any material and geometry information can be defined within a cross-section, there are no comprehensible correlations of input and output parameters. Therefore, a targeted manipulation of cross-sectional properties is limited.

Compared to the finite element techniques, analytical solution based on Classical Lamination Theory, which is an extension of the classical plate theory to laminated plates, is fast and reasonably accurate. It also directly derives cross-sectional properties from the material and geometric data. However, in order to allow analytical analysis, the following assumptions are usually made:

- Walls are thin compared to the cross-sectional dimensions;
- Each ply is under the condition of plane stress
- Shear flow around each cell of the blade section is constant;
- Transverse shearing is negligible, and the blade section is rigid in its own plane. This assumption is fairly valid for a blade whose length far exceeds the transverse dimensions (chord and thickness).

Bir [1] developed PreComp (Pre-processor for computing Composite blade properties) at National Renewable Energy Laboratory (NREL) based on CLT. PreComp is an independent tool, which does not need a separate pre-processor to generate the input files, as such the geometric shape and internal structural layout of the blades, Moreover, it allows an arbitrary number of webs and a general layup of composite laminates. PreComp has been widely used in cross-sectional analysis of wind turbine composite blades due to its efficiency. However, PreComp ignores the effects of shear webs in the calculation of the torsional stiffness. In other words, if the number of webs on a cross-section is changed, no change in torsional stiffness will be observed using PreComp. This is invalid for a practical blade cross-section, where the torsional stiffness will be enhanced as the number of shear webs increases.

1.3 Research objectives

This work focus on the devolvement of a simplified analytical analysis based on beam theory, which is capable of rapidly and accurately determining cross-sectional properties of wind turbine composite blades. These properties are essential information for the structural dynamics and aeroelastic analysis of the wind turbine blade. An analytical tool in VBA is developed to determine axial, flapwise, edgewise, flap-edge stiffnesses, orientation of principal axes for stiffness, elastic center and shear center, which are the important section properties for static structural analysis. It is assumed that the blade undergoes small deformation. Therefore, Bernoulli-Navier hypothesis is applied with the assumptions that planes of the cross-section remain plane and perpendicular to the axis. There is no shear deformation of the blade. The effect of torsion, shear deformation and the coupling of blade extension, bending, shear, and torsion are momentarily not considered due to orthotropic laminate. Nevertheless, technical changes like number of shear web, laminate layup and material stiffness can be done in no time with this analytical model. For structural analysis, strain and stress are calculated using classical lamination theory. These are later transferred to another analytical model to carry out laminate failure, buckling and bonding analysis. Figure 2 shows the development process of the VBA tool.

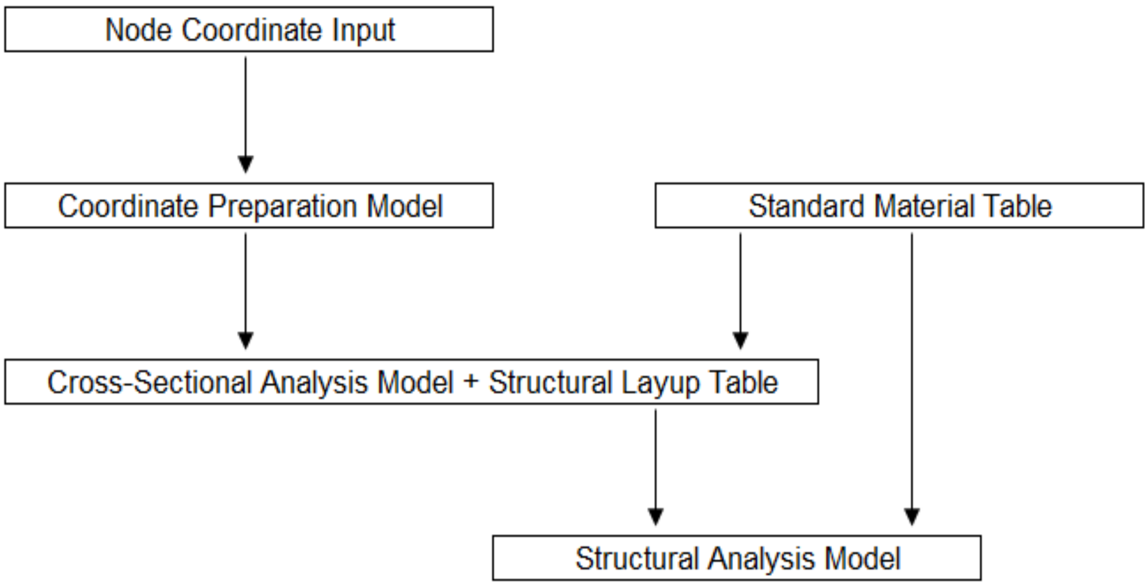

Figure 2: Flow chart of the VBA tool

2 Basics

The calculation of stiffness of a laminate and sandwich structure based on classical lamination theory are discussed in this chapter. Followed by a brief introduction of the structural design of a typical rotor blade and its cross-sectional stiffnesses.

2.1 Classical Lamination Theory

In this project, all materials are assumed to be orthotropic and under plane-stress condition [4]. Under plane-stress condition one of the normal stresses and both out-of-plane shear stresses are zero.

$$\sigma_z = \tau_{yz} = \tau_{xz} = 0 \tag{2.1}$$

Plane-stress condition may approximate the stresses in a thin-fiber-reinforced composite plate when the fibers are parallel to the x-y plane and the plate is loaded by forces along the edges such that the forces are parallel to the plane of the plate and are distributed uniformly over the thickness. The plane-stress condition does not provide the stresses exactly, not even for this thin-plate problem. Nevertheless, for many thin wall structures it is a useful approximation, yielding results within reasonable accuracy. Hence, the stress and strain of an orthotropic laminate is as followed:

$$\begin{Bmatrix} \sigma_x \\ \sigma_y \\ \tau_{xy} \end{Bmatrix} = \begin{bmatrix} \bar{Q}_{11} & \bar{Q}_{12} & 0 \\ \bar{Q}_{21} & \bar{Q}_{22} & 0 \\ 0 & 0 & \bar{Q}_{66} \end{bmatrix} \begin{Bmatrix} \epsilon_x \\ \epsilon_y \\ \gamma_{xy} \end{Bmatrix} \tag{2.2}$$

2.1.1 Stiffness and Compliance matrices of orthotropic layer

The engineering constants of the layer are used to determine the elements of the stiffness and matrix:

$$[\bar{Q}] = \begin{bmatrix} \dfrac{E_x}{1 - v_{xy}v_{yx}} & \dfrac{v_{yx}E_x}{1 - v_{xy}v_{yx}} & 0 \\ \dfrac{v_{xy}E_y}{1 - v_{xy}v_{yx}} & \dfrac{E_y}{1 - v_{xy}v_{yx}} & 0 \\ 0 & 0 & G_{xy} \end{bmatrix} \tag{2.3}$$

$$v_{yx} = v_{xy}\frac{E_y}{E_x} \tag{2.4}$$

The compliance matrix is the inverse of the stiffness matrix:

$$[\bar{S}] = [\bar{Q}]^{-1} = \begin{bmatrix} \frac{1}{E_x} & -\frac{\upsilon_{yx}}{E_y} & 0 \\ -\frac{\upsilon_{xy}}{E_x} & \frac{1}{E_y} & 0 \\ 0 & 0 & \frac{1}{G_{xy}} \end{bmatrix} \tag{2.5}$$

The stiffness matrices are transformed to the wall segment coordinate system (ξ, ζ, η) if the layer orientation is not parallel to the blade axis:

$$\begin{aligned}
\hat{Q}_{11} &= c^4\bar{Q}_{11} + s^4\bar{Q}_{22} + 2c^2s^2(\bar{Q}_{12} + 2\bar{Q}_{66}) \\
\hat{Q}_{22} &= s^4\bar{Q}_{11} + c^4\bar{Q}_{22} + 2c^2s^2(\bar{Q}_{12} + 2\bar{Q}_{66}) \\
\hat{Q}_{12} &= \bar{Q}_{12} + c^2s^2(\bar{Q}_{11} + \bar{Q}_{22} - 2\bar{Q}_{12} - 4\bar{Q}_{66}) \\
\hat{Q}_{66} &= \bar{Q}_{66} + c^2s^2(\bar{Q}_{11} + \bar{Q}_{22} - 2\bar{Q}_{12} - 4\bar{Q}_{66}) \\
\hat{Q}_{16} &= -s^3c(\bar{Q}_{12} + 2\bar{Q}_{66} - \bar{Q}_{22}) + c^3s(\bar{Q}_{12} + 2\bar{Q}_{66} - \bar{Q}_{11}) \\
\hat{Q}_{26} &= -c^3s(\bar{Q}_{12} + 2\bar{Q}_{66} - \bar{Q}_{22}) + s^3c(\bar{Q}_{12} + 2\bar{Q}_{66} - \bar{Q}_{11})
\end{aligned} \tag{2.6}$$

2.1.2 Stiffness and Compliance matrices of orthotropic structure

Stiffness matrices of the laminate are used to calculate the stiffness of the blade. Thus, the stiffness matrices of the laminate need to be calculated and are defined as

$$\begin{aligned}
A_{ij} &= \sum_{k=1}^{K} \left(\hat{Q}_{ij}\right)_k (z_k - z_{k-1}) \\
B_{ij} &= \frac{1}{2}\sum_{k=1}^{K} \left(\hat{Q}_{ij}\right)_k (z_k^2 - z_{k-1}^2) \\
D_{ij} &= \frac{1}{3}\sum_{k=1}^{K} \left(\hat{Q}_{ij}\right)_k (z_k^3 - z_{k-1}^3)
\end{aligned} \tag{2.7}$$

If the laminate is unsymmetrical, the stiffness matrices refer to neutral plane of the laminates need to be calculated as the mid plane is not equal to the neutral plane of the laminate.

$$A_{ij}^{NP} = A_{ij}$$

$$B_{ij}^{NP} = B_{ij} - \varrho A_{ij} \tag{2.8}$$

$$D_{ij}^{NP} = D_{ij} - 2\varrho B_{ij} + \varrho^2 A_{ij}$$

ϱ is the distance from the laminate mid plane to neutral plane

$$\varrho = \frac{B_{11} - \frac{A_{16}B_{16}}{A_{66}}}{A_{11} - \frac{A_{16}{}^2}{A_{66}}} \tag{2.9}$$

In orthotropic laminates, normal forces do not cause shear and bending moments do not cause twist of the laminates. Hence, there are no extension-shear, bending-twist, and extension-twist couplings. A laminate is orthotropic when every ply is orthotropic ($\hat{Q}_{16} = \hat{Q}_{26} = 0$). Fiber-reinforced plies are orthotropic under the following conditions [4]:

- When the ply is made of unidirectional fibers and all the fibers are aligned with one of the laminate's orthotropic directions;
- When the ply is a woven fabric and the ply's symmetry axes are aligned with the laminate's orthotropic directions;
- When two adjacent unidirectional plies (oriented in different directions) are treated as a single layer and the symmetry axes of this layer are aligned with the laminate's orthotropic directions

The stiffness matrices of an orthotropic laminate are as follows:

$$[A] = \begin{bmatrix} A_{11} & A_{12} & 0 \\ A_{21} & A_{22} & 0 \\ 0 & 0 & A_{66} \end{bmatrix}$$

$$[B] = \begin{bmatrix} B_{11} & B_{12} & 0 \\ B_{21} & B_{22} & 0 \\ 0 & 0 & B_{66} \end{bmatrix} \tag{2.10}$$

$$[D] = \begin{bmatrix} D_{11} & D_{12} & 0 \\ D_{21} & D_{22} & 0 \\ 0 & 0 & D_{66} \end{bmatrix}$$

where $[A]$ is the extensional stiffness matrix in $[\frac{N}{mm}]$, $[B]$ is the coupling stiffness matrix in $[N]$, $[D]$ is the bending stiffness matrix in $[Nmm]$.

The compliance matrices $[\alpha]$, $[\beta]$, $[\delta]$ are related to the stiffness matrices $[A]$, $[B]$, $[D]$ by

$$\begin{bmatrix} \alpha_{11} & \alpha_{12} & 0 & \beta_{11} & \beta_{12} & 0 \\ \alpha_{12} & \alpha_{22} & 0 & \beta_{12} & \beta_{22} & 0 \\ 0 & 0 & \alpha_{66} & 0 & 0 & \beta_{66} \\ \beta_{11} & \beta_{12} & 0 & \delta_{11} & \delta_{12} & 0 \\ \beta_{12} & \beta_{22} & 0 & \delta_{12} & \delta_{22} & 0 \\ 0 & 0 & \beta_{66} & 0 & 0 & \delta_{66} \end{bmatrix} = \begin{bmatrix} A_{11} & A_{12} & 0 & B_{11} & B_{12} & 0 \\ A_{21} & A_{22} & 0 & B_{21} & B_{22} & 0 \\ 0 & 0 & A_{66} & 0 & 0 & B_{66} \\ B_{11} & B_{12} & 0 & D_{11} & D_{12} & 0 \\ B_{21} & B_{22} & 0 & D_{21} & D_{22} & 0 \\ 0 & 0 & B_{66} & 0 & 0 & D_{66} \end{bmatrix}^{-1} \tag{2.11}$$

2.1.3 Stiffness and Compliance matrices of orthotropic sandwich plate

A sandwich consists of three main parts. Two thin, stiff and strong laminates (skin) separated by a thick core material of low density. It is often that the stiffness of the core is neglected. A sandwich structure operates in much the same way as a traditional I-beam where as much material as possible is places in the flanges situated furthest from the neutral axis. The connecting web makes it possible for the flanges to resist shear stresses. In a sandwich structure, the laminates can be considered to be the flanges of the I-beam and the core material as the web. The two forms differ in the way that in a sandwich, the core and laminates are dissimilar materials and the core provides continuous support for the laminates rather than being concentrated in a narrow web. When subjected to bending, the laminates act in unison, resisting the external bending moment so that one laminate is loaded in compression and the other in tension. The core resists transverse forces while at the same time supports the laminates and stabilizes them against buckling and wrinkling. Hence, the purpose of the sandwich structure is to increase local bending stiffness of the laminate to control local bending and prevent buckling.

A sandwich plate is orthotropic when both skins as well as the core are orthotropic and the orthotropy directions are parallel to the edges. There are no extension-shear, bending-twist, and extension-twist couplings. Like orthotropic laminate, the following elements of the stiffness matrices are zero:

$$A_{16} = A_{26} = B_{16} = B_{26} = D_{16} = D_{26} = 0 \tag{2.12}$$

The calculation of the stiffness matrices of an orthotropic sandwich plate is different than of an orthotropic laminate. The stiffness matrices of sandwich plates are evaluated by assuming that the thickness of the core remains constant under loading and the in-plane stiffnesses of the core are negligible. Under these assumptions the $[A]$, $[B]$, and $[D]$ stiffness matrices of a sandwich plate are governed by the stiffnesses of the skins.

The stiffness matrices of each laminate skin refer to its mid plane is first calculated. Then, the stiffness matrices of the sandwich plate are determined with the following equation. The superscripts t and b refer to the top and bottom skins.

$$[A] = [A]^t + [A]^b$$

$$[B] = d^t[A]^t - d^b[A]^b + [B]^t + [B]^b \tag{2.13}$$

$$[D] = (d^t)^2[A]^t + (d^b)^2[A]^b + [D]^t + [D]^b + 2d^t[B]^t - 2d^b[B]^b$$

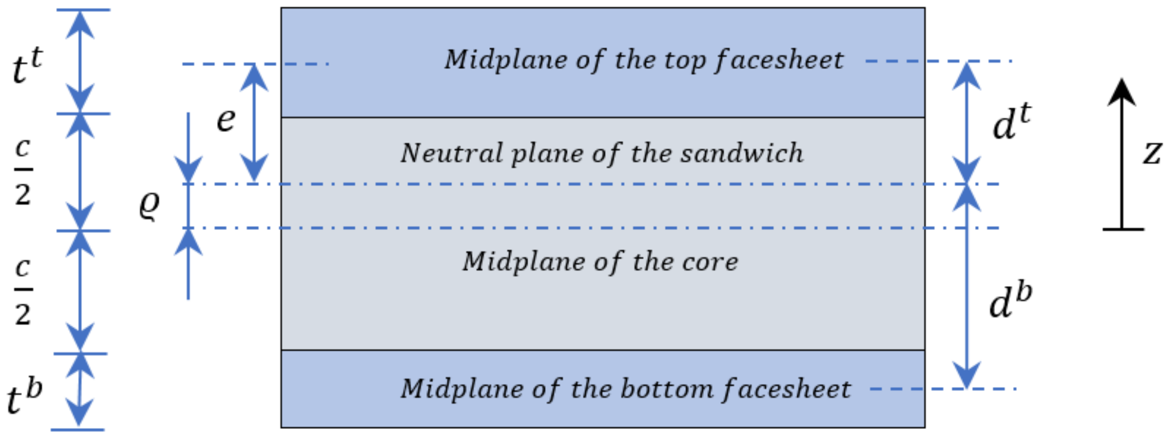

Figure 3: Unsymmetrical sandwich plate

If the sandwich plate is unsymmetrical due to different thickness of the top and bottom skins, the distance e and ϱ are calculated, in order to determine the distance d^t and d^b between the midplane of the core and the mid plane of the skin:

$$e = \frac{{A_{11}}^b \cdot \left(\frac{t^b}{2} + c + \frac{t^t}{2}\right) + {A_{11}}^c\left(\frac{c}{2} + \frac{t^t}{2}\right)}{{A_{11}}^b + {A_{11}}^c + {A_{11}}^t} \tag{2.14}$$

where e is the distance of the skin mid plane to neutral plane of the sandwich plate

$$\varrho = \frac{c}{2} + \frac{t^t}{2} - e \tag{2.15}$$

where ϱ is the distance from the mid plane of the core to the center of gravity (neutral plane) of the sandwich plate

Thus, the distance between the midplane of the core and the mid plane of the top and bottom skin

$$d^t = \frac{c}{2} + \frac{t^t}{2} - \varrho$$
$$(2.16)$$
$$d^b = \frac{c}{2} + \frac{t^b}{2} + \varrho$$

2.2 Structural design of a rotor blade

The current state-of-art wind turbine rotor blades are constructed from fiber reinforced polymers (FRP), as it is an efficient way to further improve the performance by reducing the weight of the blades. The reinforcing fibers have high strength, high stiffness, high stiffness-to-density ratio and high strength-to-density ratio and its main function is to carry the load and provide strength, stiffness, thermal stability and other structural properties to the composite blade. The purpose of is to bind the fibers together and transfer the load to fibers providing rigidity and shape to the blade structure. The failure mode during structural analysis is strongly affected by the type of matrix material used in the composites. Typically, continuous glass fiber composites are used, but as blades become longer and slender, designers are also going for carbon fibers because these stiffer fibers are becoming affordable for large wind turbine blade structure.

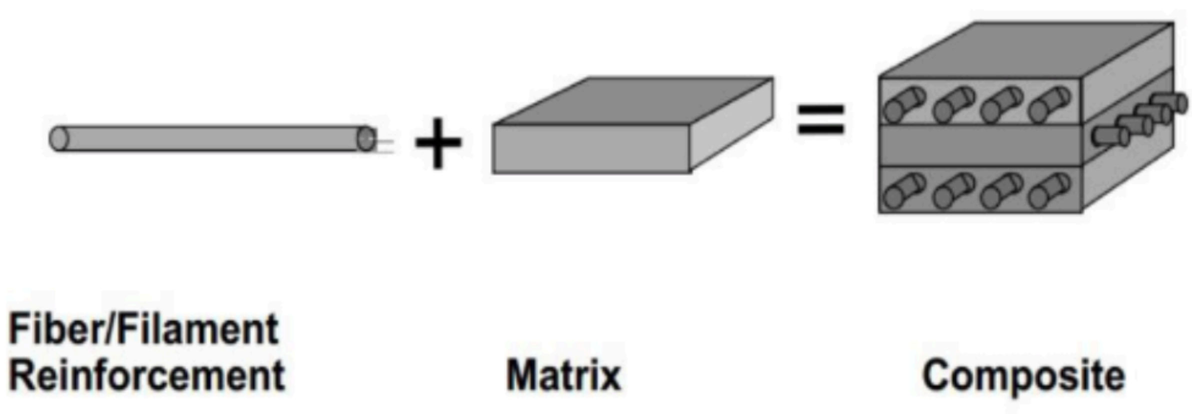

Figure 4: Composition of Composite; Source IARJSET

A wind turbine blade is predominantly loaded in flapwise and edgewise direction. A wind turbine blade cross section can be divided into load carrying parts, and parts, that are geometrically optimized for aerodynamic shape. This is a kind of compromise between the structural integrity and aerodynamic performance in a wind turbine blade. Table 1 shows the function of each part of the blade cross section. Figure 5 shows a type of layup in which the midsections cap the two shear webs. The number of lamina stacks along the section periphery, the number of laminas in each stack, and the thickness of the laminas generally vary along the blade length.

Part	Function
Leading and trailing edge panels	Sandwich panels with a form core separating layers of multi-directional laminates towards leading and trailing edges, ensuring aerodynamics geometry, low mass, resistance to torsion and high buckling resistance as well as carrying the edgewise loading. Sometimes, reinforcement in the leading and trailing edge is present to take partially the edgewise loading.
Main and tail girders	The primary function of the girder section is to carry the flapwise bending moment, and it is usually made as a thick monolithic composite laminate, which for some large blades is a hybrid glass/carbon composite. The carbon fibers are used to enhance the bending stiffness of the blade. The main girders lay-up usually includes UD-layers to provide for the bending stiffness as well as off-axis or angle-ply layers (often biax) to provide for the buckling resistance of the flange loaded in compression (suction side of airfoil).
Shear webs	The function of the webs is to carry the flapwise shear forces, and they are usually made as composite sandwich plates with polymeric or balsa core and relatively with biax laminate thin composite skins. The sandwich design is chosen in order to enhance the resistance against in-plane shear buckling.

Table 1: Structural parts of a blade and the functions

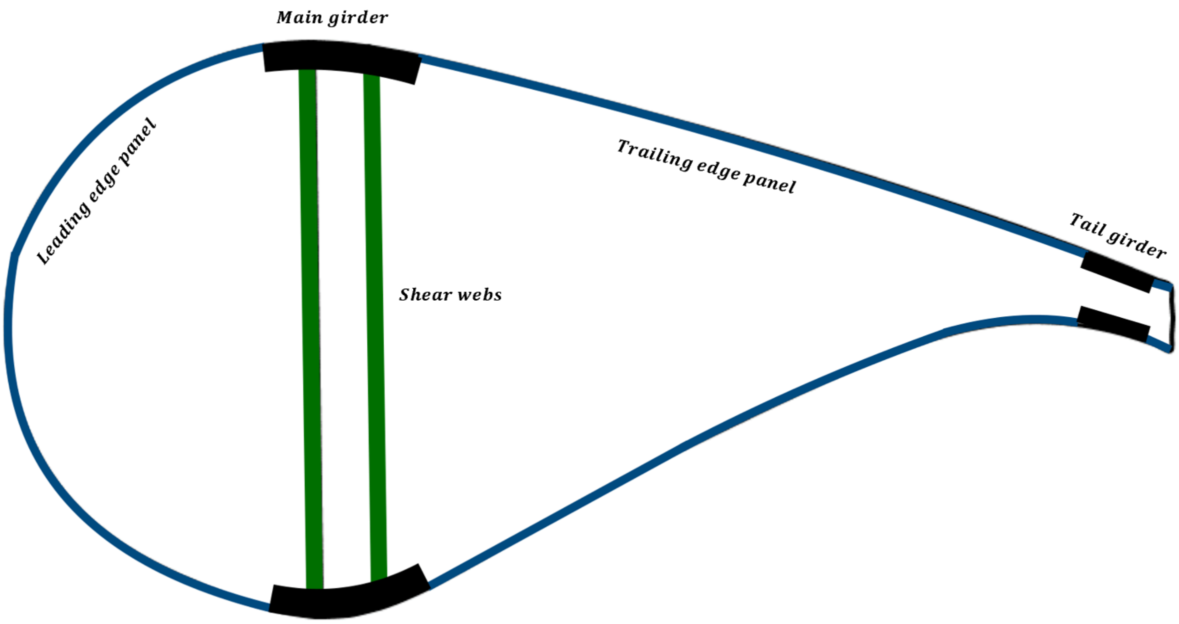

Figure 5: Example of the composite layup of at a typical blade section

2.2.1 Cross-sectional stiffness of a rotor blade

Rotor blade is considered as an orthotropic beam, as its wall is made of orthotropic laminates. Additionally, rotor blade is assumed to be undergoing small deformation and is analyzed using Bernoulli-Navier hypothesis, which the planes of the cross section remain plane and perpendicular to the axis. In another word, shear deformation of the cross section is neglected. Thus, for the typical rotor blade cross sections, the cross-sectional stiffness is given as a 4x4 matrix according to Bernoulli-Navier hypothesis

$$P = \begin{bmatrix} EA & 0 & 0 & 0 \\ 0 & EI_{yy} & EI_{xy} & 0 \\ 0 & EI_{xy} & EI_{xx} & 0 \\ 0 & 0 & 0 & GI_t \end{bmatrix} \quad (2.17)$$

with the corresponding positions of the elastic centers. The coupling between tension, bending and torsion is not considered.

3 Coordinate Systems

The following two coordinate systems are used to differentiate the coordinate system for the whole cross section and for the discretized elements.

3.1 Chord Coordinate System $(\boldsymbol{X_R}, \boldsymbol{Y_R}, \boldsymbol{Z_R})$

Chord Coordinate System is chosen as the reference coordinate system in this tool. The chord coordinate system has its origin at the leading edge of the cross section. The direction of Y_R and X_R axes are parallel and perpendicular to the chord line of the cross-section respectively. X_R axis points in the direction of the suction side, Y_R axis is orientated to blade trailing edge, and Z_R is in direction of the blade pitch axis, see Figure 8 in Chapter 4.1.2. For each cross-sectional plane, there exists a separate chord coordinate system.

3.2 Periphery Coordinate System $(\boldsymbol{\eta}, \boldsymbol{\zeta}, \boldsymbol{\xi})$

The periphery coordinate system of Figure 6 follows the cross-sectional contour. The contour of the cross-section is discretized into small elements. A periphery coordinate system with the origin at the neutral plane of each element is defined. At each point in the element ξ is parallel to the Z_R coordinate, η is tangential to the contour and ζ is defined to be perpendicular to the contour and orientated toward the interior of the cross-section.

The coordinate of the shear webs starts from the pressure side. On the suction and pressure side, the coordinate starts from the leading edge to trailing edge or flat back. It is important due to the definition of the layup build-up of the layer in the layup table for suction side contour, pressure side contour and shear webs, respectively.

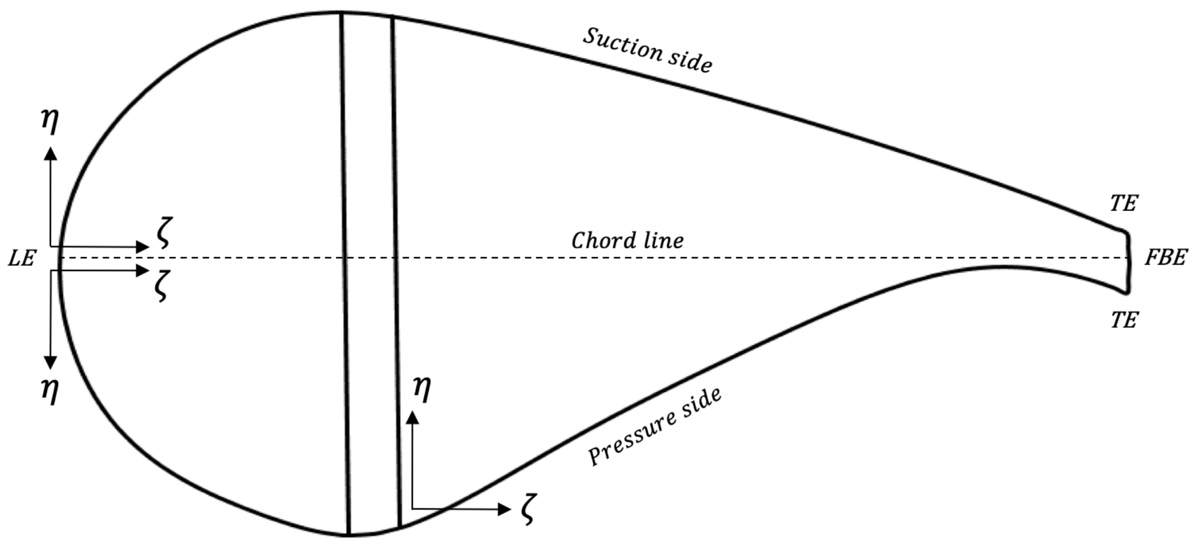

Figure 6: Periphery Coordinate System (η, ζ, ξ)

4 Cross-sectional analysis model

A cross-sectional analysis model is developed to extract cross-sectional properties of wind turbine composite blades rapidly and accurately using VBA. The tool is capable to be used for different shape of the cross-section of the blade, including different position and number of shear webs. The calculated cross-sectional properties are compared with the results from finite-element analysis for validation. As this tool works based on Classical Lamination Theory, there are assumptions need to be made for analytical analysis, as mentioned in Chapter 2.

In order to determine the cross-sectional properties of wind turbine blades, all cross-sectional laminates are discretized into many elements. Each element encloses several layers of laminates with or without core. Stiffness and Compliance matrices of each orthotropic laminate or sandwich elements are determined in Chapter 2.1 using Classical Lamination Theory, which are used to calculate elastic center, shear center, principle axes, axial stiffness, flapwise stiffness and edgewise stiffness of the cross-section. Based on the above strategy, a mathematical model for cross sectional analysis is developed. The flowchart of the model is shown below. Each step of the flow chart is detailed as follows:

Data input

↓

Coordinate Transformation

↓

Point Definition

↓

Discretization of the cross-section into many elements

↓

Layup Definition

↓

Calculation of stiffness and compliance matrices of each elements using CLT

↓

Calculation of the elastic center and bending stiffness of the cross-section

↓

Calculation of axial strain and axial load

↓

Calculation of shear flow and shear center

Flow chart of the mathematical model

4.1 Data preparation

Due to different type of profile data given by the customer, the profile data must be adapted accordingly so that they are compatible for this mathematical model. Besides, standard material table for a cross section is prepared in advanced.

4.1.1 Profile Data

The profile data are in the form of a defined number of nodes, along the blade axis. These are separately given for pressure side, suction side, shear webs and where required also for flat back. Each node is defined with a node number. Each node has its coordinate (x, y, z). Table 2 shows an example of the profile data. Z-values are used for the definition for material start and end locations along the blade. These values are measured in the Blade Coordinate System, where the origin is at the aerodynamic center, see Figure 7. The zero point $(Z = 0)$ is at the blade root cut surface, where all given Z-values are perpendicular to the root cut surface, thus perpendicular to the (x, y)-plane in the blade coordinate system. One blade station is analyzed at one time and the profile data of the specific blade station is transferred to Coordinate Preparation Model for point definition and coordinate transformation if necessary. Z-axis is directed into the page.

Pressure side / Suction side / Shear web / Flat back			
Node	**X**	**Y**	**Z**
[-]	**[mm]**	**[mm]**	**[mm]**
6354	349.99	1504.838	1500
6535	398.499	1492.719	1500
6539	422.539	1485.858	1500
⋮	⋮	⋮	⋮
89110	776.394	2689.316	13750
89111	779.805	2639.433	13750
89115	781.401	2614.484	13750
⋮	⋮	⋮	⋮
156572	43.206	1849.205	30000
156573	55.021	1800.622	30000
156577	60.679	1776.271	30000
⋮	⋮	⋮	⋮

Table 2: Example of the profile data

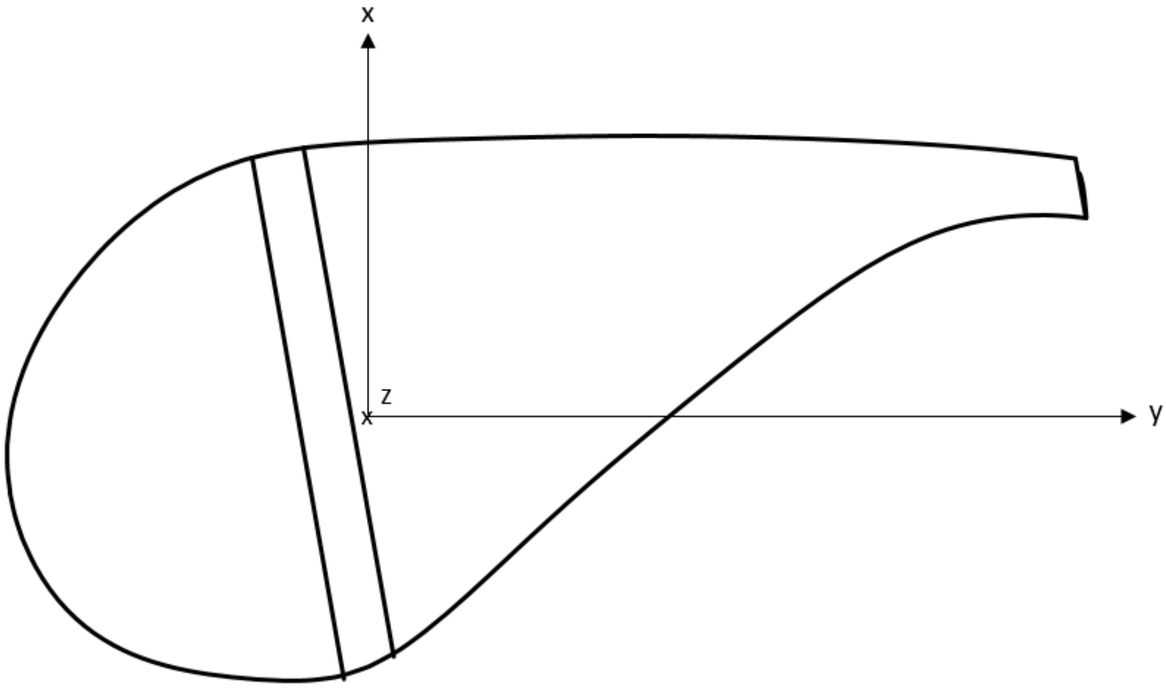

Figure 7: Blade coordinate system

4.1.2 Coordinates Transformation

Chord Coordinate System axes are chosen as the reference axes, which the origin is at the leading edge and the direction of Y_R and X_R are parallel and perpendicular to the chord direction of the blade cross-section respectively. This is due to that bending stiffness including both flapwise and edgewise stiffness is referred to the elastic center of a principal coordinate system, of which the principal axes are generally very near to the reference axes. Besides, it is much easier to determine the element angle α_k in order to build up the layers inwards in chord coordinate system, see Chapter 4.2. Therefore, it is necessary to add a step to transfer the input airfoil data to reference axes with an origin at the leading edge if the input data refer to different axes. The twist angle is calculated by determining the angle of the chord line to the horizontal axis. With the twist angle the origin coordinates system is transformed to chord coordinate system, see Figure 8. For pressure and suction side of the profile, the coordinates always start at leading edge LE and end with TE/FBE, whereas the coordinates of shear webs always start from the suction side (SWLE-X) and end with the pressure side (SWLE-O)

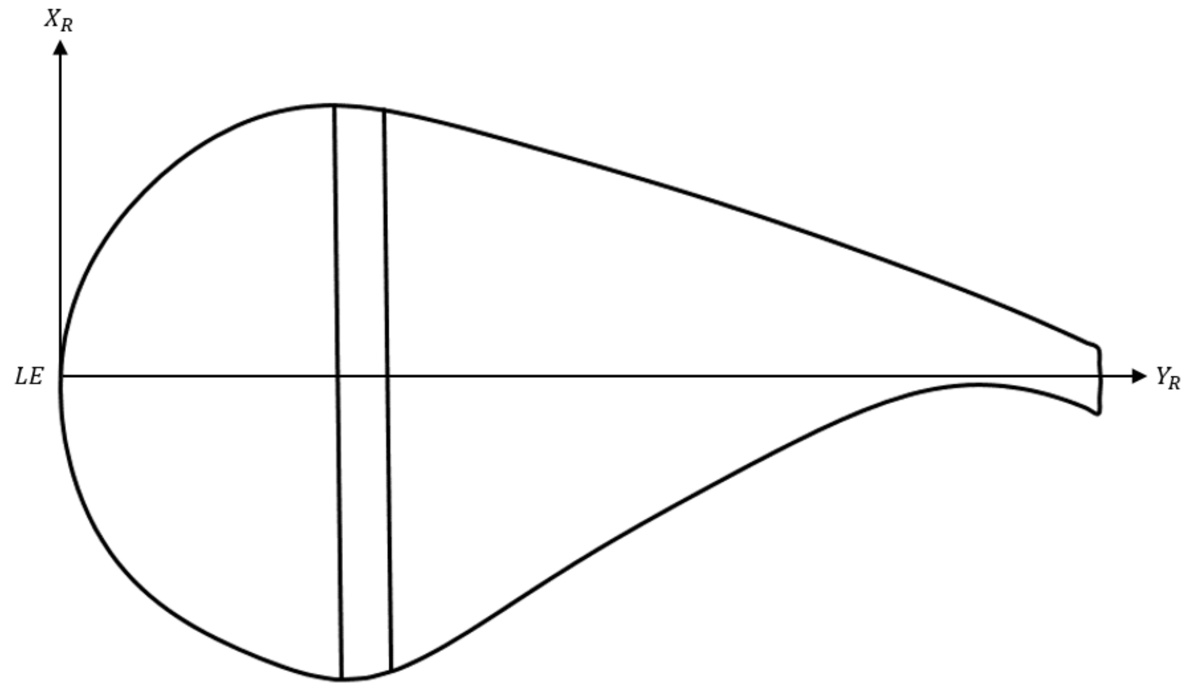

Figure 8: Chord coordinate system with an origin at leading edge

4.1.3 Points Definition

Table 3 shows the essential points on the contour of the cross-section. These points need to be labeled beforehand, for both pressure (X) and suction (O) side. The location of starting point of the main girder and tail girder as well as the width of the girders are defined by the user.

LE	Leading edge
TE	Trailing edge
FBE	Flat back edge
SWLE	Shear web leading edge
SWTE	Shear web trailing edge
MGLE	Main girder leading edge
MGTE	Main girder trailing edge
TGLE	Tail girder leading edge
TGTE	Tail girder trailing edge
a	Distance from main girder leading edge to shear web leading edge (Suction side)
b	Main girder width (Suction side)
c	Distance from main girder leading edge to shear web leading edge (Pressure side)
d	Main girder width (Pressure side)
e	Distance from tail girder trailing edge to trailing edge (Suction side)
f	Tail girder width (Suction side)

g	Distance from tail girder trailing edge to trailing edge (Pressure side)
h	Tail girder width (Pressure side)

Table 3: Labels and parameters across the profile

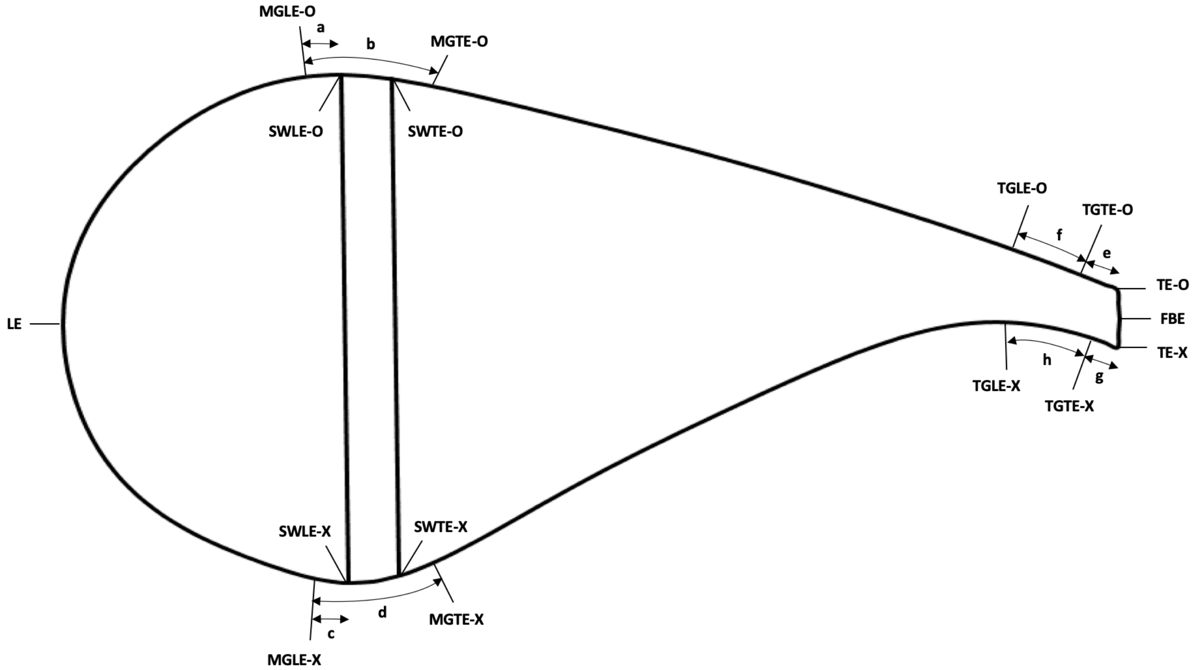

Figure 9: Labels and parameters to be defined

4.1.4 Structural Layup Table

The structural layup at a section is thus characterized by the variation of composite laminas that stack along the section periphery and over the web cross-section. This layup varies from section to section. At any section, the composite structural layup is within the confines of the section external shape. External shape at a section is characterized by its chord length and airfoil geometry.

A layup table of the stacking sequence of layers for the specific cross-section is created for pressure side, suction side and shear webs, respectively. The model runs across the tables from the top to the bottom to build the stack-up sequence of the layers by referring to the chord start and chord end across the contour. The value behind the label is the distance from the labeled node and it is set by the user by referring to the calculated accumulated distance. A positive value is measured from leading edge towards the trailing edge, or from the trailing edge towards the flat back edge. A negative value is measured from the trailing edge to the leading edge, or from the flat back edge to the trailing edge. When the chord start is LE and the chord end is TE/FBE, it means that the layer covers the whole pressure side or suction side of the profile. The 0°layer orientation means that the layup is put parallel to the blade pitch axis. For example, if the layer is biaxial, the resulting fiber orientation is +45°/-45° with respect to the blade pitch axis, whereas for a UD layer, it is always put in the direction of the blade pitch axis.

Pressure side / Suction side			
Layer	**Chord start**	**Chord end**	**Layer orientation**
[-]	**[mm]**	**[mm]**	**[°]**
Biax	LE	TE	0
Biax	LE	FBE	0
Core	TE-i	TE	0
Biax	NE	NE+60	0
UD	MGLE	MGTE	0
UD	MGLE	MGTE	0
Biax	MGTE	MGTE+93	0
⋮	⋮	⋮	⋮

Table 4: Example of a structural layup table for pressure and suction side

Shear web			
Layer	**Chord start**	**Chord end**	**Layer orientation**
[-]	**[mm]**	**[mm]**	**[°]**
Biax	SWLE	SWLE	0
Biax	SWLE	SWLE	0
Core	SWLE	SWLE	0
Biax	SWLE	SWLE	0
Biax	SWLE	SWLE	0
⋮	⋮	⋮	⋮

Table 5: Example of a structural layup table for shear web leading edge

4.1.5 Material Table

A standardized material table is prepared. Material engineering constants, material ID, layer thickness, layer orientation, layup (ply angle), and density are the necessary as inputs.

4.2 Discretization of the cross-section into many elements

In this step, the cross section is discretized into many elements according to the given nodes. Each element encloses several laminates with or without core. The starting and ending node of all the elements are given with a label, which corresponds to the labeling system in the structural layup table, as this is important for the layup definition later.

The distance between these two nodes represent the width of the element. The resolution of the cross-sectional model for the calculation of the cross-sectional properties depends on the width of the element, as each element has different width. A new coordinate is created in the middle of each element using the two adjacent nodes, as the intersection point of the η, ζ, ξ axes. It has its own coordinate system with an angle α_k from reference Y_R-axis to η-axis. Y_R-axis is parallel to the chord line. α_k is positive in clockwise and negative in counterclockwise direction.

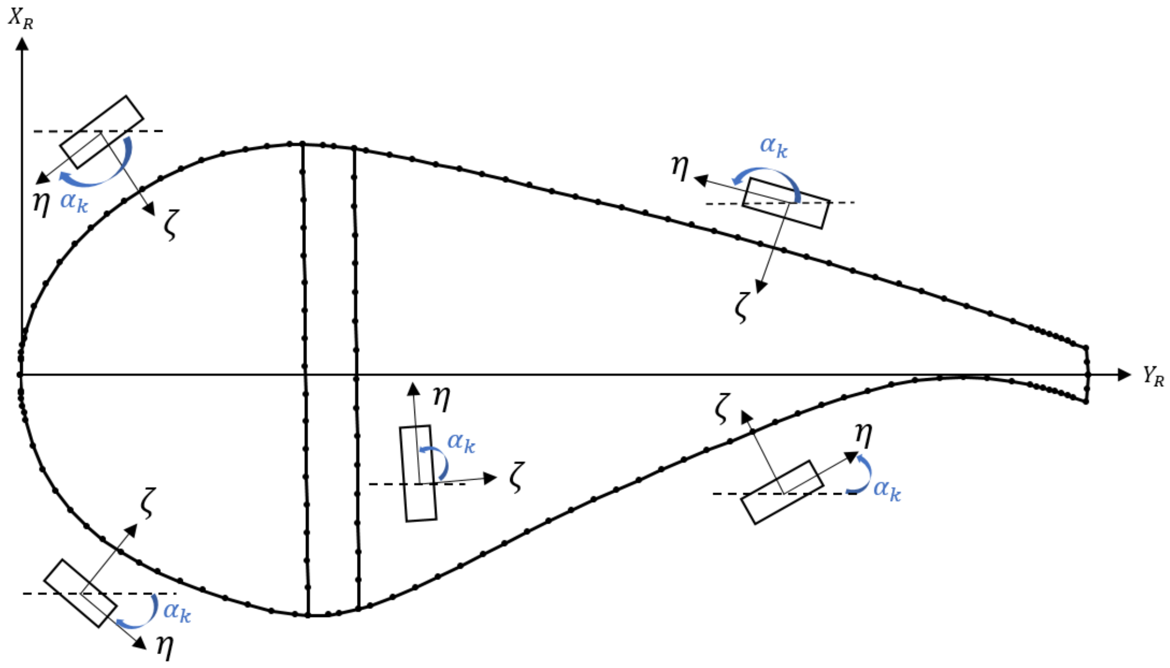

Figure 10: Discretization of the cross section

Element number	Start node	End node	Element width	Element angle	⋯
[-]	[-]	[-]	[mm]	[°]	⋯
1	NE	NE+50	50	-92.93	⋯
2	NE+50	NE+60	10	-96.07	⋯
⋮	⋮	⋮	⋮	⋮	⋮
22	MGLE	MGLE+51	51	-179.64	⋯
23	MGLE+51	MGLE+131	80	177.68	⋯
⋮	⋮	⋮	⋮	⋮	⋮
27	MGTE	MGTE+93	93	171.85	
28	MGTE+93	MGTE+186	93	170.61	
⋮	⋮	⋮	⋮	⋮	⋮
62	TE-75	TE-50	25	162.29	
63	TE-50	TE	50	162.03	
⋮	⋮	⋮	⋮	⋮	⋮

Table 6: Example of an element data table of a discretized cross-section

4.3 Layup definition

The layup definition serves to distribute material along the webs and cross-sectional contour. The layup definition is done by comparing the start and end node of the element with the chord start and chord end in the structural layup table.

According to table below, number of layers with the corresponding material on each element are defined according to the structural layup table with the help of layup definition. The properties of the layer like the orientation, thickness and layup are listed in the table for further calculation. In Table 7, for example, biax layers and core are distributed on the region of the leading edge (Element 1), forming a symmetrical sandwich structure. All layers are orientated parallel to the blade axis. On the other hand, element 22 is an element in the main girder, which consist 7 UD layers.

Element number	**…**	**Number of layers**	**Material**	**Layer orientation**	**Layer thickness**	**Layup**
[-]	**…**	**[-]**	**[-]**	**[°]**	**[mm]**	**[-]**
1	…	5	Biax	0	0.576	+45 -45
			Biax	0	0.576	+45 -45
			Core	0	12.7	NA
			Biax	0	0.576	+45 -45
			Biax	0	0.576	+45 -45
⋮	⋮	⋮	⋮	⋮	⋮	⋮
22	…	7	UD	0	1.9	0
			UD	0	1.9	0
			UD	0	1.9	0
			UD	0	1.9	0
			UD	0	1.9	0
			UD	0	1.9	0
			UD	0	1.9	0
⋮	⋮	⋮	⋮	⋮	⋮	⋮

Table 7: Example of element with layer stack-up

4.4 Calculation of stiffness and compliance matrices of each elements

The material engineering constants are imported from the material table into the model. The ABD matrices referring to the midplane of the element are first calculated, followed by the determination of the neutral plane. The stiffness matrices are evaluated at the neutral plane of each element, where the bending moment M_ξ does not cause axial strain ϵ_ξ and N_ξ does not cause curvature κ_ξ in this surface.

Besides, it is important to identify either the element is an orthotropic laminate or sandwich plate due to different calculation of the stiffnesses. The stiffness matrices of sandwich plates are evaluated by assuming that the thickness of the core remains constant under loading and the in-plane stiffnesses of the core are negligible. The calculation methods of ABD matrices referring to the neutral plane of the element, for both laminate and sandwich element, are explained in detail in Chapter 2.1.

Element number	⋯	**Thickness of same material**	**Plate**	A_{ij}	B_{ij}	D_{ij}
[-]	⋯	**[mm]**	**[-]**	**[N/mm]**	**[N]**	**[Nmm]**
1	⋯	5.76	Laminate	⋯	⋯	⋯
⋮	⋮	⋮	⋮	⋮	⋮	⋮
		1.728				
3	⋯	12.7	Sandwich	⋯	⋯	⋯
		1.728				
⋮	⋮	⋮	⋮	⋮	⋮	⋮
22		22.8	Laminate	⋯	⋯	⋯
⋮	⋮	⋮	⋮	⋮	⋮	⋮
		20.2				
24	⋯	25.4	Sandwich	⋯	⋯	⋯
		5.76				
⋮	⋮	⋮	⋮	⋮	⋮	⋮

Table 8: ABD-Matrices of the elements

4.5 Calculation of the elastic center and bending stiffness of the cross-section

Elastic center (Centroid) and shear center of a blade cross-section are two important sectional properties that are used to determine the structural response. The elastic center is defined as the location where an axial load does not cause a change in curvature and a bending moment does not produce axial strain. Likewise, shear forces acting at the shear center do not cause twist. In other words, the load acting at the elastic center decouples the structural response between axial extensions and bending, whereas, shear center decouples bending and twisting. For the beam made of isotropic material, the locations of elastic center and shear center are purely dependent of geometric cross-section of the beam. Composite material exhibits unique structural coupling characteristic. For example, a composite beam with rectangular cross-section subjected to axial force exists an extension/twist coupling and applied pure bending moment exists a bending/twisting coupling. Hence, the location of elastic center and shear center of a laminated composite closed-section beam is not only a function of the geometry but also the material properties and layup of the sectional laminate. Determination of these locations depends on the stiffness of each segment laminate of the entire cross-section.

The elastic center, axial and bending stiffnesses are calculated according to the source [4] based on Classical Beam Theory. The calculated ABD matrices for orthotropic laminates and sandwich plate are used for the calculation. The elastic center (bending centroid) of a cross-section is important because it tells where the neutral axis (Neutral fiber) lies. If a constant cross section beam is bent, the neutral axis is the plane on which there is no axial strain.

Coordinates of the elastic center (bending centroid) are determined as follows:

$$y_{EC} = \frac{\sum_{k=1}^{K} b_k \left(\bar{y}_k \frac{(\delta_{11})_k}{(D)_k} + \frac{(\beta_{11})_k}{(D)_k} \sin \alpha_k \right)}{\sum_{k=1}^{K} \frac{b_k (\delta_{11})_k}{(D)_k}}$$

$$x_{EC} = \frac{\sum_{k=1}^{K} b_k \left(\bar{x}_k \frac{(\delta_{11})_k}{(D)_k} - \frac{(\beta_{11})_k}{(D)_k} \cos \alpha_k \right)}{\sum_{k=1}^{K} \frac{b_k (\delta_{11})_k}{(D)_k}} \tag{4.1}$$

where $D = \alpha_{11}\delta_{11} - {\beta_{11}}^2$

x_{EC} and y_{EC} are the distance from the origin to the elastic center, whereas $\bar{x}_k$ and $\bar{y}_k$ are the distance from the element neutral plane centroid to the origin of the reference axes X_R and Y_R respectively.

On the other hand, the determination of the axial and bending stiffnesses with respect to reference axes and elastic center takes place in the form of a summation of the stiffnesses of every single elements of a cross-section.

Axial stiffness:

$$EA = \sum_{k=1}^{K} \frac{(\delta_{11})_k b_k}{(D)_k} \tag{4.2}$$

Bending stiffness:

$$EI_{yy} = \sum_{k=1}^{K} \frac{(\delta_{11})_k b_k}{(D)_k} \left(b_k {x_k}^2 + \frac{{b_k}^3 sin^2 \alpha_k}{12} \right) - \frac{2(\beta_{11})_k}{(D)_k} b_k x_k \cos\alpha_k + \frac{(\alpha_{11})_k}{(D)_k} b_k cos^2 \alpha_k$$

$$EI_{xx} = \sum_{k=1}^{K} \frac{(\delta_{11})_k b_k}{(D)_k} \left(b_k {y_k}^2 + \frac{{b_k}^3 cos^2 \alpha_k}{12} \right) + \frac{2(\beta_{11})_k}{(D)_k} b_k y_k \sin\alpha_k + \frac{(\alpha_{11})_k}{(D)_k} b_k sin^2 \alpha_k \tag{4.3}$$

$$EI_{xy} = \sum_{k=1}^{K} \frac{(\delta_{11})_k b_k}{(D)_k} \left(-b_k x_k y_k + \frac{{b_k}^3 \cos\alpha_k \sin\alpha_k}{12} \right) - \frac{(\beta_{11})_k}{(D)_k} b_k (x_k \sin\alpha_k - y_k \cos\alpha_k) + \frac{(\alpha_{11})_k}{(D)_k} b_k \cos\alpha_k \sin\alpha_k$$

where x_k and y_k are the distance of the element neutral plane centroid to the elastic center of the reference axes X_R and Y_R, respectively.

The cross-sectional stiffness of a wind turbine blade is defined about the principal axis of inertia at each blade station. Therefore, it is important to determine the section principal axis orientation and its stiffness values. It is not always the case that the principal axis is parallel and perpendicular to the chord line. The bending stiffnesses in the principal coordinate system are the maximum (EI_{max}) and minimum (EI_{min}) values for the cross-section, which are also called edgewise and flapwise bending stiffness, respectively. The principal bending stiffness are found using equation (4.5).

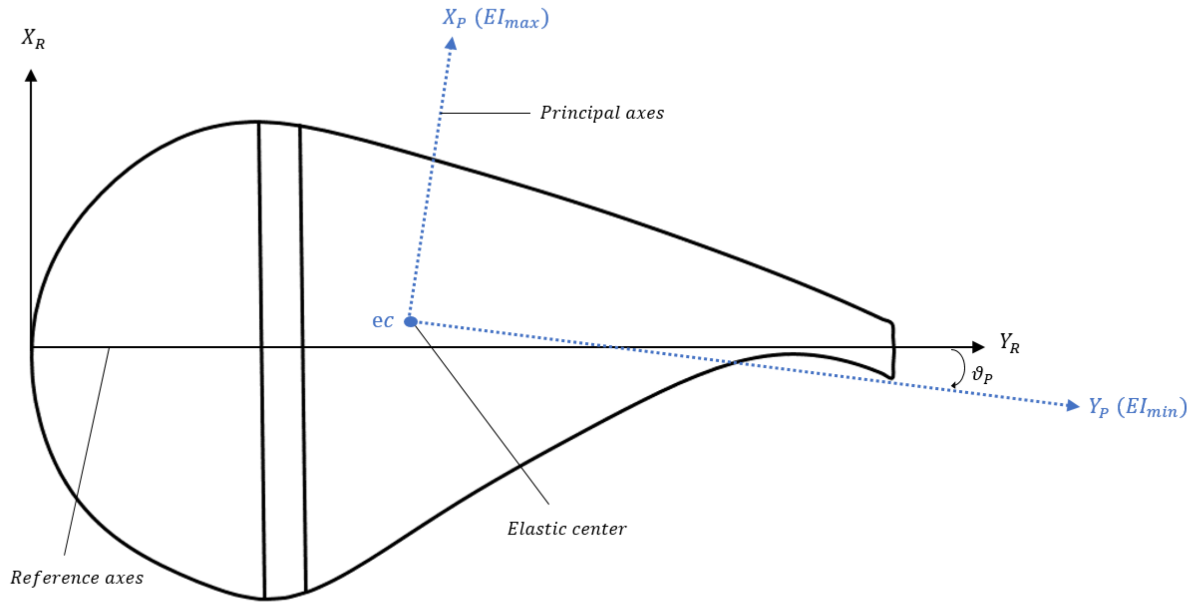

Figure 11: Coordinate systems at a blade section

Principal axis angle:

$$\vartheta_p = \frac{1}{2}\tan^{-1}\frac{-2 * EI_{xy}}{(EI_{yy} - EI_{xx})}; \rightarrow \vartheta_{p1}, \vartheta_{p2} \tag{4.4}$$

Principal stiffnesses:

$$EI_{max} = \frac{EI_{yy} + EI_{xx}}{2} + \frac{1}{2}\sqrt{(EI_{yy} - EI_{xx})^2 + 4EI_{xy}{}^2}$$

$$EI_{min} = \frac{EI_{yy} + EI_{xx}}{2} - \frac{1}{2}\sqrt{(EI_{yy} - EI_{xx})^2 + 4EI_{xy}{}^2} \tag{4.5}$$

To determine which ϑ_p value corresponds to EI_{max} and to EI_{min}:

$$EI_{max/min} = \frac{EI_{yy} + EI_{xx}}{2} + \frac{EI_{yy} - EI_{xx}}{2}cos2\vartheta_{pi} - EI_{xy}sin2\vartheta_{pi} \tag{4.6}$$

4.6 Calculation of axial strain and axial load

Wind blades are treated as transversely loaded thin-walled beams [4]. The applied transverse load, with components p_y and p_x, produces bending moments M_y, M_x, a torque T and transverse shear forces Q_y, Q_x. The bending moments M_y and M_x give rise to an axial stress

σ_ξ while the internal forces Q_y and Q_x, and T give rise to shear stress $\tau_{\xi\eta}$ in the wall of the cross section.

The force-strain relationship for an orthotropic beam is shown below. From the equation (4.7), there is no tension-bending-torsion coupling in an orthotropic beam.

$$\begin{Bmatrix} N \\ M_y \\ M_x \\ T \end{Bmatrix} = \begin{bmatrix} EA & 0 & 0 & 0 \\ 0 & EI_{yy} & EI_{xy} & 0 \\ 0 & EI_{xy} & EI_{xxx} & 0 \\ 0 & 0 & 0 & GI_t \end{bmatrix} \begin{Bmatrix} \epsilon_z \\ \dfrac{1}{\rho_y} \\ \dfrac{1}{\rho_x} \\ \vartheta \end{Bmatrix} \tag{4.7}$$

There is no applied axial load N and additionally torque T is neglected for the current development stage of this VBA model. Only resultant bending moments are taken into consideration.

In general, the strains in the wall of the element, which is treated as a plate, are calculated as follows:

$$\begin{Bmatrix} \epsilon_\xi \\ \epsilon_\eta \\ \gamma_{\xi\eta} \end{Bmatrix}_k = \begin{Bmatrix} \epsilon_\xi^0 \\ \epsilon_\eta^0 \\ \gamma_{\xi\eta}^0 \end{Bmatrix}_k + \zeta \cdot \begin{Bmatrix} \kappa_\xi \\ \kappa_\eta \\ \kappa_{\xi\eta} \end{Bmatrix}_k \tag{4.8}$$

However, in this project, only the strains in the neutral plane is calculated and the curvatures of the element are neglected, as the size of the element is insignificant compared to the size of the cross-section. Furthermore, ϵ_η is assumed zero. Hence, the simplified equation for strain calculation of the element is

$$\begin{Bmatrix} \epsilon_\xi \\ 0 \\ \gamma_{\xi\eta} \end{Bmatrix}_k = \begin{Bmatrix} \epsilon_\xi^0 \\ 0 \\ \gamma_{\xi\eta}^0 \end{Bmatrix}_k \tag{4.9}$$

axial strain ${\epsilon_\xi}^0$ and shear strain ${\gamma_{\xi\eta}}^0$ are the most important strains and therefore are calculated for current development stage of the tool. The calculation of ${\gamma_{\xi\eta}}^0$ is discussed in Chapter 4.7.

For instance, there are only resultant bending moment applied in the cross-section. Therefore, the axial strain of the element ϵ_ξ is not affected by the axial strain of the cross-section ϵ_z, which is due to axial load N, but only affected by the curvature of the blade $\frac{1}{\rho_y}$ and $\frac{1}{\rho_x}$. According to the Bernoulli-Navier hypothesis states that the axial strain varies linearly with the curvature of the blade.

$$\epsilon_{\xi k}{}^{0} = -y_k \frac{1}{\rho_x} + x_k \frac{1}{\rho_y} \tag{4.10}$$

The curvatures of the blade's axis depend on the stiffnesses of the cross-section and the magnitude of the resultant bending moments, which are the inputs for the tool. M_y is the flapwise bending moment about Y_R axis (chord line) and M_x is the edgewise bending moment about X_R axis.

$$\begin{gathered}\frac{1}{\rho_y} = \frac{EI_{xx}M_y - EI_{xy}M_x}{EI_{yy}EI_{xx} - (EI_{xy})^2} \\ \frac{1}{\rho_x} = \frac{EI_{yy}M_x - EI_{xy}M_y}{EI_{yy}EI_{xx} - (EI_{xy})^2}\end{gathered} \tag{4.11}$$

The coordinates are transformed to the principal coordinate system with the following equation.

$$\begin{bmatrix} y \\ x \end{bmatrix}_{principal} = \begin{bmatrix} cos\vartheta_p & -sin\vartheta_p \\ sin\vartheta_p & cos\vartheta_p \end{bmatrix} \cdot \begin{bmatrix} y \\ x \end{bmatrix}_{GL\ ChordCS} \tag{4.12}$$

The curvature of the blade can be also calculated using the maximum and minimum stiffness and the principal bending moments.

$$\begin{gathered}\frac{1}{\rho_y} = \frac{M_{yp}}{EI_{min}} \\ \frac{1}{\rho_x} = \frac{M_{xp}}{EI_{max}}\end{gathered} \tag{4.13}$$

According to [4], the axial strain-force relationships with the compliance matrix in the wall of an orthotropic element is as follows:

$$N_{\xi k} = \frac{(\delta_{11})_k}{(D)_k} \cdot \epsilon_{\xi k}{}^{0} \tag{4.14}$$

$$F_{\xi k} = N_{\xi k} \cdot b_k \tag{4.15}$$

where $N_{\xi k}$ is the axial force per unit length in N/mm and $F_{\xi k}$ is the axial force in N.

4.7 Calculation of shear flow and shear center

The shear stresses and shear center are calculated by assuming constant shear flow for each cell following the traditional method used for thin-walled beams made of isotropic, homogeneous materials. The results are calculated from the requirement that pure shear force load acts on the shear center causing no twist of the cross section in the chord coordinate system.

4.7.1 Boundary nodes naming definition

First, the boundary nodes of each segment must be defined to separate the profile into 3 cells (for the cross-section with 2 shear webs). The definition of the boundary nodes is performed using the node number of the corresponding node label.

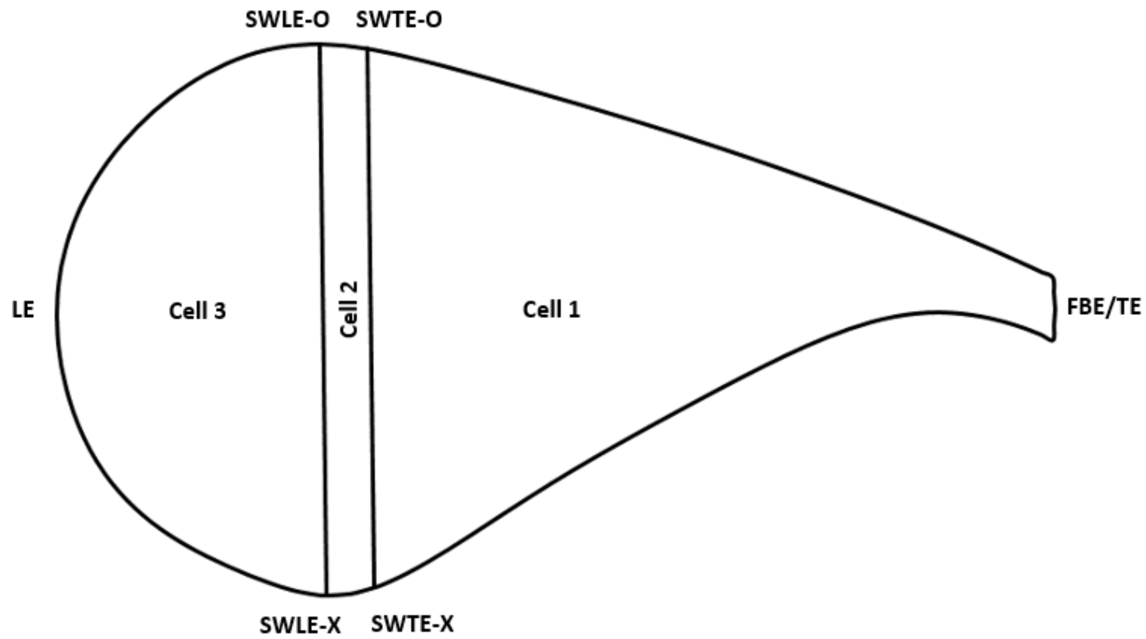

Figure 12: Boundary nodes with label

4.7.2 Shear load and shear strain

The calculation of the shear flows is done according to the source [4]. When there is no load applied in the axial direction, the blade is pure transversely loaded, the shear flows are defined as line integral over the partial derivative of the axial load with respect to ξ along the periphery coordinate system.

$$q^{op}(s) = -\int_0^s \frac{\partial N_\xi}{\partial \xi} d\eta \tag{4.16}$$

where q^{op} is the shear flow of the open section and N_ξ is the axial force (per unit length) at the neutral plane of each element, η is the coordinate along the wall and s is the distance from the free edge to the point of interest. Since the wall of the cross-section is discretized into elements and each element is flat, the integrals in equation above can be replaced by summations.

$$\int_0^s ()\, d\eta = \sum_{k=1}^{n} \int_0^{b_k} ()\, d\eta \tag{4.17}$$

where b_k is the width of the kth element and n is the total number of the element

The blade with two shear webs is equivalent to three cells closed-section beam. Each cell is cut longitudinally, thereby producing an open-section beam. According to [4], open-section shear flow of orthotropic layup is calculated by using the compliance matrices of each element, bending stiffness in the chord coordinate system attached to the elastic center of the cross-section and the applied shear forces Q_y and Q_x at the shear center. Thus, the blade does not twist.

$$\begin{aligned} q_x^{op} &= -\frac{Q_x}{EI_{xx} \cdot EI_{yy} - \left(EI_{xy}\right)^2} \cdot \left[EI_{xx} \cdot \sum_{k=0}^{K} b_k \cdot (x_k \cdot \frac{\delta_{11}}{D} - cos\, \alpha_k \cdot \frac{\beta_{11}}{D}) \right. \\ &\qquad \left. + EI_{xy} \cdot \sum_{k=0}^{K} b_k \cdot (y_k \cdot \frac{\delta_{11}}{D} + \sin \alpha_k \cdot \frac{\beta_{11}}{D}) \right] \\ q_y^{op} &= -\frac{Q_y}{EI_{xx} \cdot EI_{yy} - \left(EI_{xy}\right)^2} \cdot \left[-EI_{yy} \cdot \sum_{k=0}^{K} b_k \cdot (y_k \cdot \frac{\delta_{11}}{D} + \sin \alpha_k \cdot \frac{\beta_{11}}{D}) \right. \\ &\qquad \left. - EI_{xy} \cdot \sum_{k=0}^{K} b_k \cdot (x_k \cdot \frac{\delta_{11}}{D} - cos\, \alpha_k \cdot \frac{\beta_{11}}{D}) \right] \end{aligned} \tag{4.18}$$

$$q^{op} = q_x^{op} + q_x^{op} \tag{4.19}$$

The shear flow of the open section is determined by the sums of the shear flows of the kth element. It is summed separately along the perimeter coordinates of the contour and stops at the end of the last element of the shear webs. The shear flow of the contour element after the last element of the shear web is increased by adding up with the shear flow from the previous contour element.

$$q_{6,first}^{op} = q_{5,last}^{op} + q_{8,last}^{op}$$
$$q_{3,first}^{op} = q_{2,last}^{op} + q_{6,last}^{op} \quad (4.20)$$

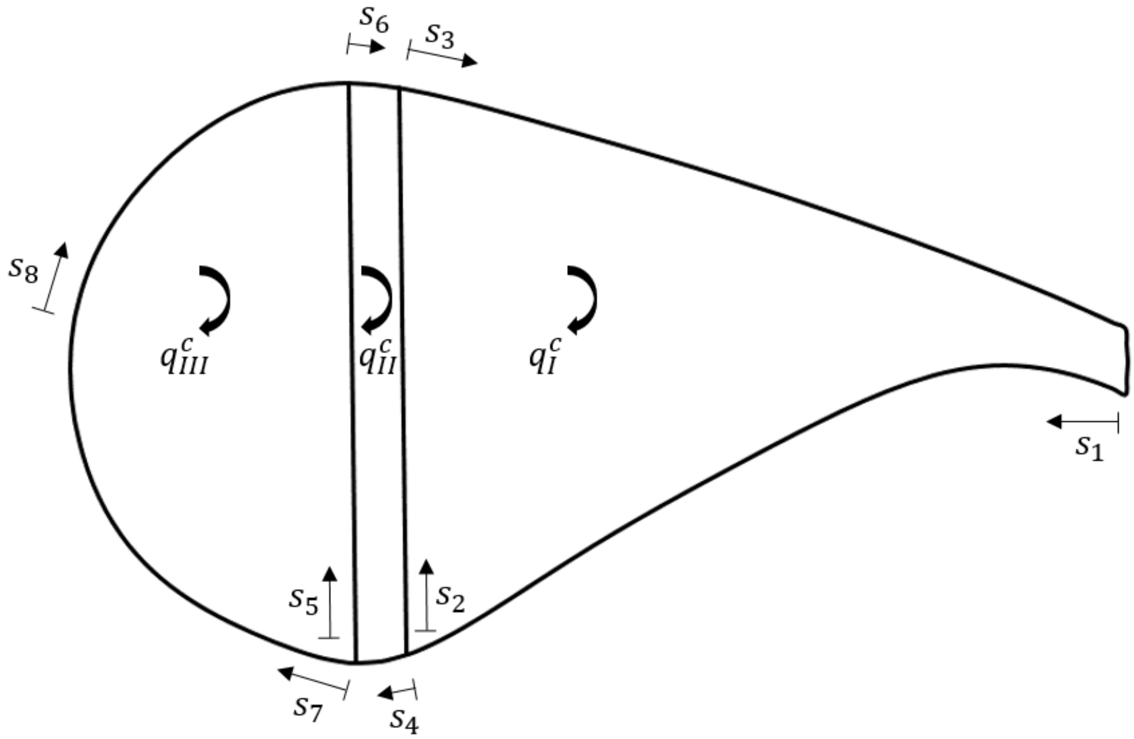

Figure 13: Cell definition of a 3-cells cross section for shear flow calculation

When the cross section is cut, the shear flows become zero at the cut which is generally not the case in the real structure. Therefore, constant shear flow ${q^c}_i$ must be introduced at the cut in order to close the gap and restore compatibility that exists in the real structure with closed cross sections. Hence, the required compatibility condition is that the shear deformation, summed around the perimeter coordinate of each cell, must be equal to zero (no twist of the cells):

$$\oint_i {\gamma_{\xi\eta}}^0 \, ds = 0; \; i = 1, 2, 3 \text{ cells} \quad (4.21)$$

${\gamma_{\xi\eta}}^0$ is the in-plane shear strain at the neutral plane of each element and it can be expressed in term of shear flow:

$$\gamma_{\xi\eta}{}^{0} = \frac{q}{Gt} = \alpha_{66} \cdot q \tag{4.22}$$

Thus,

$$\oint_i \frac{q}{Gt} ds = 0 \tag{4.23}$$

Shear flow q is the summation of open shear flow q^{op} and constant shear flow q^c

$$q = q^{op} + q^c \tag{4.24}$$

Expanding the equation above for each cell i yields the constant shear flow of each cell:

$$\begin{gathered}
\oint \frac{q^{op}{}_I}{G_I t_I} ds + q^c{}_I \oint \frac{ds}{G_I t_I} - q^c{}_{II} \int \frac{ds_2}{G_2 t_2} = 0 \\
\oint \frac{q^{op}{}_{II}}{G_{II} t_{II}} ds + q^c{}_{II} \oint \frac{ds}{G_{II} t_{II}} - q^c{}_I \int \frac{ds_2}{G_2 t_2} - q^c{}_{III} \int \frac{ds_5}{G_5 t_5} = 0 \\
\oint \frac{q^{op}{}_{III}}{G_{III} t_{III}} ds + q^c{}_{III} \oint \frac{ds}{G_{III} t_{III}} - q^c{}_{II} \int \frac{ds_5}{G_5 t_5} = 0
\end{gathered} \tag{4.25}$$

Expressing in matrix form:

$$\begin{Bmatrix} q^c{}_I \\ q^c{}_{II} \\ q^c{}_{III} \end{Bmatrix} = \begin{bmatrix} \oint \frac{ds}{G_I t_I} & -\int \frac{ds_2}{G_2 t_2} & 0 \\ -\int \frac{ds_2}{G_2 t_2} & \oint \frac{ds}{G_{II} t_{II}} & -\int \frac{ds_5}{G_5 t_5} \\ 0 & -\int \frac{ds_5}{G_5 t_5} & \oint \frac{ds}{G_{III} t_{III}} \end{bmatrix}^{-1} \cdot \begin{Bmatrix} -\oint \frac{q^{op}{}_I}{G_I t_I} ds \\ -\oint \frac{q^{op}{}_{II}}{G_{II} t_{II}} ds \\ -\oint \frac{q^{op}{}_{III}}{G_{III} t_{III}} ds \end{Bmatrix} \tag{4.26}$$

The cycle integral of the shear flow of the open section over the circumference of the respective cell is expressed in the following equations:

$$\begin{gathered}
Cell\ I\!: \quad \oint \frac{q^{op}{}_I}{G_I t_I} ds = \int \frac{q_1}{G_1 t_1} ds_1 + \int \frac{q_2}{G_2 t_2} ds_2 + \int \frac{q_3}{G_3 t_3} ds_3 \\
Cell\ II\!: \quad \oint \frac{q^{op}{}_{II}}{G_{II} t_{II}} ds = \int \frac{q_4}{G_4 t_4} ds_4 + \int \frac{q_5}{G_5 t_5} ds_5 + \int \frac{q_6}{G_6 t_6} ds_6 - \int \frac{q_2}{G_2 t_2} ds_2
\end{gathered} \tag{4.27}$$

$$Cell\ III\colon\ \oint \frac{q^{op}{}_{III}}{G_{III}t_{III}} ds = \int \frac{q_7}{G_7 t_7} ds_7 + \int \frac{q_8}{G_8 t_8} ds_8 - \int \frac{q_5}{G_5 t_5} ds_5$$

The integrals over the compliances are performed analogously, with all components of a cell being added together.

$$\oint \frac{ds}{G_I t_I} = \int \frac{ds_1}{G_1 t_1} + \int \frac{ds_2}{G_2 t_2} + \int \frac{ds_3}{G_3 t_3}$$

$$\oint \frac{ds}{G_{II} t_{II}} = \int \frac{ds_4}{G_4 t_4} + \int \frac{ds_5}{G_5 t_5} + \int \frac{ds_6}{G_6 t_6} + \int \frac{ds_2}{G_2 t_2} \tag{4.28}$$

$$\oint \frac{ds}{G_{III} t_{III}} = \int \frac{ds_7}{G_7 t_7} + \int \frac{ds_8}{G_8 t_8} + \int \frac{ds_5}{G_5 t_5}$$

The total shear flow of each element of the shear webs is

$$q_2 = q^{op}{}_2 + q^c{}_I - q^c{}_{II}$$

$$q_5 = q^{op}{}_5 + q^c{}_{II} - q^c{}_{III} \tag{4.29}$$

4.7.3 Shear center

As mentioned, shear forces acting at the shear center do not cause twist. The location of the shear center is defined by the distances x_{sc} and y_{sc} from the elastic center (bending centroid). The calculation of the shear center is done through moment equilibrium. The torque of the external force about the elastic center is equal to the torque produced by the internal shear flow:

$$x_{sc} = -\frac{1}{Q_y} \sum_{k=1}^{n} \int_0^{b_k} \left(q_y p\right)_k d\eta$$

$$y_{sc} = -\frac{1}{Q_x} \sum_{k=1}^{n} \int_0^{b_k} (q_x p)_k\, d\eta \tag{4.30}$$

where p is the distance of point at the neutral plane of each element to the elastic center

5 Structural analysis

The long-term reliability of wind turbines is very important for sustainable and economically viable wind energy utilization. Therefore, wind turbine designs must be optimized to minimize costs and maximize lifetime. This requires performance and durability characteristics of wind turbine materials, components and structures to be understood extensively. The most critical component of a wind turbine is the composite rotor blade. A rotor blade failure can have a significant impact on turbine downtime and safety. To avoid a blade failure, knowing the strength of the composite rotor blades is essential. Verification of a composite blade resistance must be checked by structural analysis. Hence, with the validated cross-sectional properties, a structural analysis model is developed in VBA to carry out laminate strength analysis, buckling analysis and bonding analysis under extreme loads analytically. The analyses presented here follows the GL 2010 guideline [5].

5.1 Partial safety factors for the material

The analyses are carried out with characteristic values which are determined from test results. Verification shall be provided in such a way that the design values of the actions S_d are smaller than the design values of the component resistances R_d, which is equal to the characteristic value R_k divided by the partial safety factor for the material γ_{Mx}:

$$S_d \leq \frac{R_k}{\gamma_{Mx}} = R_d \tag{5.1}$$

The characteristic value R_k is the 95 % survival probability with 95 % confidence value extracted from material tests. The characteristic values could be stiffness, strength, stress or strain. For buckling analysis, the characteristic stiffness values are the mean values, which are reduced by the stability partial safety factor, see equation (5.14) and (5.15).

$$\sigma_{allow} \leq \frac{R_k}{\gamma_{Mx}} \tag{5.2}$$

The partial safety factors for material γ_{Mx} are determined separately for

- The laminate failure analysis (x=a)
- The stability analysis (x=c)
- The bonding analysis (x=d)

These factors are obtained by multiplying the partial safety factor γ_{M0} with the reduction factors C_{ix}

$$\gamma_{Mx} = \gamma_{M0} \cdot \prod C_{ix} \tag{5.3}$$

For all analyses, the partial safety factor γ_{M0} is:

$$\gamma_{M0} = 1.35 \tag{5.4}$$

5.1.1 Analysis for Fiber Failure

In the short-term strength verification, γ_{Ma} is determined by multiplication of γ_{M0} with the reduction factors C_{ia}.

$$\gamma_{Ma} = \gamma_{M0} \cdot \prod C_{ia} \tag{5.5}$$

To take account of influences on the material properties, the following reduction factors are used:

C_{1a}	$= 1.35$	influence of ageing
C_{2a}	$= 1.1$	temperature effect
C_{3a}	$= 1.1$	laminate produced by prepregs, winding techniques, pultrusion or resin infusion method
C_{4a}	$= 1.0$	post-cured laminate

The partial safety factor for fiber failure analysis is:

$$\gamma_{Ma} = 1.35 \cdot 1.35 \cdot 1.1 \cdot 1.1 \cdot 1.0 = 2.205 \tag{5.6}$$

The analysis for fiber failure is carried out for areas under tensile, compressive and/or shear loading using the corresponding design strength value.

$$R_{new} = \frac{R_d}{\gamma_{Ma}} \tag{5.7}$$

5.1.2 Analysis for Inter-fiber Failure

The inter fiber failure is verified by computational means for each individual layer of laminate. To determine the permissible failure stresses and failure strains parallel and transverse to the fibers and for shear that are necessary for this verification, the mean of the tested strength values $R_{k,mean}$ is divided by the product of the partial safety factor γ_{M0} and the following reduction factor C_{IFF}:

$$\gamma_{MIFF} = \gamma_{M0} \cdot C_{IFF} \tag{5.8}$$

C_{IFF}	$= 1.25$	to account for changes of material properties due to temperature, ageing etc.

The partial safety factor for inter-fiber failure analysis is:

$$\gamma_{MIFF} = 1.35 \cdot 1.25 = 1.6875 \tag{5.9}$$

$$R_{new} = \frac{R_{k,mean}}{\gamma_{MIFF}} \tag{5.10}$$

5.1.3 Buckling Analysis

Material partial safety factors for buckling analysis have been derived from GL guidelines. The stability against buckling and wrinkling of parts under tensile, compressive and/or shear loading are verified based on the design values of material stiffnesses of the laminate. At any location, the least favorable combination of bending, compression and shear is determined and used for the verification. γ_{Mx} is determined by multiplying the partial safety factor γ_{M0} with the following reduction factors C_{ic}:

$$\gamma_{Mc} = \gamma_{M0} \cdot \prod C_{ic} \tag{5.11}$$

C_{1c}	$= 1.1$	to account for the scattering of the moduli
C_{2c}	$= 1.1$	temperature effect
C_{3c}	$= 1.25$	for linear computations
	$= 1.0$	for analytical approach

The stability partial safety factor for the laminate for analytical approach is:

$$\gamma_{Mc} = 1.35 \cdot 1.1 \cdot 1.1 \cdot 1.0 = 1.634 \tag{5.12}$$

For core, the scattering for moduli effect is dropped off. Therefore, the stability partial safety factor for the core is:

$$\gamma_{Mc} = 1.35 \cdot 1.1 \cdot 1.0 \cdot 1.0 = 1.485 \tag{5.13}$$

The design values of material stiffness of the laminate are reduced by dividing with the stability partial safety factor:

$$E_{new} = \frac{E_d}{\gamma_{Mc}} \tag{5.14}$$

$$G_{new} = \frac{G_d}{\gamma_{Mc}} \tag{5.15}$$

5.1.4 Bonding Analysis

The partial safety factor for the material γ_{Md} for bonding analysis is calculated by multiplying the partial safety factor γ_{M0} by the following reduction factors C_{id}:

$$\gamma_{Md} = \gamma_{M0} \cdot \prod C_{id} \tag{5.16}$$

C_{1d}	$= 1.5$	influence of ageing
C_{2d}	$= 1.0$	temperature effect
C_{3d}	$= 1.1$	bonding surface reproducibility
C_{4d}	$= 1.0$	post-cured bond

The partial safety factor for bonding analysis is:

$$\gamma_{Md} = 1.35 \cdot 1.5 \cdot 1.0 \cdot 1.1 \cdot 1.0 = 2.2275 \tag{5.17}$$

For the static strength verification, a characteristic shear stress $\tau_{R_k} = 7\ N/mm^2$ can be used for the case of multi-component thermosetting adhesives. No further verification is needed and this value is approved by GL, only for adhesives. This value may be assumed for bonded joints of shell and web. The allowable shear stress is therefore:

$$\tau_{allow} = \frac{\tau_{R_k}}{\gamma_{Md}} = 3.14\ \frac{N}{mm^2} \tag{5.18}$$

5.2 Laminate Failure Analysis

Deformation, strains and stresses are generally calculated using the methods of elasto-statics and for many components which are designed for maximum stiffness dimensioning might be finished with the calculation of all strains. However, for typical light-weight-constructions the knowledge of stresses and strains is not sufficient. The designing engineer has to guarantee that the component will not fail in service. This implies a failure analysis and the determination of a margin of safety which might be required for technical approval of the structure. To determine the safety against failure is the task of a strength analysis or failure analysis.

Generally, strength analysis correlates the load applied to the structure to the maximum bearable load. In the case of FRP-laminates a laminate lay- up which fulfills the requirements concerning the margin of safety results from strength analysis. The necessary input for FRP-strength analysis are the stresses of the laminae resulting from stress analysis. Usually, strength analysis is done on the level of the unidirectional UD-lamina. Therefore, the calculated strains in the (ξ, ζ, η) coordinate system have to be transformed to fiber coordinate system $(1,2,3)$ to acquire the correct strains for strength analysis. The Stiffness and Compliance Matrices of each ply j in fiber coordinate are then used to calculate the stresses of the unidirectional UD-lamina. The calculated ply stress and strain are validated with Compositor.

$$\begin{Bmatrix} \varepsilon_1 \\ \varepsilon_2 \\ \gamma_{12} \end{Bmatrix}_j = \begin{bmatrix} c^2 & s^2 & cs \\ s^2 & c^2 & -cs \\ -2cs & 2cs & c^2 - s^2 \end{bmatrix}_j \begin{Bmatrix} \varepsilon_\xi \\ 0 \\ \gamma_{\xi\eta} \end{Bmatrix}_j \tag{5.19}$$

$$s = \sin(-\alpha); c = cos(-\alpha)$$

$$\begin{Bmatrix} \sigma_1 \\ \sigma_2 \\ \tau_{12} \end{Bmatrix}_j = \begin{bmatrix} Q_{11} & Q_{12} & 0 \\ Q_{21} & Q_{22} & 0 \\ 0 & 0 & Q_{66} \end{bmatrix}_j \begin{Bmatrix} \varepsilon_1 \\ \varepsilon_2 \\ \gamma_{12} \end{Bmatrix}_j \tag{5.20}$$

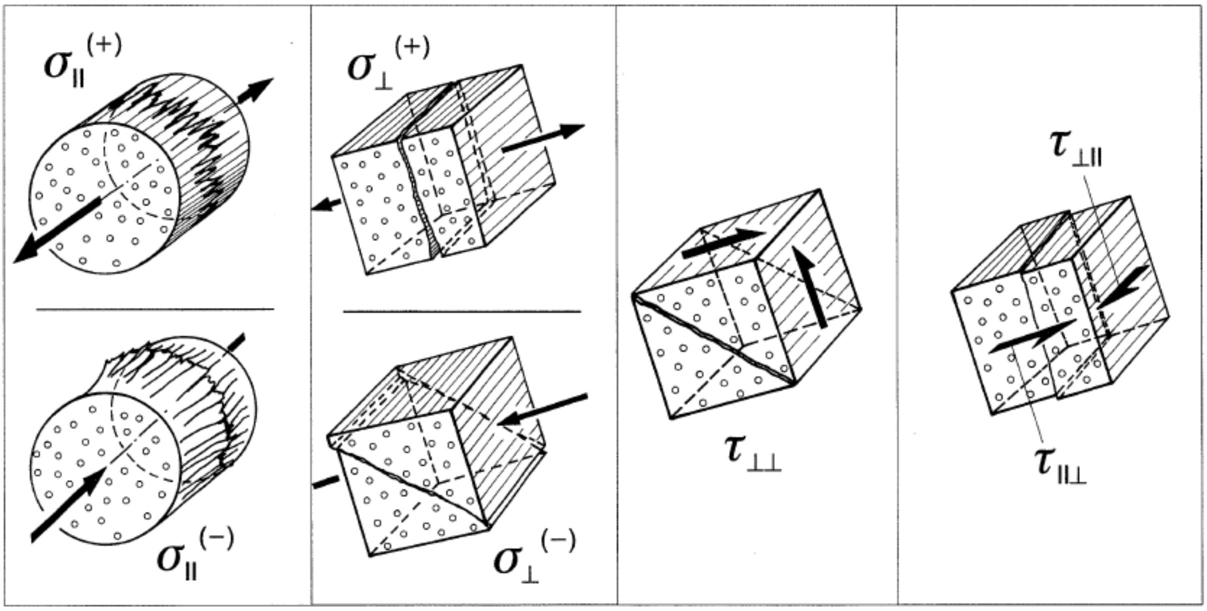

Figure 14: The basic stressings of a UD-composite element [6]

$\sigma_{\parallel}(\sigma_1)$ stressing is responsible for fiber failure (FF), while $\sigma_{\perp}(\sigma_2)$, $\tau_{\perp\perp}(\tau_{23})$, $\tau_{\parallel\perp}(\tau_{12})$ stressings cause inter-fiber failure (IFF).

5.2.1 Fiber Failure Criteria

Puck failure criteria [12] are one the most commonly used and well-established criteria for the assessment of composite laminate strength. Puck's failure criteria are implemented for the evaluation of stress results of unidirectional ply. Woven fabric like biaxal and triaxal weave are assumed to be formed by 2 and 3 UD layers, respectively, for a simplified laminate analysis. Fracture criterion is being formulated with the stress exposure $f_{E,FF}$:

$$f_{E,FF}^{t} = \frac{\sigma_1}{R_{\parallel}^{t}} \qquad for\ \sigma_1 > 0 \tag{5.21}$$

$$f_{E,FF}^{c} = \frac{\sigma_1}{-R_{\parallel}^{c}} \qquad for\ \sigma_1 < 0 \tag{5.22}$$

where $f_{E,FF}^{t}$ and $f_{E,FF}^{c}$ are stress exposures for fiber failure under tension and compression loading cases. σ_1 is the stress value in fiber direction, $R_{\parallel}^{t}$ and $R_{\parallel}^{c}$ are tensile and compressive strengths in fiber direction, respectively. For a preliminary analysis, this simple fracture criterion is sufficient.

5.2.2 Inter-fiber Failure Criteria

Figure above shows the fracture curve (σ_2, τ_{21}) in the section plane where $\sigma_1 = 0$ and the three independent fracture conditions for the fracture modes A, B and C. The intersection points with the axes are given by the tensile strength $R_{\perp}^{t}$, compressive strength $R_{\perp}^{c}$ and the shear strength $R_{\perp\parallel}$. σ_2 is the stress value in the transverse fiber direction and shear stress τ_{21}.

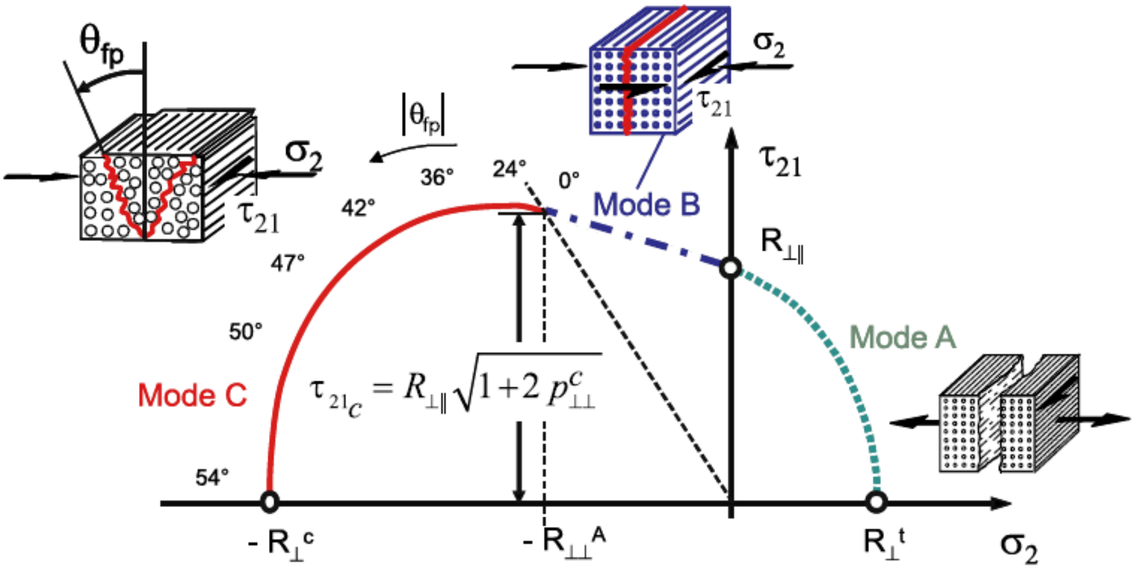

Figure 15: Fracture curve (σ_2, τ_{21}) [6]

Below are the equations for fracture modes A, B and C. Mode A is caused by tensile and shear stresses. Modes B occurs under compressive and shear stresses. Mode C is a dangerous failure mode in compressive shearing which may lead to ultimate failure. If the value of failure exposure ($f_{E,IFF}$) exceeds 1, failure initiation occurs.

Mode A: $\theta_{fp} = 0°$; $\sigma_2 \geq 0$

$$f_{E,IFF} = \sqrt{\left(\frac{\tau_{21}}{R_{\perp\parallel}}\right)^2 + \left(1 - p_{\perp\parallel}^{t}\frac{R_{\perp}^{t}}{R_{\perp\parallel}}\right)^2 \cdot \left(\frac{\sigma_2}{R_{\perp}^{t}}\right)^2} + p_{\perp\parallel}^{t}\frac{\sigma_2}{R_{\perp\parallel}} \tag{5.23}$$

Mode B: $\theta_{fp} = 0°$; $\sigma_2 < 0$; $0 \leq \left|\frac{\sigma_2}{\tau_{21}}\right| \leq \frac{R_{\perp\perp}^{A}}{|\tau_{21c}|}$

$$f_{E,IFF} = \frac{1}{R_{\perp\parallel}} \cdot \left(\sqrt{\tau_{21}{}^2 + \left(p_{\perp\parallel}^{c}\sigma_2\right)^2} + p_{\perp\parallel}^{c}\sigma_2\right) \tag{5.24}$$

Mode C: $cos\theta_{fp} = \sqrt{\frac{R_{\perp\perp}^{A}}{-\sigma_2}}$; $\sigma_2 < 0$; $0 \leq \left|\frac{\tau_{21}}{\sigma_2}\right| \leq \frac{|\tau_{21c}|}{R_{\perp\perp}^{A}}$

$$f_{E,IFF} = \left[\left(\frac{\tau_{21}}{2(1 + p_{\perp\perp}^{c}) \cdot R_{\perp\parallel}}\right)^2 + \left(\frac{\sigma_2}{R_{\perp}^{c}}\right)^2\right] \cdot \frac{R_{\perp}^{c}}{\sigma_2} \tag{5.25}$$

$p^t_{\perp\parallel}$, $p^c_{\perp\parallel}$ and $p^c_{\perp\perp}$ represent inclination parameters that control the shape of the failure envelope. The value of the parameter $p^t_{\perp\parallel}$ and $p^c_{\perp\parallel}$ are taken from GL-Guideline, where $p^c_{\perp\parallel} = 0.25$ and $p^t_{\perp\parallel} = 0.3$. $R^A_{\perp\perp}$ is the resistance of the action plane against its fracture due to transverse shear stressing $\tau_{\perp\perp}$ acting in that plane.

$$R^A_{\perp\perp} = \frac{R_{\perp\parallel}}{2p^c_{\perp\parallel}}\left(\sqrt{1 + 2p^c_{\perp\parallel}\frac{R^c_{\perp}}{R_{\perp\parallel}}} - 1\right) \tag{5.26}$$

$$p^c_{\perp\perp} = p^c_{\perp\parallel}\frac{R^A_{\perp\perp}}{R_{\perp\parallel}} \tag{5.27}$$

$$\tau_{21_c} = R_{\perp\parallel}\sqrt{1 + 2p^c_{\perp\perp}} \tag{5.28}$$

5.3 Stability Analysis (Buckling)

Buckling is an instability that leads to structural failure. Buckling refers to the loss of stability of a component and is usually independent of material strength. This loss of stability usually occurs within the elastic range of the material. The load at which buckling occurs depends on the stiffness of a component and the boundary conditions, not upon the strength of its materials. Buckling strength is generally increased by increasing the core thickness in sandwich panels. Increasing the core thickness will lead to the increase of the bending moment of inertia, which in turn increases the stiffness of the sandwich structure and hence, suppresses buckling. It must be understood that core optimization is a natural part of the blade design optimization as it affects weight, cost and structural performance.

Local buckling of orthotropic rotor blade that arise due to axial compressive stresses introduced by bending moments and shear stresses introduced by shear forces. Therefore, a buckling analysis need to be implemented to predict the critical buckling stresses. In this project, local buckling analyses of the rotor blade will be carried out are generally performed by modeling the wall segments of the rotor blade as long plates or shells and by assuming that edges common to two or more plates remain straight.

The structure is divided into individual sections, which are assumed to be infinitely long. There are shear webs, main girders, tail girders, shell panels at pressure and suction side. Die disadvantages of splitting the structure into individual sections are that fixed condition is uncertain and no coupling or interaction is considered. However, this method is efficient and sufficient accurate to perform local buckling analysis of the rotor blade.

Effective mechanical properties of the laminate and sandwich structure are computed using CLT, and the structure's young modulus, thickness, curvature and width all contribute to the prediction of the critical buckling stresses. The buckling criteria, S_G is defined by equation (5.45).

The approach for calculating the critical stress at which local buckling occurs is illustrated in Table 9. The buckling criterion are applied to each of the individual sections of the rotor blade under different extreme loading conditions. For a conservative buckling analysis, the edges of each section are assumed to be parallel to the Z-axis are simply supported, and the edges perpendicular to the Z-axis are free. In reality, all edges would have a finite restraint to rotation due to the adjoining panels, and the buckling resistance would be somewhat enhanced. Furthermore, the nonlinear geometric and inelastic effects are ignored in order to keep the analysis simple [7]. The following buckling analyses are available in the analytical tool.

Structural part	**Material**	**Geometry**	**Loading condition**
Shear webs	Isotropic	Laminate or Sandwich plate	Bending, shear
Shell panels	Isotropic	Sandwich shell	Compression, shear
Leading and trailing edges	Isotropic	Laminate Shell	Compression, shear
Spar caps and tail caps	Anisotropic	Laminate shell	Compression, shear

Table 9: Recommended buckling analysis conditions for different part of the section

When the structure is a shell, the shell curvature must be taken into account as well as the respective buckling coefficients needs to be corrected for the pressure and shear load. With the aid of the shell width and the middle shell radius r, the curvature parameter Ω is determined for isotropic and anisotropic structure separately.

$$r = \frac{h}{2} + \frac{b^2}{8h} \tag{5.29}$$

$$\Omega_{isotropic\_laminate} = \frac{12 \cdot (1 - \nu^2) b^4}{r^2 t^2} \tag{5.30}$$

$$\Omega_{isotropic\_sandwich} = \frac{4 \cdot (1 - \nu^2) b^4}{r^2 d^2} \tag{5.31}$$

$$\Omega_{anisotropic} = \frac{b^4}{r^2} \sqrt{\frac{A_{11} A_{22}}{D_{11} D_{22}}} \tag{5.32}$$

where b is the width, h is the height and t is the thickness of the shell

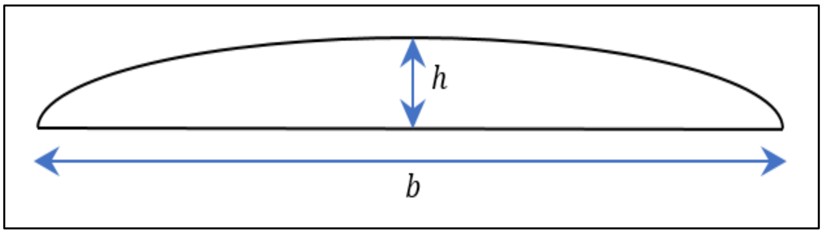

Figure 16: Parameter of a shell

5.3.1 Isotropic buckling condition

In all structural parts, which consist predominantly of $\pm 45°$ laminate (Shear webs and shell panels), the stiffness parameter is bigger than 1 and the verification can be carry out for isotropic condition. The poisson's ratio of the structure is approximately 0.3. Therefore, the buckling coefficient values for isotropic structural are suitable.

Poisson's ratio:

$$\nu = \frac{D_{12}}{D_{12} + 2D_{66}} \approx 0.3 \tag{5.33}$$

Stiffness parameter:

$$\eta = \frac{D_{12} + 2D_{66}}{\sqrt{D_{11} D_{22}}} > 1 \tag{5.34}$$

The critical stresses for an isotropic structure are calculated as follows:

Axial stress:

$$\sigma_{c\ cr} = k_d \cdot E_w \cdot \left(\frac{t}{b}\right)^2 \tag{5.35}$$

Bending stress:

$$\sigma_{b\ cr} = k_b \cdot E_w \cdot \left(\frac{t}{b}\right)^2 \tag{5.36}$$

Shear stress:

$$\tau_{cr} = k_\tau \cdot E_w \cdot \left(\frac{t}{b}\right)^2 \tag{5.37}$$

The critical loads are then calculated from the critical stress by multiplying with the thickness of the structure.

Axial or bending load:

$$p_{cr} = \sigma_{cr} \cdot t \tag{5.38}$$

Shear load:

$$q_{cr} = \tau_{cr} \cdot t \tag{5.39}$$

In order to determine the buckling coefficient k_i from the diagrams for isotropic plate and shell structure, Figure 17 and Figure 21 ($\nu = 0.3$), an effective E-Modulus need to be calculated for an anisotropic structure, especially for those consist of multiple layers with different engineering constants, assuming that the material volume is evenly distributed over the thickness. For a sandwich structure, the bending stiffness is therefore also reduced depending on the skins thickness relationship [8].

$$E_w = \sqrt{D_{11} \cdot D_{22}} \cdot \frac{12(1 - 0.3^2)}{t^3} \tag{5.40}$$

5.3.2 Anisotropic buckling condition

Isotropic buckling condition is not suitable for those anisotropic structure, like main and tail girders, which consist of mainly UD-lamina. The critical loads for orthotropic structure are calculated using equation (5.41) and (5.42). Buckling coefficient k is taken from the buckling analysis diagrams for anisotropic structure, Figure 18 and Figure 22.

Axial load:

$$p_{cr} = k \cdot \left(\frac{\pi}{b}\right)^2 \cdot \sqrt{D_{11} \cdot D_{22}} \tag{5.41}$$

Shear load:

$$q_{cr} = k \cdot \left(\frac{\pi}{b}\right)^2 \cdot \sqrt[4]{D_{11} \cdot {D_{22}}^3} \tag{5.42}$$

A long plate structure of constant thickness is considered, whose length is large compared with its width.

Effective length-to-width ratio α_ω:

$$\alpha_\omega = \frac{a}{b} \cdot \sqrt[4]{\frac{D_{22}}{D_{11}}} = \infty \tag{5.43}$$

Effective width-to-length ratio β_ω:

$$\beta_\omega = \frac{b}{a} \cdot \sqrt[4]{\frac{D_{11}}{D_{22}}} = 0 \tag{5.44}$$

Finally, the buckling criteria S_G is estimated with the combination of loads:

$$S_G = \frac{1}{\frac{p_c}{p_{c\,cr}} + \left(\frac{p_b}{p_{b\,cr}}\right)^2 + \left(\frac{q}{q_{cr}}\right)^2} \geq 1 \tag{5.45}$$

For a shell structure, it is important to calculate differently for isotropic laminate, isotropic sandwich and anisotropic laminate structure, due to the complexity of determining the curvature parameter of the shells using equation (5.30), (5.31) and (5.32). If the shell is bent harder (with strong curvature), several buckling waves appear over its width b in the arc direction. The influence of the width is not significant anymore (as r is not >> b anymore), which leads to the linear increase of buckling coefficient k over $\sqrt{\Omega}$, see Figure 18. The buckling coefficient can be applied for the full shell as well as the partial shell. When the height of the shell is very small ($r \rightarrow \infty$), the horizontal axis value is near to 0. The graph of a plate is used ($\alpha_\omega = \infty$). The long shell behaves like a long plate.

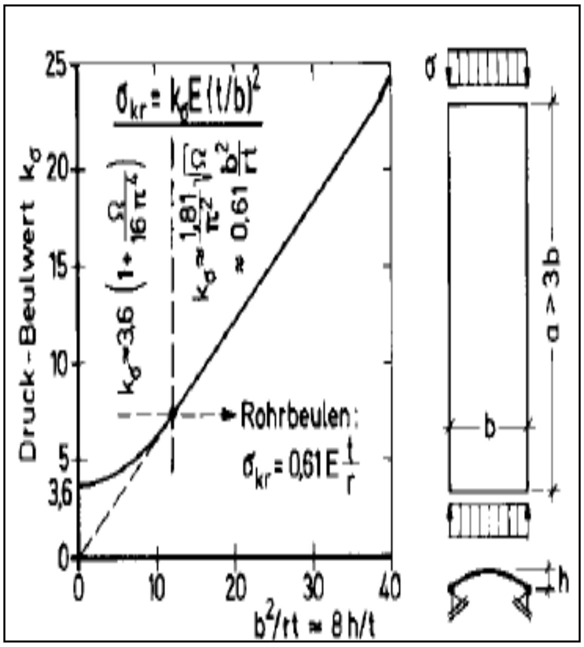

Figure 17: Isotropic laminate shell; simple supported; compressive loading [9]

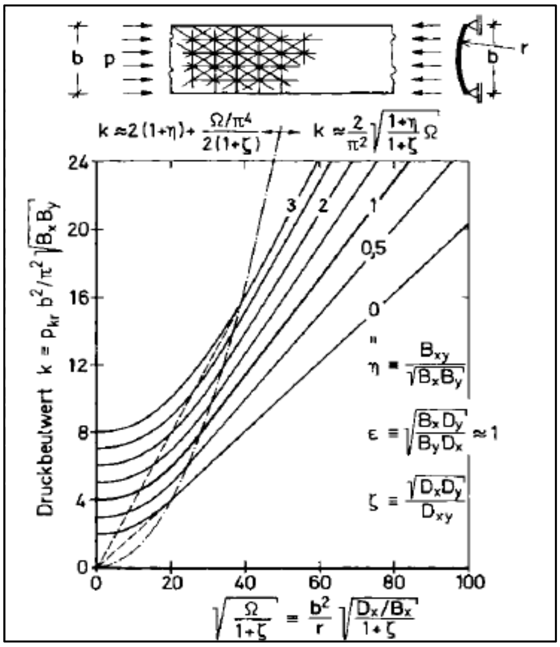

Figure 18: Orthotropic laminate shell; simple supported; compressive loading [9]

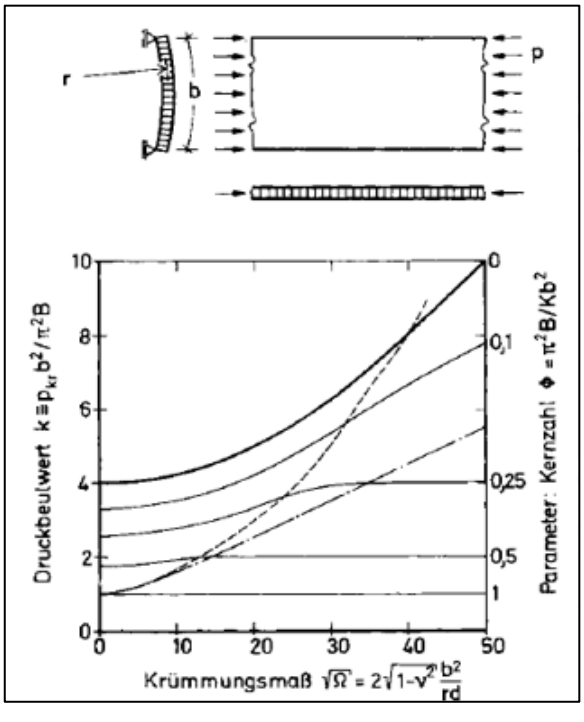

Figure 19: : Isotropic sandwich shell; simple supported; compressive loading [9]

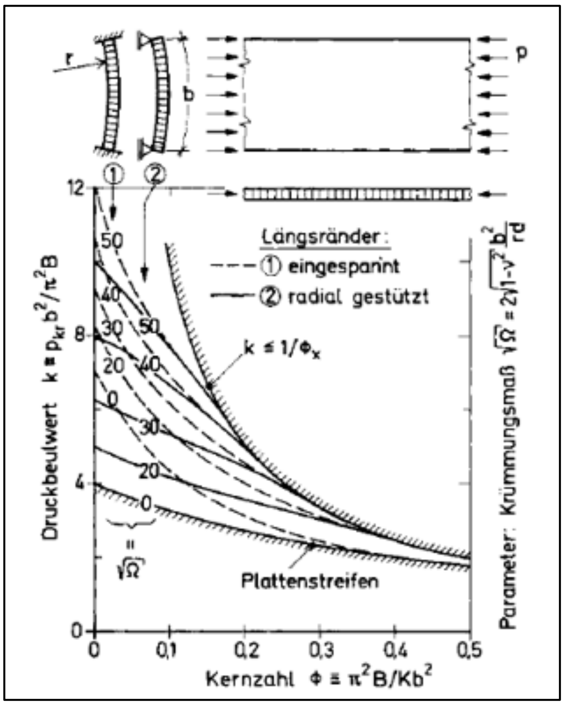

Figure 20: Isotropic sandwich shell; simple supported and fixed supported; compressive loading [9]

Figure 21 and Figure 22 are suitable for both laminate and sandwich plate, because no curvature of the structure needs to be calculated separately.

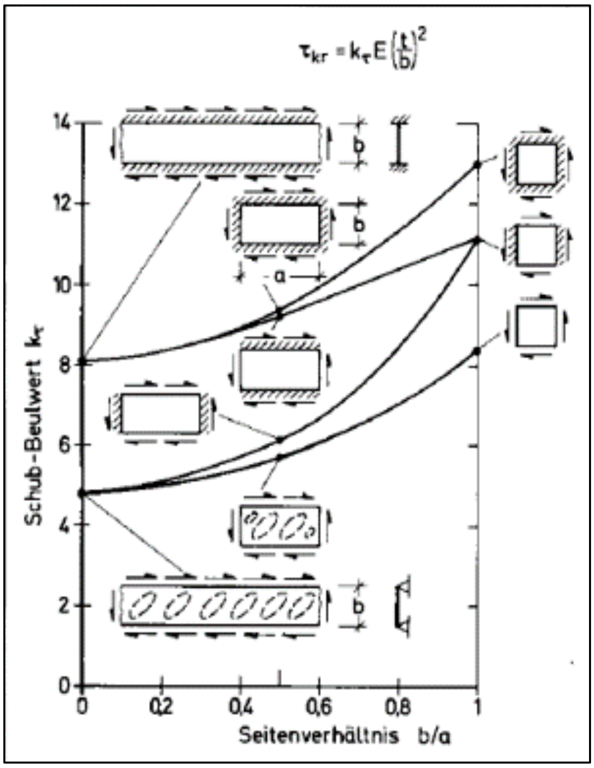

Figure 21: Isotropic plate; simple supported; shear loading [9]

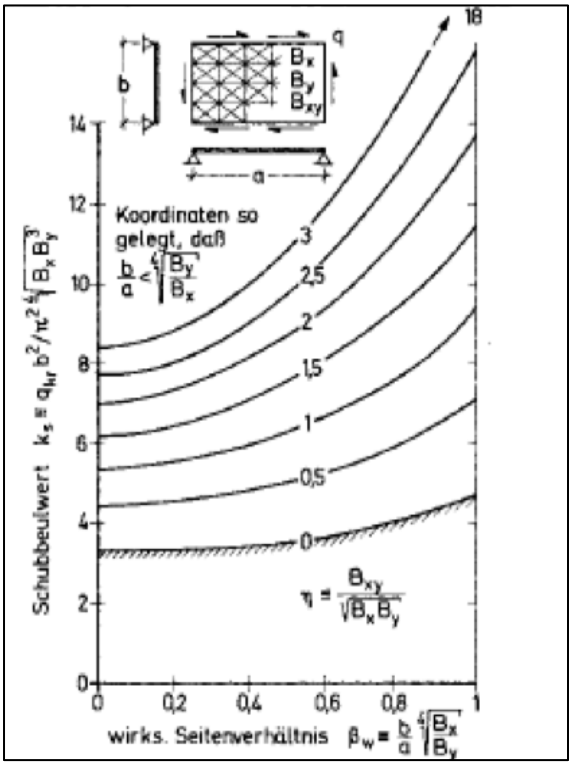

Figure 22: Orthotropic plate; simple supported; shear loading [9]

5.3.3 Deviation of isotropic buckling analysis for composite structure

As mentioned, for composite structure, which consist predominantly of $\pm 45°$ laminate, buckling analysis can be carried under isotropic condition. An analysis is performed to show the deviation in the critical buckling loads of a same structure calculated under isotropic and anisotropic condition.

When the stiffness parameter η is significantly bigger than 1, the calculation with isotropic condition is slightly too conservative. This will be the case that the biax-layer has different value of E_x and E_y. The bigger the difference of η value from 1, the bigger the error assuming an anisotropic structure as isotropic, as the k_σ value from the isotropic graph is smaller. Taking the boundary condition of simple support and loading condition of a shell structure as example, see Figure 17 and Figure 18, the only η-curve in Figure 17 for isotropic shell ($\eta = 1$) shows that $k_{\sigma min} = 3{,}62 \rightarrow \; k_{min} = 4$, where $\nu = 0.3$

$$k = \frac{12(1-\nu^2)}{\pi^2} k_\sigma \tag{5.46}$$

which is smaller than the case $\eta > 1$ in Figure 18. The k_{min} value of the η-curve Figure 18 for anisotropic plate under constant axial load and simply supported is higher, when η value is higher. The difference in the value of critical buckling load under isotropic and anisotropic condition is shown in Chapter 6.5.4.

5.4 Bonding Analysis

The verification for bonding joints is based on the assumption that the shear stress on the bonded joints must be transferred through the adhesive layer. It is assumed that the shear stress is transferred linearly over the entire thickness of the adhesive layer.

The force to be transferred across the adhesive layer is:

$$\mathrm{F} = \mathrm{q} \cdot \mathrm{L} \tag{5.47}$$

The shear stress in the bonded joints is calculated by dividing the force with the area of the adhesive layer

$$\tau_{bond} = \frac{\mathrm{F}}{b \cdot L} = \frac{q}{b} \tag{5.48}$$

$$\tau_{bond} = \frac{\mathrm{F}}{b \cdot L} = \frac{q}{b} \tag{5.49}$$

According to GL Guideline 2010 [5], the shear stress in the bonded joints should be exceed the allowable shear stress, which is calculated in Chapter 5.1.4

$$\tau_{bond} \leq \frac{\tau_{R_k}}{\gamma_{Md}}$$

And therefore, the minimum width of the adhesive layer is determined, see Figure 44.

$$b_{min} = \frac{\gamma_{Md}}{\tau_{R_k}} \cdot q \tag{5.50}$$

6 Validation with finite-element method

In order to investigate the correctness of the analytical tool, the results are validated with finite element method.

6.1 FE Model Setup

A constant cross-section of composite beam is used to validate the analytical VBA code for the cross-sectional properties' calculation. The FE model is made up of SHELL 181 element in ANSYS Workbench. This is a four-node element with six degrees of freedom at each node: three translation and three rotational Degree of Freedom (DOF) in and about x, y and z directions respectively. This type of element is used for analyzing thin to moderately thick shell structures. The element size is 100 mm in this model, which is fine enough for linear applications. In order to define different stack-up of the layers on different part of the geometry, the geometry is made up of several faces.

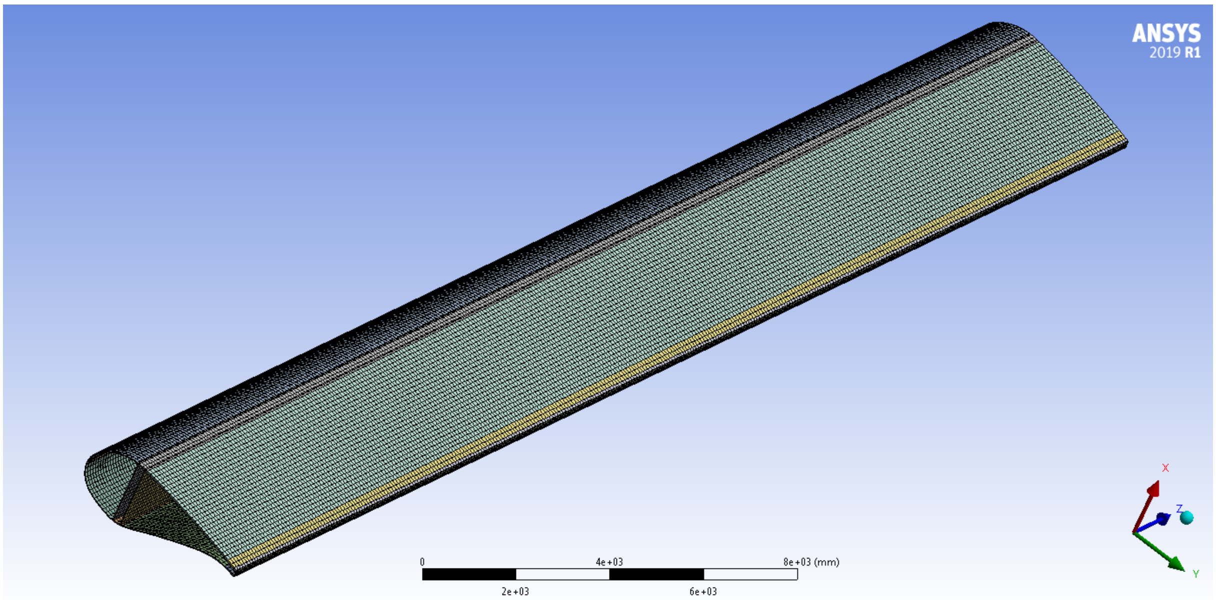

Figure 23: Meshed geometry of a constant cross section blade with several faces

With the help of ANSYS Composite PrepPost (ACP), the composite design of the blade is built up. Orthotropic mechanical properties of each layer are defined by 9 constants:

- Young's Modulus in x, y, z-direction (EX, EY, EZ)
- Shear Modulus in the xy, yz, xz-plane (GXY, GYZ, GXZ)
- Poisons Ratio in the xy, yz, and xz-plane (PRXY, PRYZ, PRXZ)

The composite layups is defined separately for each segment of the blade, as well as the fiber directions and orientations. The layup direction is towards inside of the cross-section. In the Figure 24 the section cut shows the lay-up definition on the section plane. The leading edge shell panels are with relatively thinner core compared to trailing edge shell panels. Tail girders consist of the largest amount of UD layers for higher edgewise stiffness of the blade.

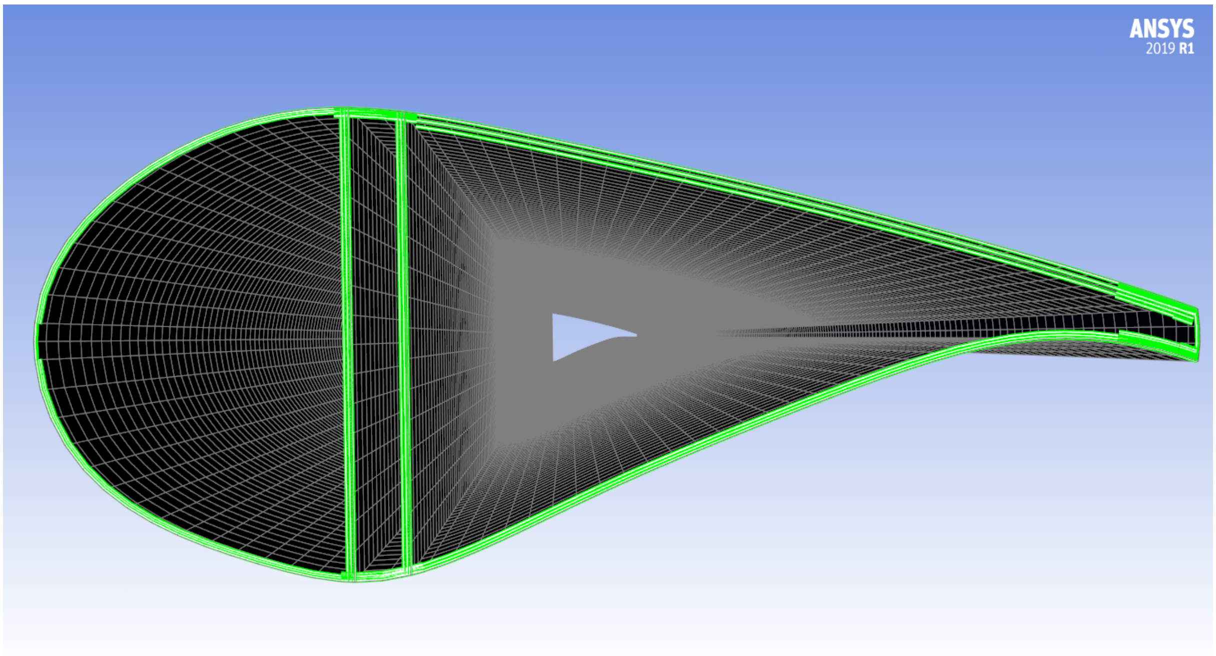

Figure 24: Section cut of the blade

Static structural analysis is then performed. In the end, the stresses/strains in the layer is evaluated and compared to the VBA code output.

6.2 Determining cross-sectional properties using FE Model

The bending stiffness of the FEM-Model is determined based on 1D Beam theory. The boundary and load condition are as follows: The left end of the beam is free, and the right end is fixed. Only bending moment is applied. By getting the maximum deflection of the blade in x and y direction, respectively, the bending stiffnesses are obtained.

$$EI_{xx} = \frac{M_x L^2}{2u_y} \tag{6.1}$$

$$EI_{yy} = \frac{M_y L^2}{2u_x} \tag{6.2}$$

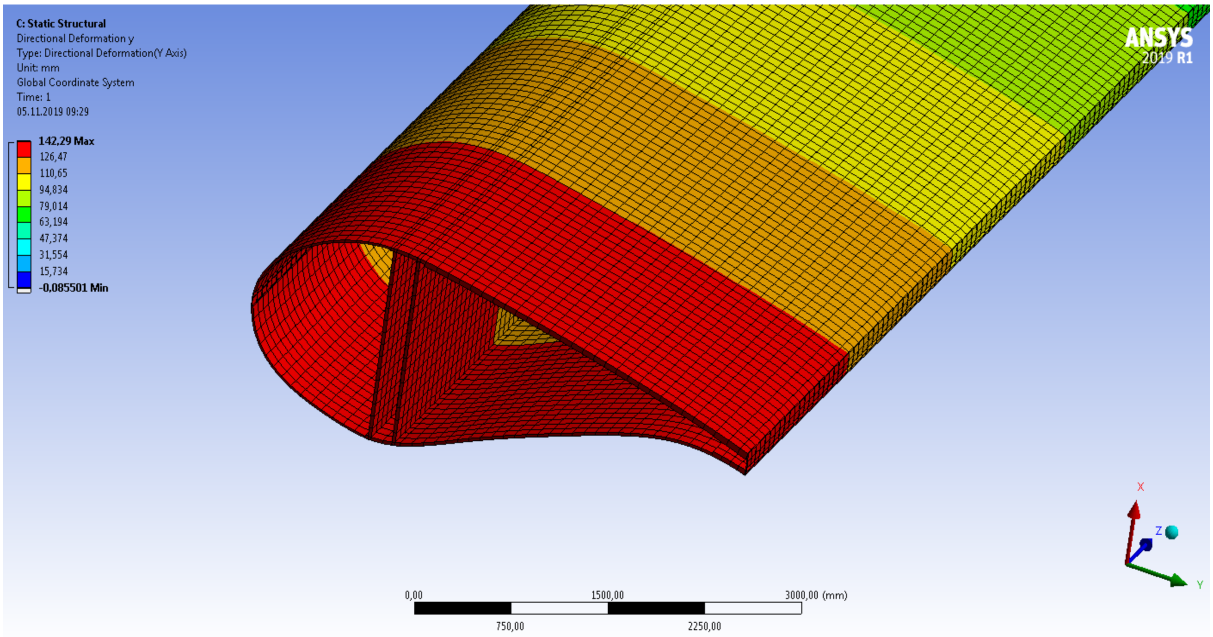

Figure 25: Maximum deflection uy due to Mx

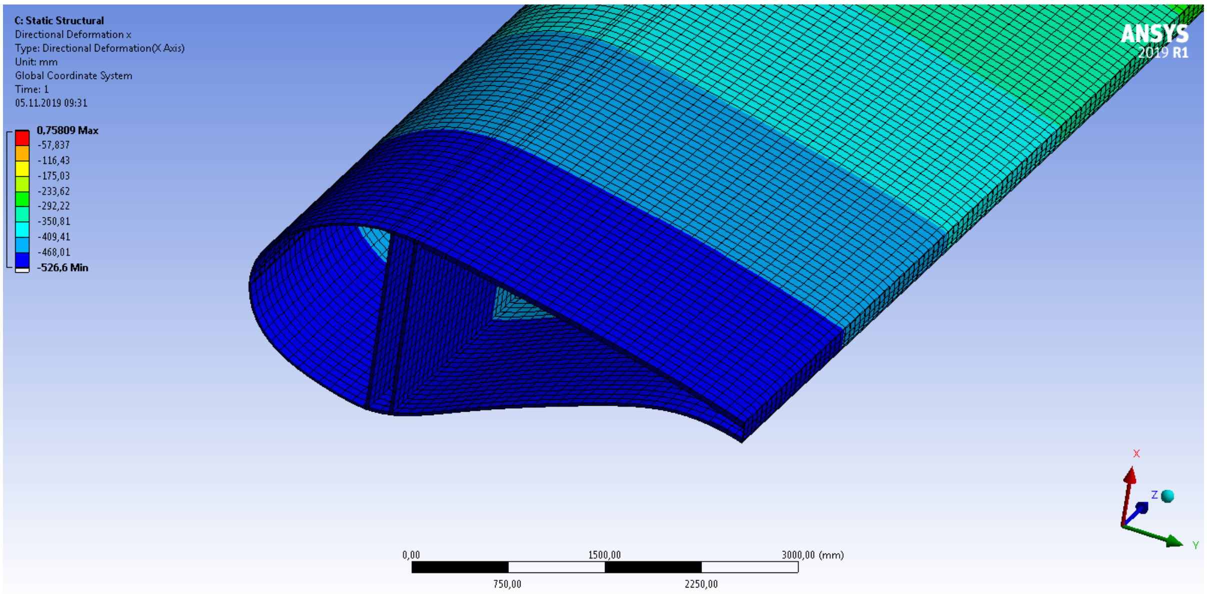

Figure 26: Maximum deflection ux due to My

On the other hand, the elastic center is determined by extracting the axial displacement at the origin due to pure bending moment. The influence of the flap-edge stiffness EI_{xy} is negligible as the principal axis angle is very small. x_{EC} and y_{EC} are the distance from the origin to the elastic center.

$$y_{EC} = -\frac{u_{z_{origin}}}{L} \cdot \frac{EI_{xx}}{M_x} \tag{6.3}$$

$$x_{EC} = \frac{u_{z_{origin}}}{L} \cdot \frac{EI_{yy}}{M_y} \tag{6.4}$$

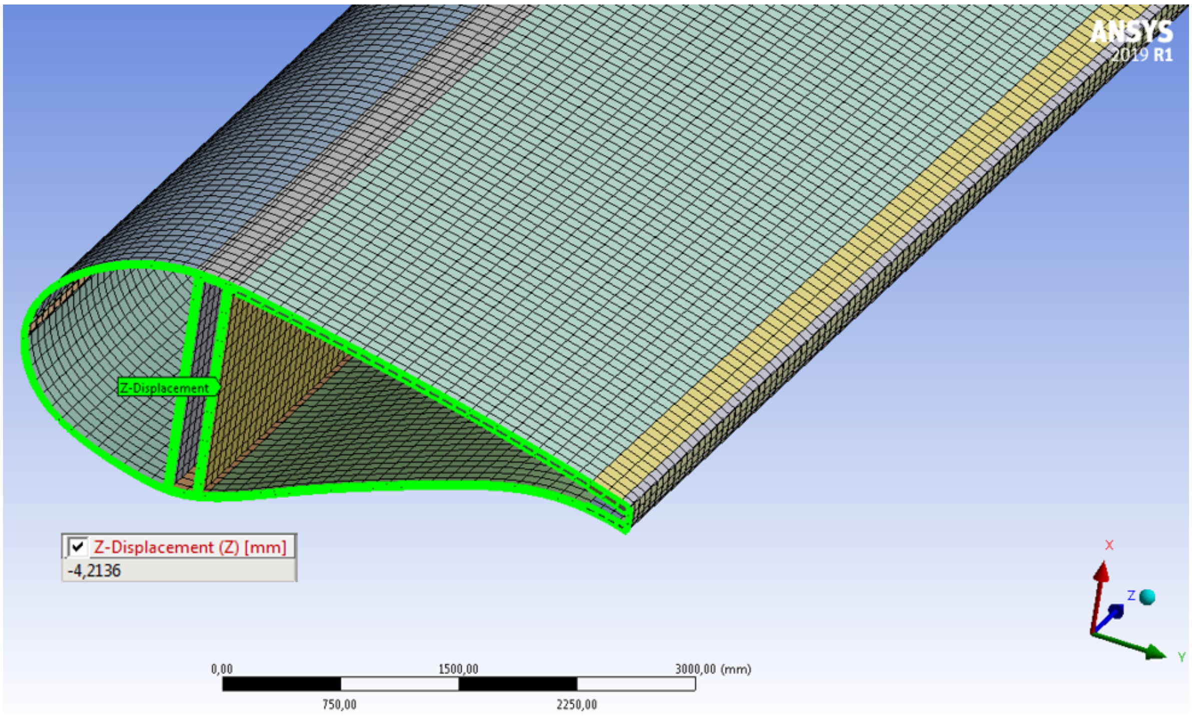

Figure 27: Axial displacement at the origin due to bending moment Mx

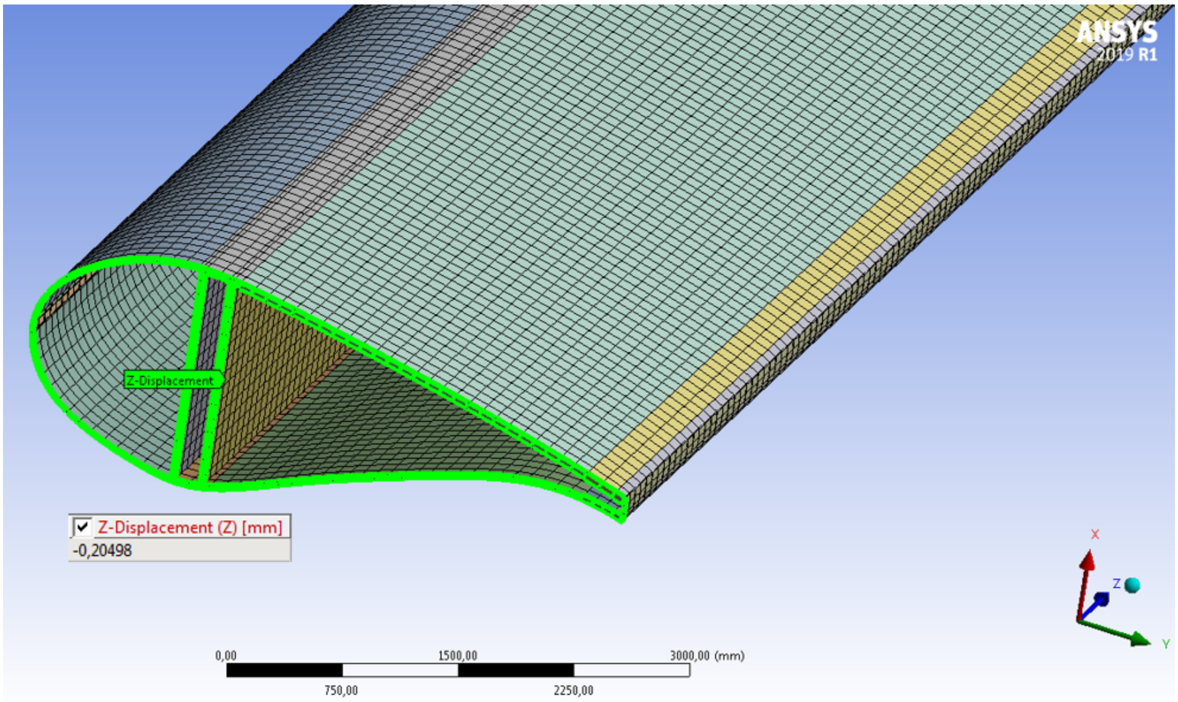

Figure 28: Axial displacement at the origin due to bending moment My

After finding the elastic center, an axial force is applied at the elastic center to determine the axial stiffness of the cross-section. The axial displacement is obtained from the FE Model.

$$EA = \frac{F_z \cdot L}{u_{z_{EC}}} \tag{6.5}$$

As mentioned, shear forces acting at the shear center do not cause twist. Therefore, the shear forces Q_x and Q_y are adjusted accordingly. The location of the shear center is obtained when the twist angle about z-axis is nearly zero, for both loading condition.

6.3 Axial Strain and Shear Stress obtained from FE Model

Bending moments $M_x = -3.55e9\ Nmm$ and $M_y = -7.38e9\ Nmm$ are applied at cross section is study the axial strain distribution of the wall of the cross section.

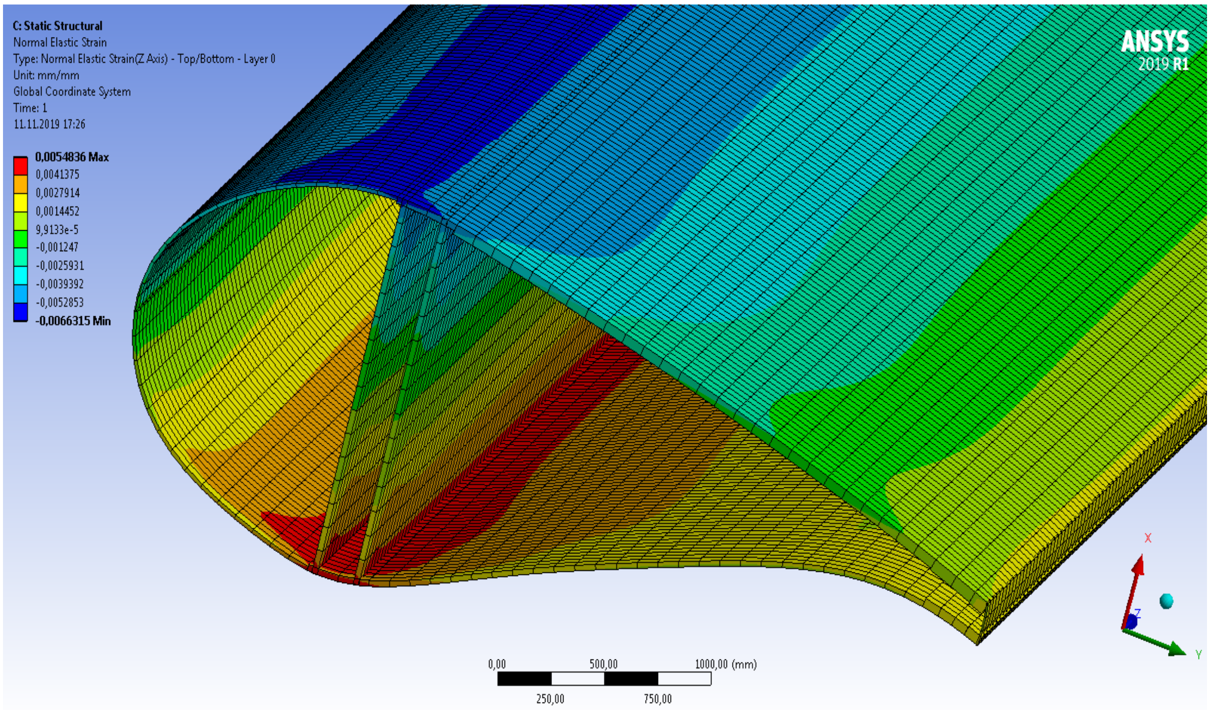

Figure 29: Axial strain of the cross section due to bending moments Mx and My

Shear force $Q_x = 1e5\ N$ is applied at the shear center of cross section is study the shear stress distribution of the wall of the cross section. It can be seen in Figure 30 and Figure 31 that the shear stress in the core layer is much lower than the shear stress in the biax skin layer as due to lower stiffness of the core.

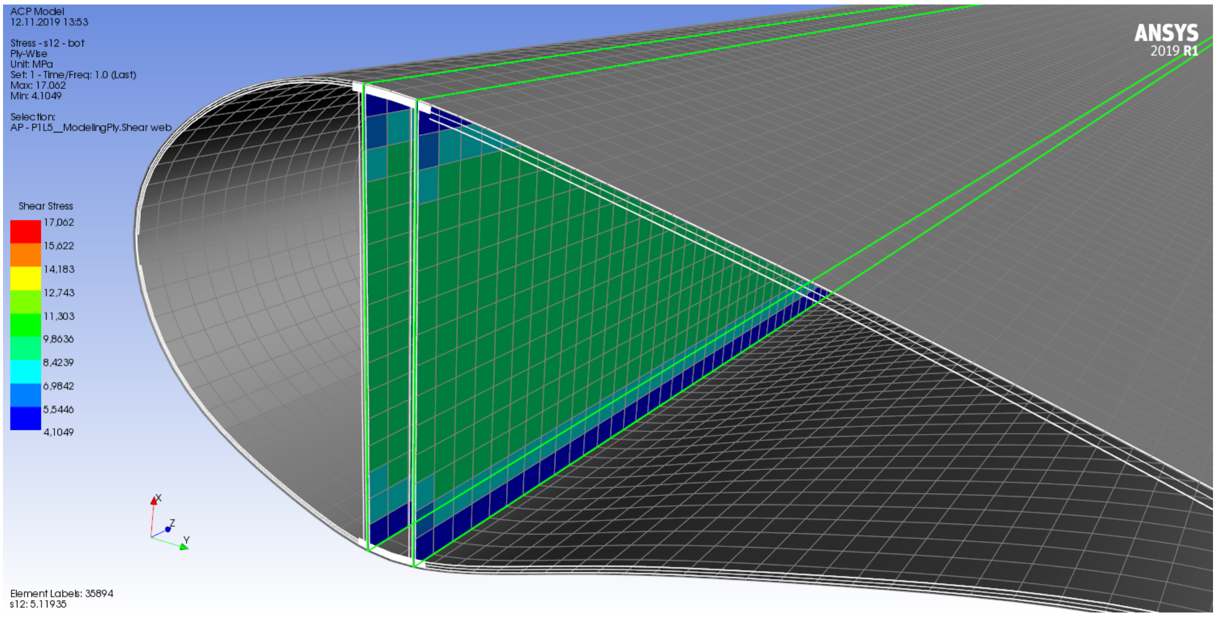

Figure 30: Shear stress distribution in the skin layer of the shear web

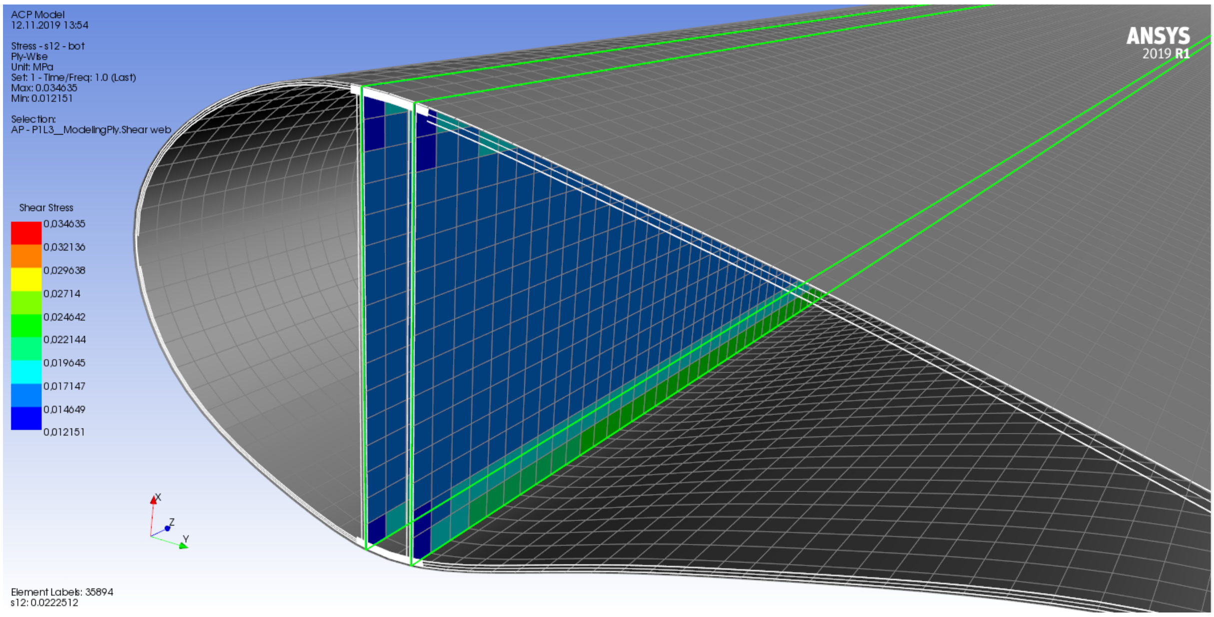

Figure 31: Shear stress distribution in the core layer of the shear web

6.4 Buckling Analysis in FEM

Linear buckling analysis of the simplified blade model is carried out in ANSYS Workbench. The 1st buckling mode of the model is investigated and compared with the analytical results in order to validate the analytical buckling calculation of the VBA tool. Critical buckling load from the FE model is calculated by multiplying the applied load with the load multiplier.

$$p_{cr} = p_{applied} \cdot LM \tag{6.6}$$

When the cross section is loaded by only bending moments, the segment in which the compressive stress is the highest is the most susceptible to buckling. The first buckling mode is found in the leading edge shell panel due to thinner core in this segment. Therefore, buckling analysis of this section is performed. Buckling analysis for a shell structure is more complicated than for the plate due to complex buckling behavior of shells and it is affected by curvature and boundary condition. For this work, the buckling behavior of shells is not investigated in depth. Only simple shell buckling analysis in FEM is carried out for both full model and leading edge shell panel segment model to check the validity of the analytical shell buckling analysis. The end short edge of the segment model is fixed, while displacement in x and y is restrained for the other three edges. A remote force is applied in z direction to create quasi-constant axial load across the width in the structure, see Figure 32. For the full model, constant axial load is applied at the segment. The first buckling mode in the center of the structure is taken for validation.

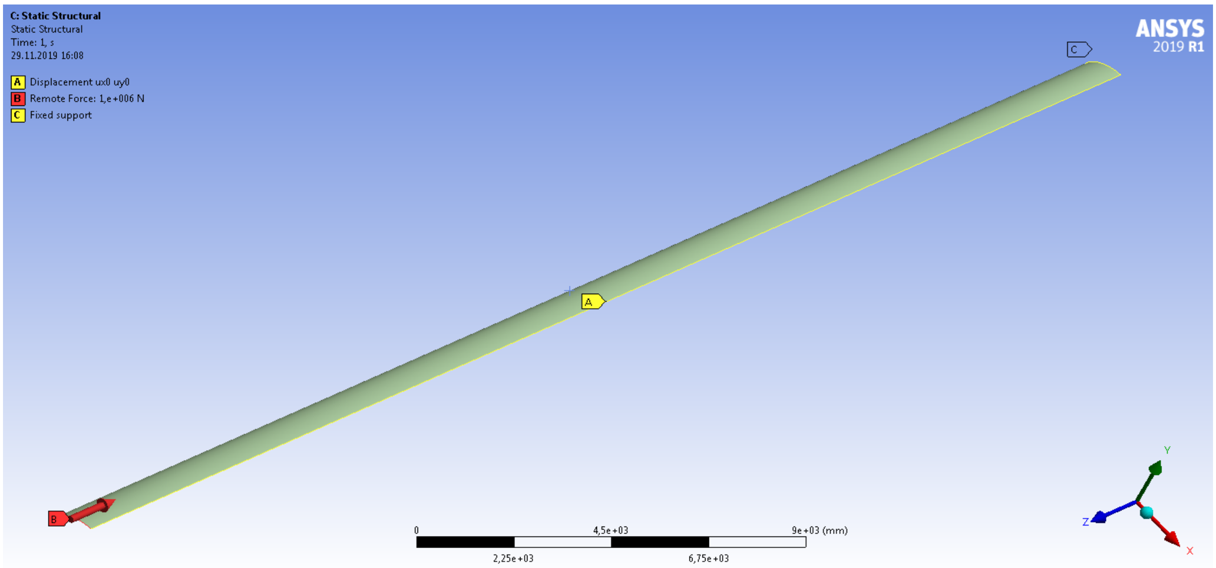

Figure 32: Boundary and loading condition of leading edge shell panel

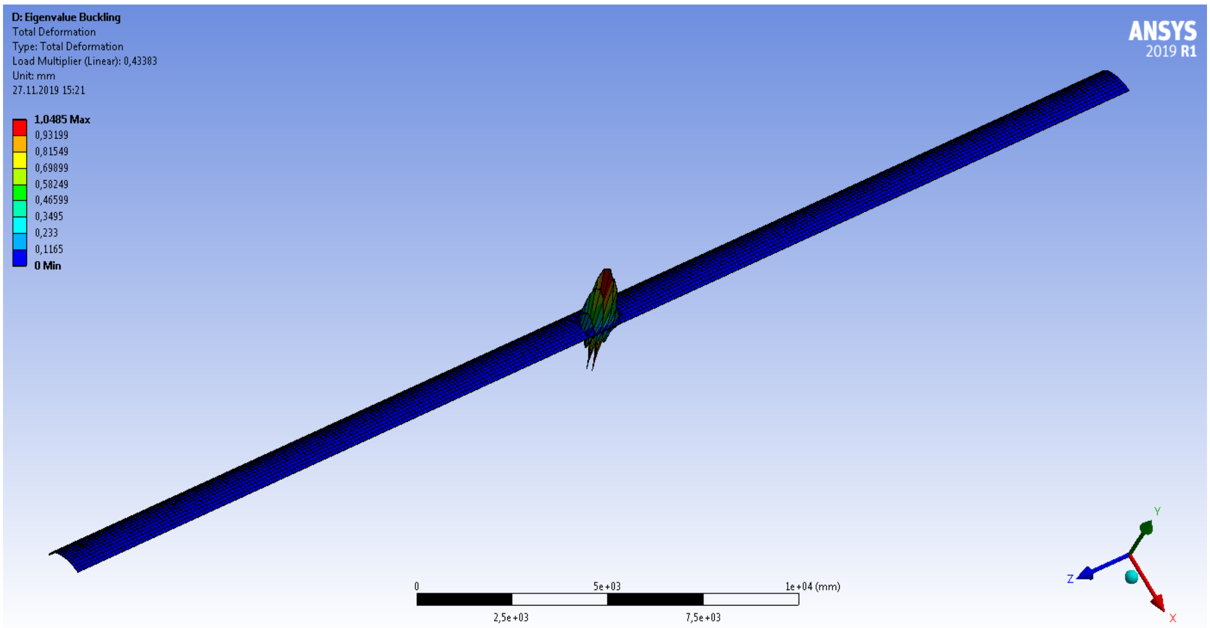

Figure 33: First buckling mode segment shell model due to constant axial load

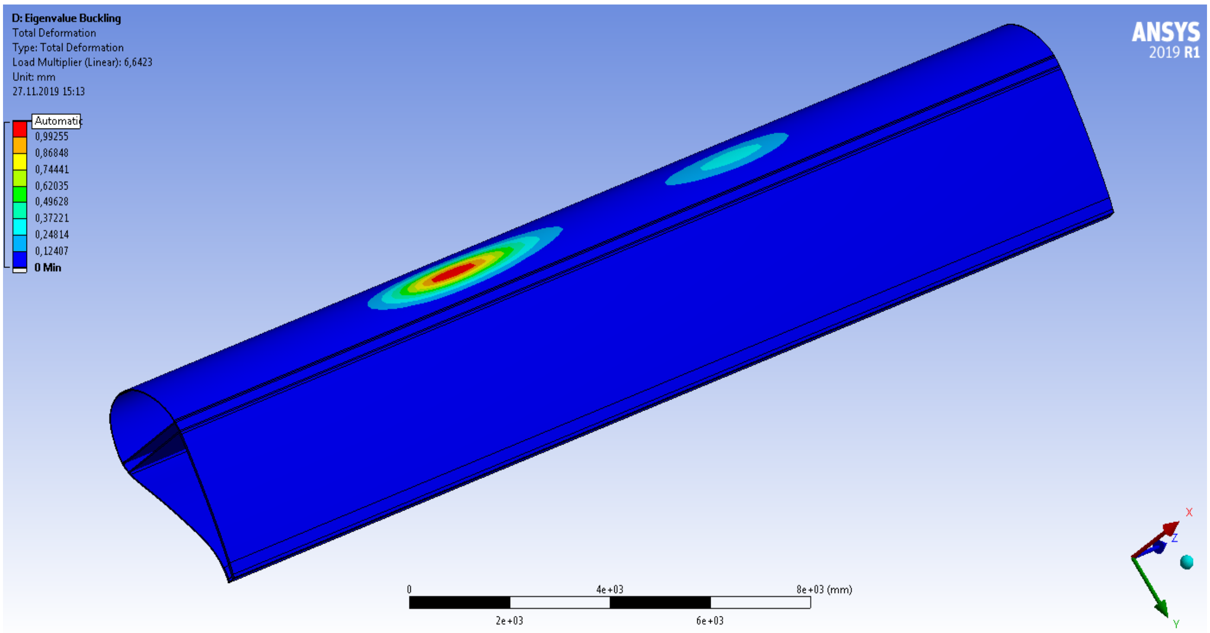

Figure 34: First buckling mode of whole model due to constant axial load

Furthermore, shear web is chosen for plate buckling comparison because it is one of the most critical part in a wind turbine blade. Linear buckling analysis for three loading conditions, bending, shear and compression, are carried out in ANSYS. The segment model of shear web is simply supported at all edges.

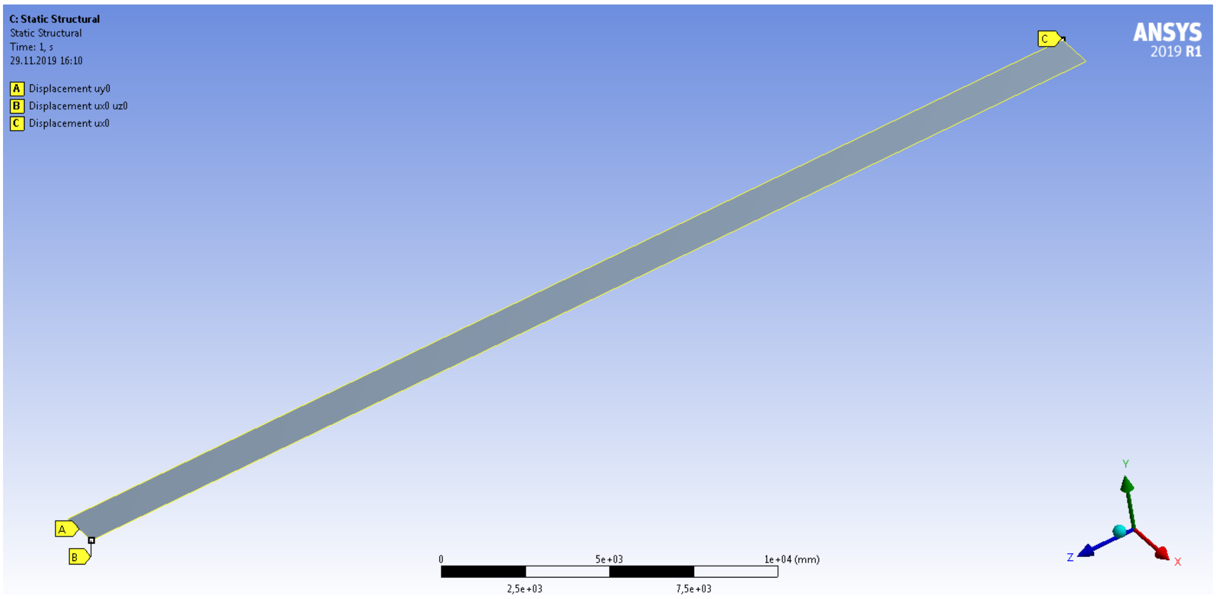

Figure 35: Plate simply supported at all edges

First, bending moments are applied at the two short edges. The applied bending load is calculated using equation (6.7), as the shear web is a sandwich structure. For analytical approach, the critical buckling load is calculated under isotropic condition because shear web consists of predominantly biaxial layers. Additionally, buckling analysis of the full model is performed. In order to obtain the critical bending load at the shear web, a thinner core is used for the shear web so that it is most likely to buckle first due to the effect of reduced bending stiffness. A concentrated load is acted in z direction at the top of the shear web and another concentrated load is acted in negative z direction at the bottom of the shear web to create bending load in the shear web, see Figure 36.

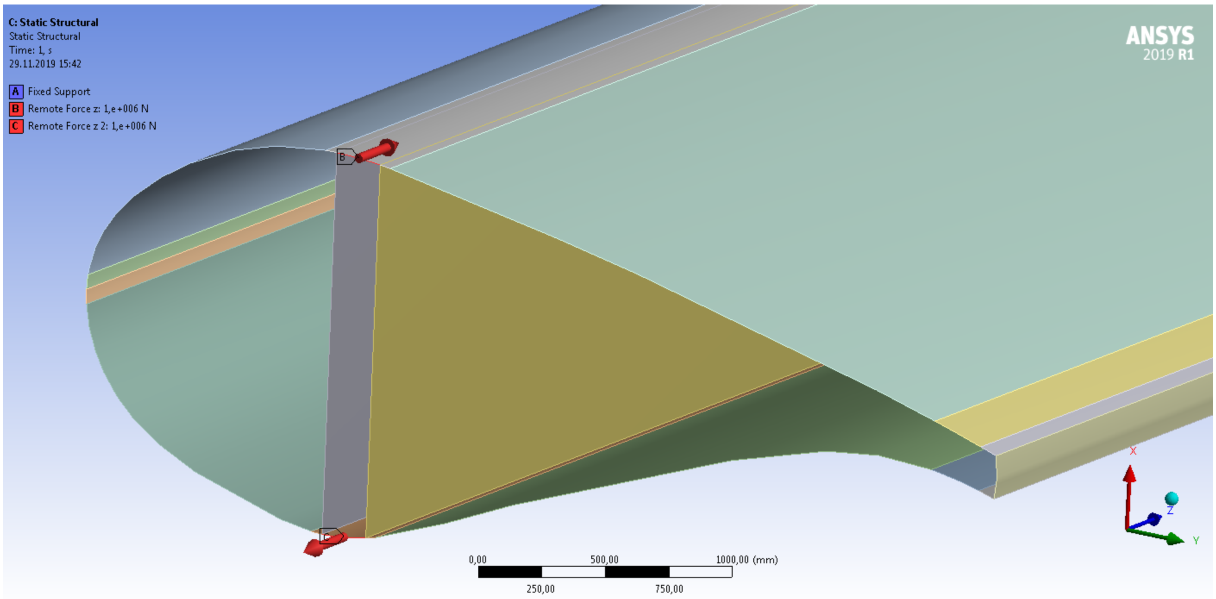

Figure 36: Bending loading at the shear webs

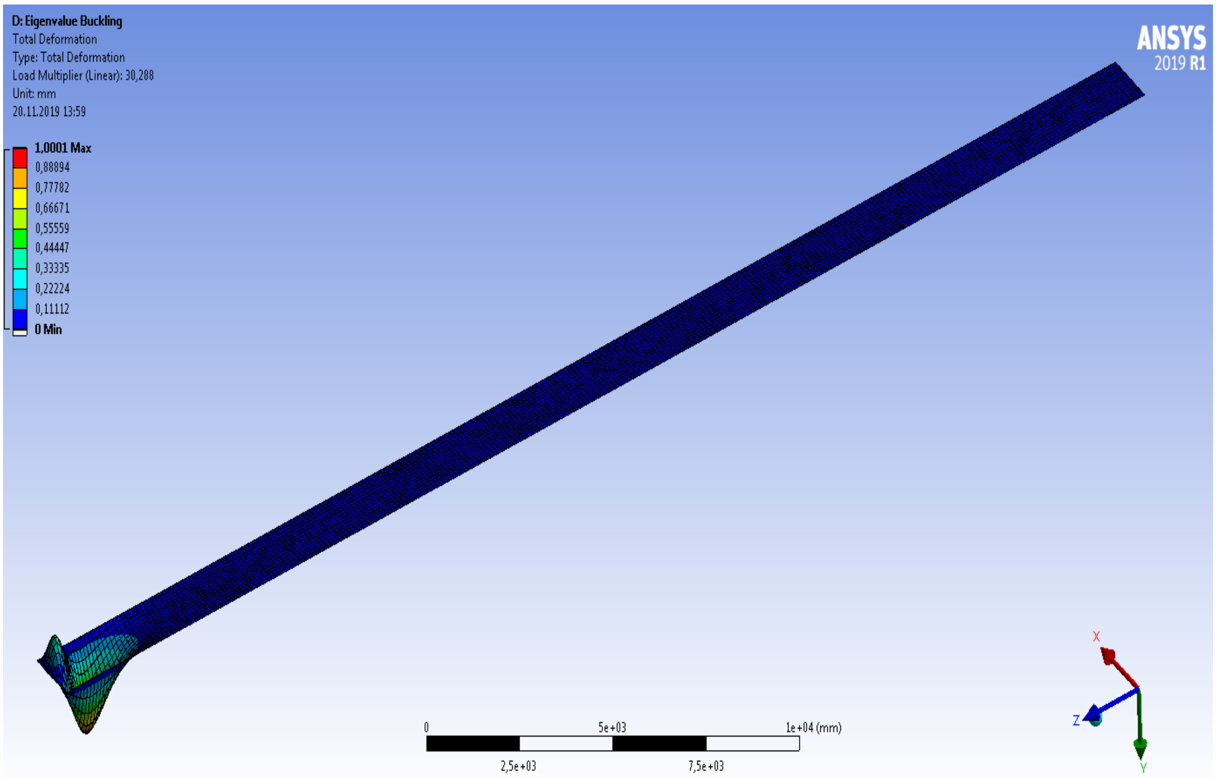

Figure 37: First buckling mode of segment plate model due to bending load

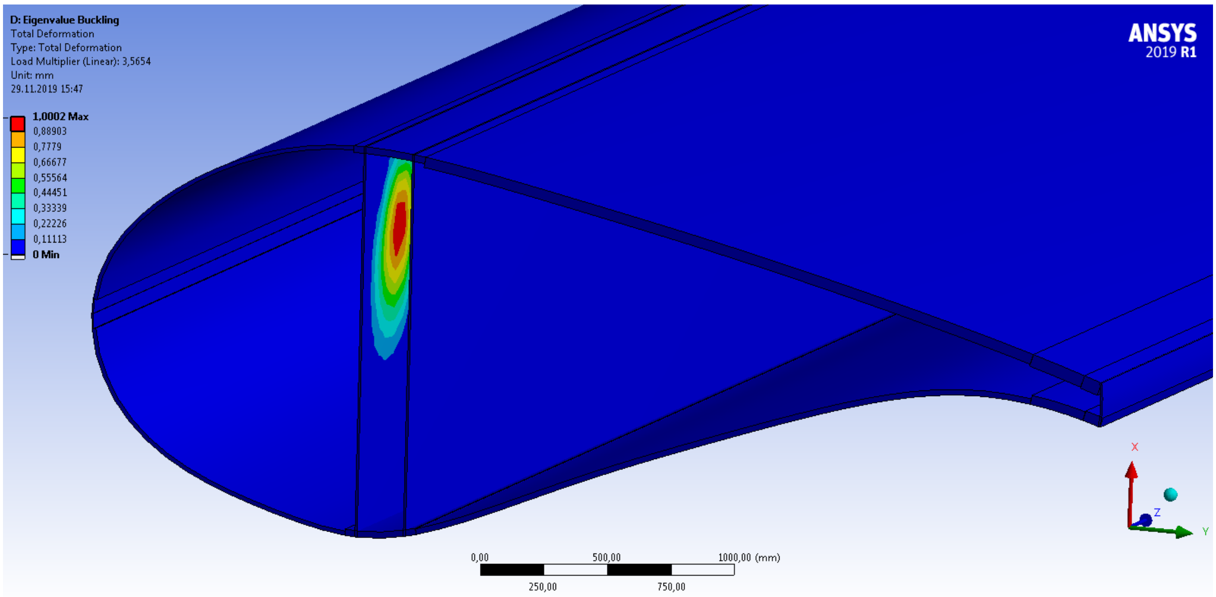

Figure 38: First buckling mode of whole model due to bending load

Buckling analysis under shear and compression loading of the shear web can only carried out using shear web segment model. Shear loads are applied at all edges of the shear web. Lastly, linear buckling analysis under constant axial load at the short edges are also performed with the FE Model and the results are compared with the analytical outputs.

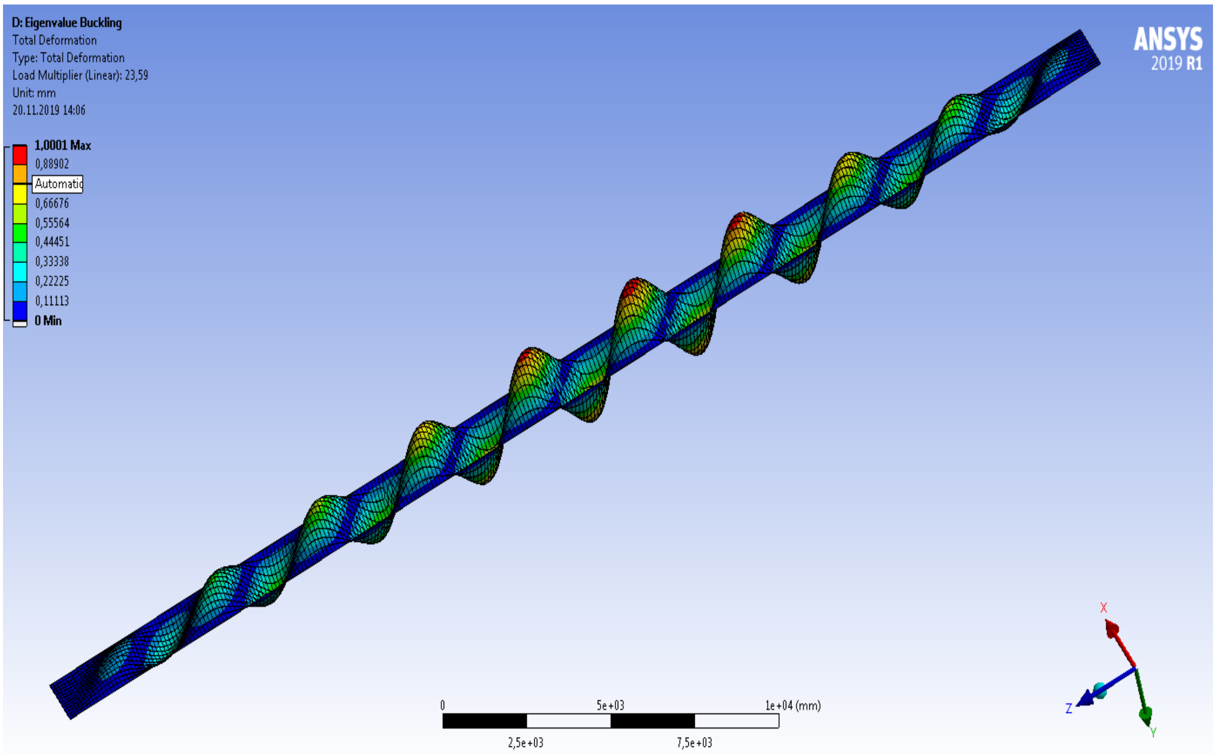

Figure 39: First buckling mode of segment plate model due to shear load

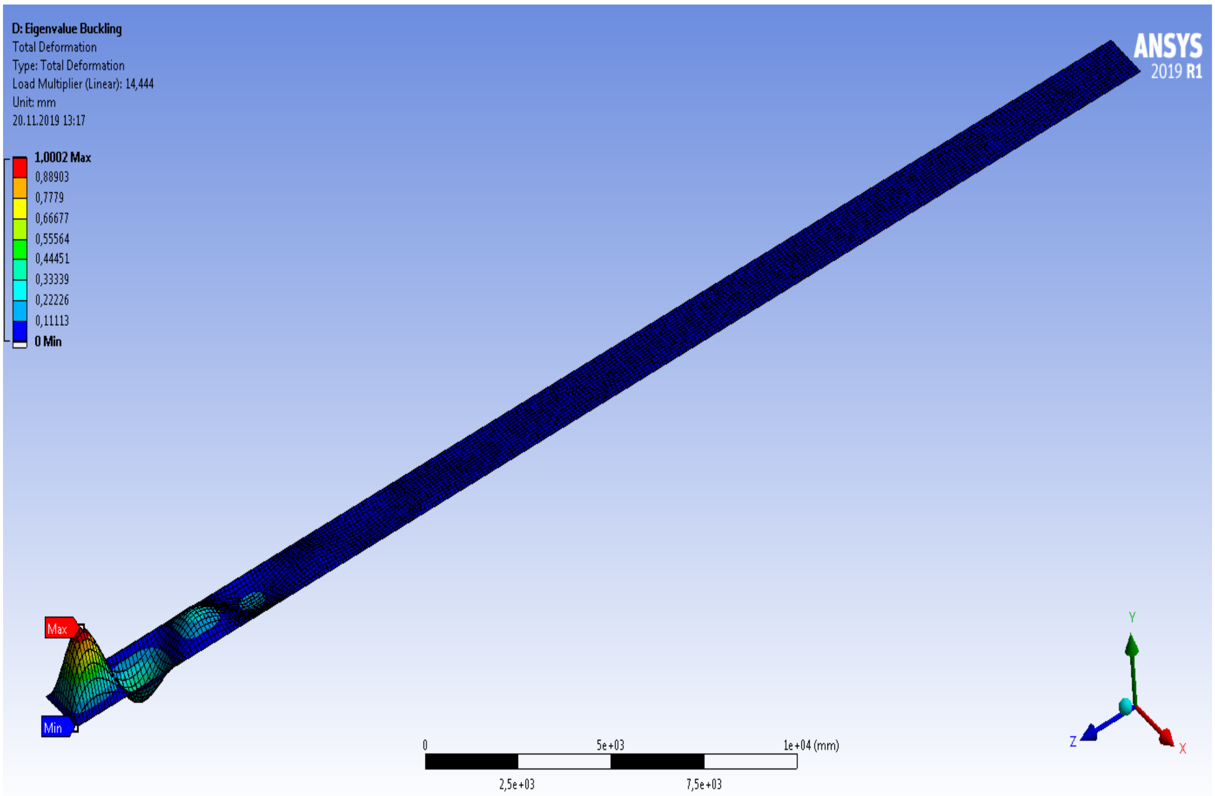

Figure 40: First buckling mode segment plate model due to constant axial load

6.5 Result Comparison

The results obtained from the analytical model are compared with the results from finite element, followed by the evaluation.

6.5.1 Cross-sectional Properties

Sectional properties	Analytical	FEM
Axial stiffness EA $[N]$	2.92E+09	2,92E+09
Flapwise stiffness EI_{min} $[Nmm^2]$	1.16E+15	1,16E+15
Edgewise stiffness EI_{max} $[Nmm^2]$	4.29E+15	4,30E+15

Table 10: Comparison of properties extracted from the analytical VBA model of station 15.5 m with FE values

In Table 10, both analytical and numerical method produced identical stiffnesses results. This proves that the analytical model is very accurate to calculate the stiffnesses of the cross section. Furthermore, Figure 41 shows that the analytical calculated elastic center's location match well with those of FE-Model. However, shear deformation of the FE-Model leads to the deviation of the location of the shear center. As ANSYS is always taking the shear deformation of the beam into account, it means that this is one of the reasons that leads to deviation of the results, especially in the x-direction as the shear stiffness in x-direction is relatively smaller than in y-direction. Furthermore, the stiffness of the core material is ignored, and a constant shear strain is across the element thickness assumed in the analytical VBA model, which is not the case for the FE model, especially an element with a sandwich structure. The shear strain distribution in the shell element is linear, and therefore causing a deviation in the value of the shear flow.

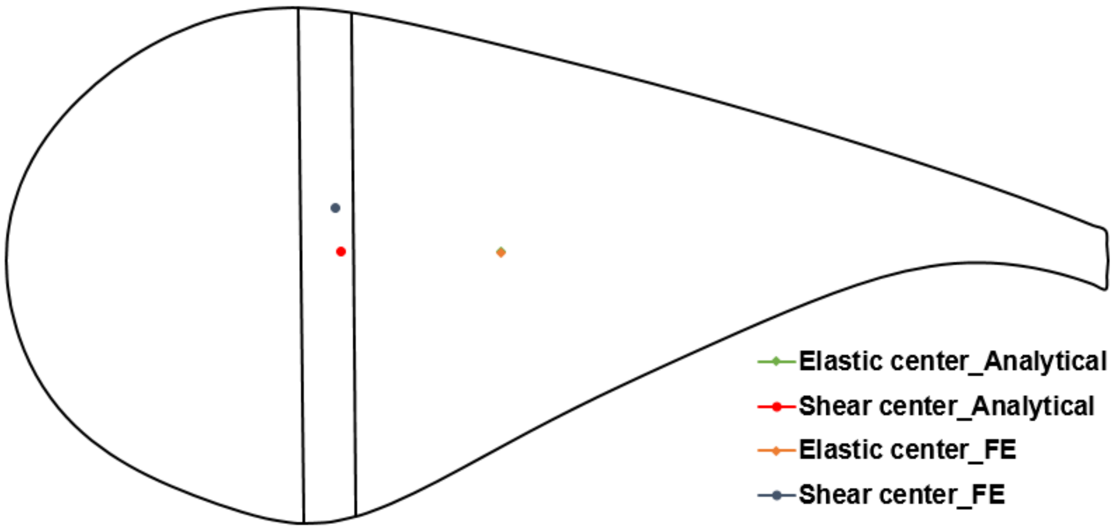

Figure 41: Comparison of elastic and shear center of a cross section

6.5.2 Maximum axial strain in the laminate

The analytically calculated stress and strain are validated by the FE results. Bending moments M_x and M_y are applied at the cross section. The maximum axial strains ϵ_ξ are calculated with the analytical model as well as validated with FE model. Figure 42 represents the maximum axial strain comparison between analytical and finite element method at several points across the contour of the cross section. The results show that analytical model is able to determine the axial strain accurately.

When there is only bending in a rotor blade section, the axial strain is zero along the neutral fiber axis which its origin at the elastic center of the cross section. It increases linearly as the distance to neutral fiber increases. In Figure 29 and Figure 42, it can be seen that axial strain is negative above the neutral fiber and positive below the neutral fiber, which matches well with the theory, see Figure 43.

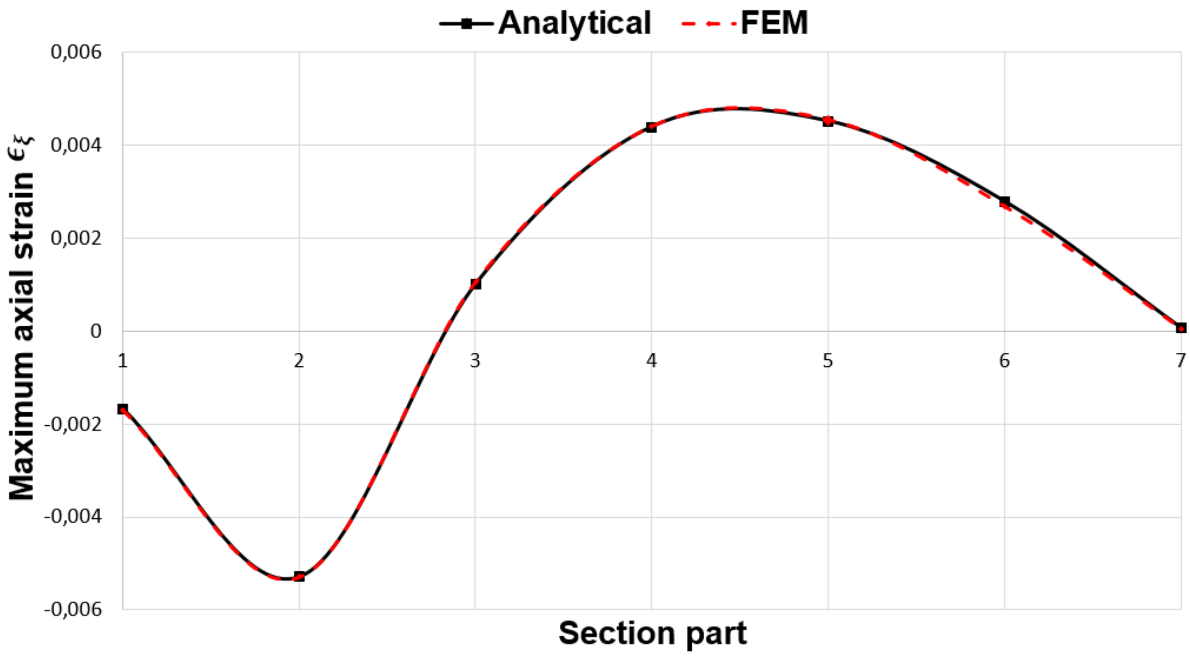

Figure 42: Maximum axial strain comparison between analytical and FE model

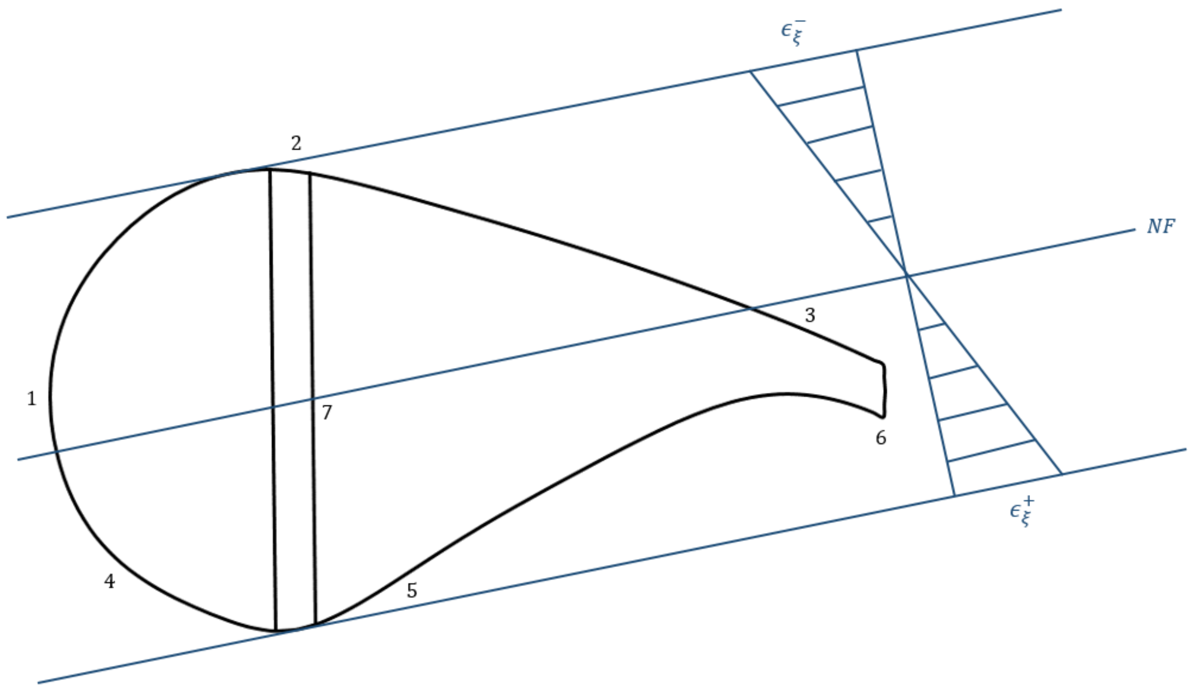

Figure 43: Axial strain linearly distributed in the cross section

Axial load at the node of the element is calculated for sandwich and laminate structure with the following equations:

$$p_{sandwich} = \sigma_{\xi b} \cdot t_{skin_b} + \sigma_{\xi c} \cdot t_c + \sigma_{\xi t} \cdot t_{skin_t} \tag{6.7}$$

$$p_{laminate} = \sigma_{\xi} \cdot t_{laminate} \tag{6.8}$$

6.5.3 Shear load in the bonding joints

The shear loads in the bonding joints are calculated for bonding analysis to determine the minimum width of the adhesive layer to bond the two parts together. There are six bonded joints for a cross section with two shear webs. As the shear webs are made up of a sandwich plate, the shear loads in the bonded joints connected with shear webs are calculated using equation (6.9) whereas the shear load at leading and trailing edge are determined using equation (6.10). The numbering of the bonded joints is displayed in Figure 44.

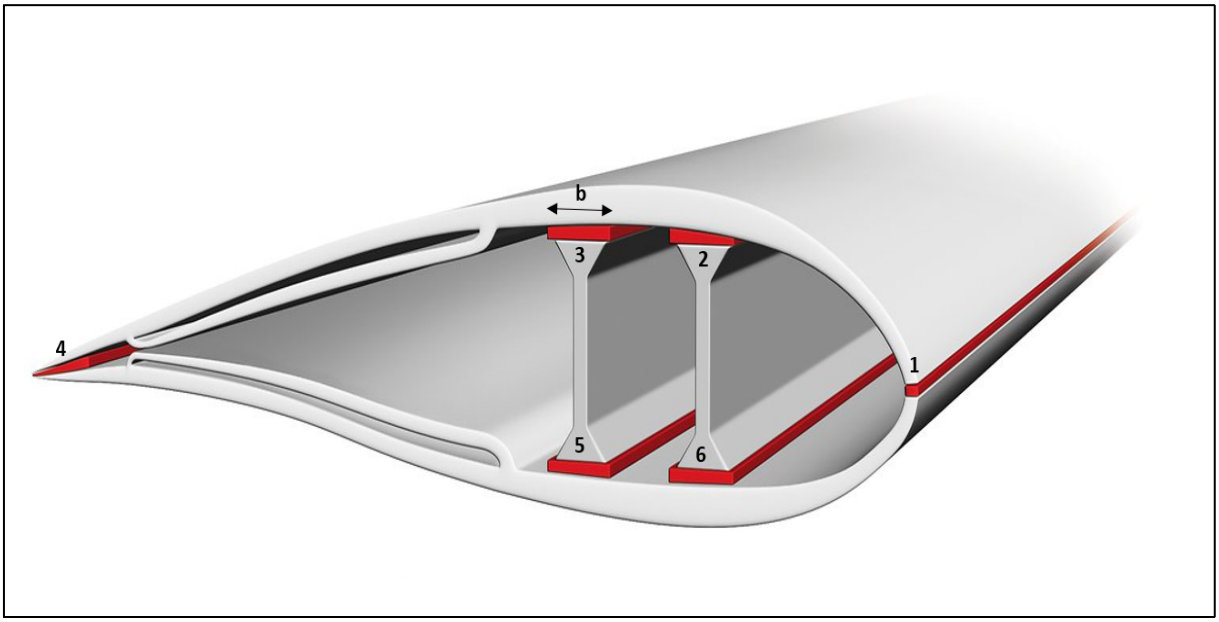

Figure 44: Rotor blade cross-section with adhesive points (red) [11]

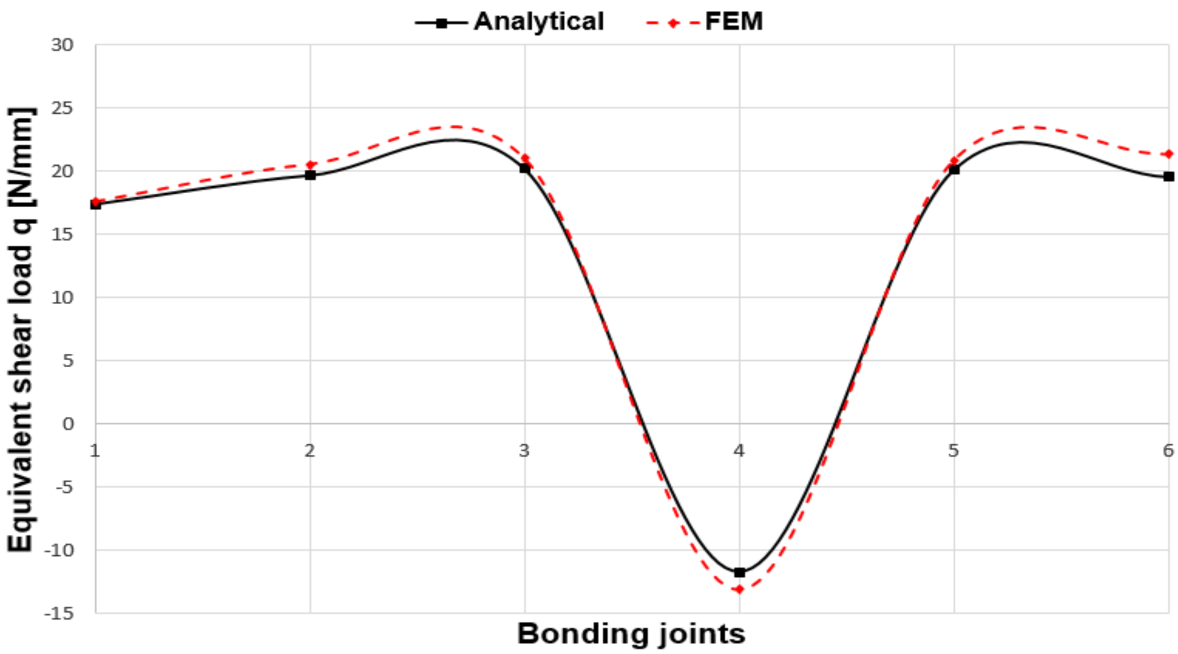

Figure 45: Shear loads comparison between analytical and FE model

The cross section is loaded by a shear force Q_x. A comparison of the value of shear load q using analytical method and FE method is performed. Shear load is not possible to be extracted directly from the FE model. Therefore, shear loads are calculated from the shear stress. In the analytical model, shear stress and shear strain are assumed to be evenly distributed across the thickness of the cross-section. It is acceptable in the case of a thin-walled cross section. However, it is not the case for a FE model. It is important to notice that the shear stress is not constant across the wall of the finite element, especially if the finite element consists of a sandwich structure. The shear strain is linearly distributed, and the shear stress is very low in the core material. Hence, for a sandwich structure, the shear load is calculated by adding up the multiplication of shear stress of the skins and core and its thickness, respectively:

$$q_{sandwich} = \tau_{\xi\eta\_b} \cdot t_{skin_b} + \tau_{\xi\eta_c} \cdot t_c + \tau_{\xi\eta\_t} \cdot t_{skin_t} \tag{6.9}$$

The shear load of a laminate structure is easier to be calculated, by multiplying shear stress of the laminate with the total thickness:

$$q_{laminate} = \tau_{\xi\eta} \cdot t_{laminate} \tag{6.10}$$

Figure 45 shows that the shear load calculated analytically is lower than the value of FE, with an underestimation of maximum 10%. The reason is that the stiffness of the core is neglected in the analytical model. Additionally, twist is also not considered, which leads the further deviation of the results. Nevertheless, increasing analytically calculated shear load by 10% is recommended for more conservative and reliable bonding analysis.

6.5.4 Critical buckling load

As mentioned in Chapter 5.3.3, the isotropic condition is slightly over conservative, if the biax layer has different value of stiffness in 0°and 90° layer direction. It is proven in Figure 46 for plate buckling analysis of the shear web. The analytically calculated critical buckling load under isotropic condition is relatively low compared with value obtained from FE Model. On the other hand, the results from the calculation under anisotropic condition is closer to the FE results. Hence, it is recommended to calculate analytically the critical buckling load under fixed support edges as well, and then determine the mean value of the critical loads from both boundary conditions for more realistic buckling analysis of the wind turbine blade.

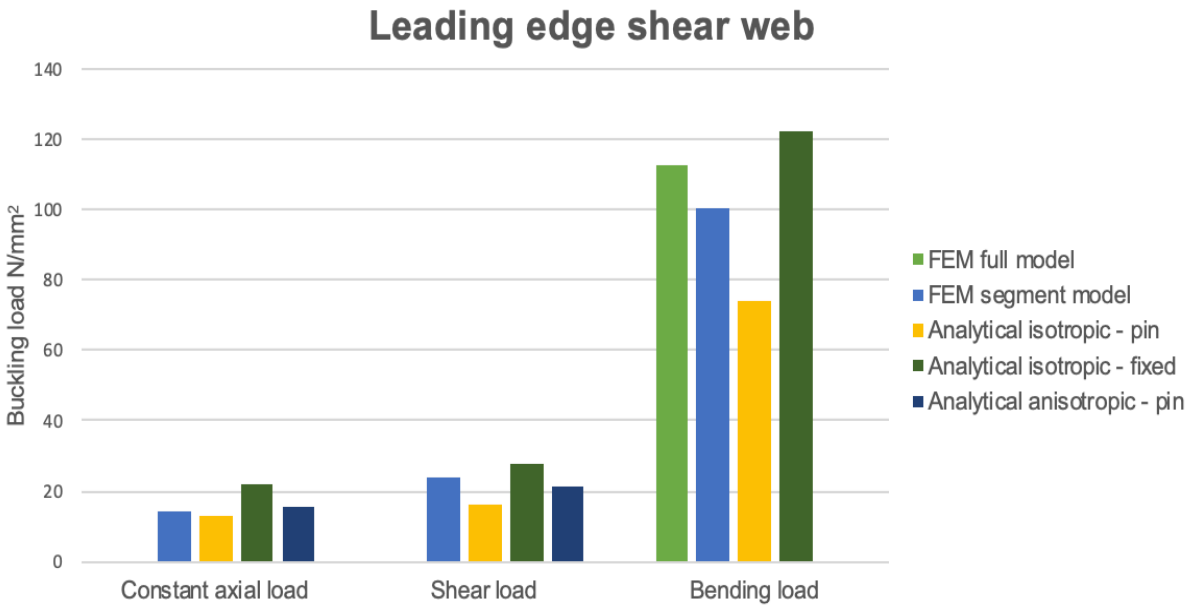

Figure 46: Plate buckling analysis of the shear web

Furthermore, due to the limitation of the analytical shell buckling analysis, only the buckling case of the shell panel under constant axial load and simply supported is carried out. Figure 47 shows that simply supported boundary condition of isotropic analytical analysis is too conservative comparing to FE full and segment model. For the future work, fixed support edges and anisotropic buckling analysis need to be implemented to the tool for more accurate shell buckling analysis.

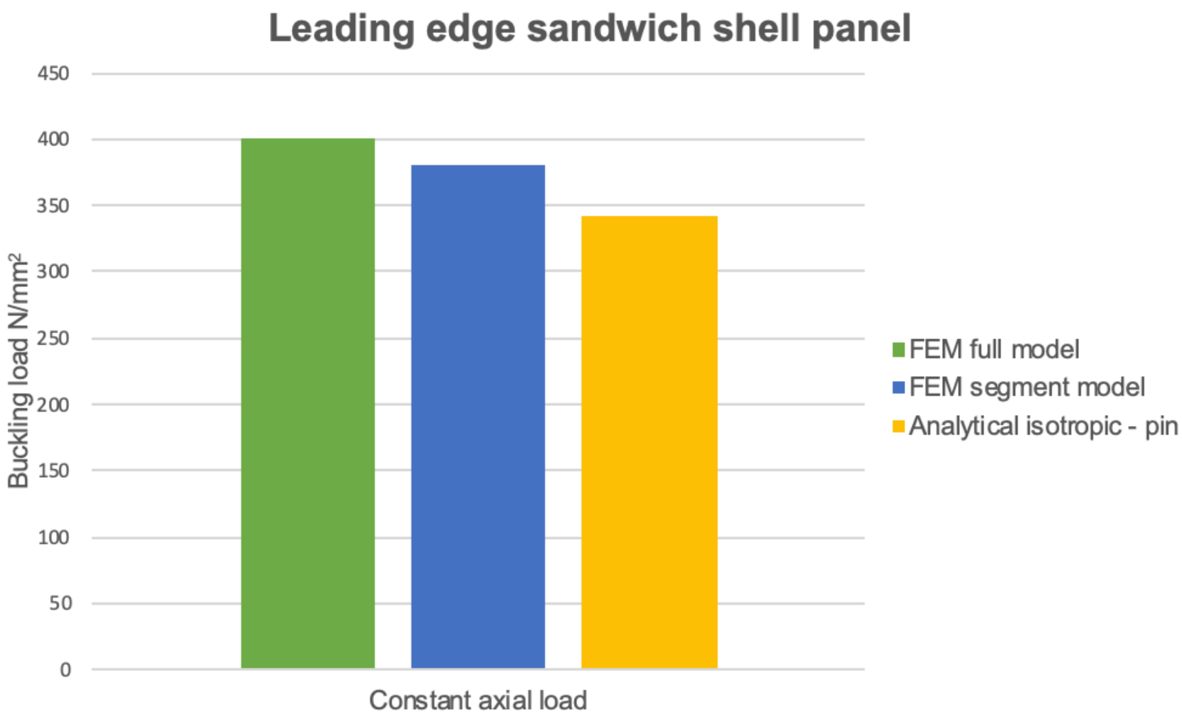

Figure 47: Shell buckling analysis of the blade shell panel

7 Conclusion

This chapter summarizes the research work carried out for this thesis and lays some recommendations and scope for future research concerning the further development of the analytical model.

7.1 Summary

An analytical model based on Classical Lamination Theory was developed to determine the cross-sectional properties of a rotor blade. Firstly, it was necessary to prepare the given profile data from the customer accordingly, by transforming the coordinates to chord coordinate system with origin at the leading edge. The cross section is then discretized into elements. The ABD-Matrices of each elements are calculated to determine the stiffnesses of the cross section. The results matched with results from the simplified FE model. Moreover, stresses and strains of each element are also validated with FE model. The results show small deviation from the FE model due to simplified analytical assumptions.

This analytical VBA tool is not finite element based and therefore cannot provide detailed load-displacement or load-stress distribution the way a sophisticated 3-D finite-element approach. However, it directly computes the cross-sectional properties and runs fast, usually in a fraction of a second. It also eliminates the need for an interactive approach and requires only a modest knowledge of composites and laminate layups typically used in blades. The advantage of this tool lies in its efficiency because it is not based on the finite element method. It is also general enough to deal most of wind turbine blades with very few restrictions. However, because of its adoption of oversimplified analytical assumptions, there are some concerns about its accuracy.

Structural analysis was carried out to verify the ultimate strength and buckling resistance of the composite laminate against extreme loads. Partial safety factors for material are considered for the analysis. Fiber and inter-fiber failure analysis were performed with the calculated axial strain and shear strain of each element as inputs. Fiber failure analysis is done to verify the stress in fiber direction does not excess tensile and compressive strength of the ply. On the other hand, inter-fiber failure analysis considered three independent fracture conditions with the fracture modes A, B and C. The ply stresses and strains are validated using Compositor.

Shear strain was assumed to be constant across the sandwich structure in the analytical model, which is not the case in the FE model. However, it did not have big influence on the accuracy of predicting of the shear center. Furthermore, it was accurate enough to calculate the shear load for bonding analysis at the bonded joints. Buckling analysis was carried out with some limitations. Each parts of the cross section were analyzed separately by assuming all edges simply supported and the load were assumed to be the same from both sides. The isotropic buckling condition for shear webs and shell panels was slightly too conservative. Furthermore, the result comparison from the buckling analysis using analytical method and finite element method shows that simply supported edges is conservative as the critical stress from the tool is lower than from the FE model. Thus, additional buckling analysis with fixed edges is needed to perform. The mean value of the critical load from both boundary conditions should be determined for more accurate buckling load calculation. There are limitations of analytical buckling analysis. The structure to be investigated must be either laminate or sandwich. If for example leading edge shell panel, which consists of laminate and sandwich, majority is considered with is sandwich, buckling analysis assuming the whole structure is sandwich is carried out, which causes inaccuracy of the analysis.

7.2 Scope for Future Works

In this tool, the flapwise and edgewise bending moments as inputs are expected to be respect to the chord coordinate system in Chapter 3.1. But it might be not the case for the bending moments given by some customers. Hence, additional code for the calculation of the bending moments due to transformation of the coordinate system should be implemented. As mentioned, the tool can calculate the cross-sectional properties of one cross section of the blade at one time and structural analyses were performed for the blade with only one constant cross section. Therefore, this tool must be further developed to be able to calculate the structural properties for the entire cross sections of the blade. Besides, the calculation of torsional stiffnesses of the cross section including the effect of constrained warping can be added to the analytical tool, because free warping assumption is not valid near a constrained blade root section.

Furthermore, it would be more practical if buckling analysis with more other loading and boundary conditions like linear varying load and rotationally restrained can be done by the tool, as they are closer to the real situation, especially for shell buckling analysis. Non-linear buckling analysis of the FEM-Model with the consideration of the deformation of the geometry would be also a more accurate approach. The calculation of the transverse shear stresses on the shear webs for further verification for inter-fiber failure can also be introduction for future works. The blade is also subjected to fatigue loads. Hence, for the continuation of this work it would be interesting to implement fatigue analysis of the laminate in the tool.

8 Bibliography

[1] „Evolution of Wind Turbine Heights and Output," [Online]. Available: http://www.cleanfuture.co.in/2017/09/22/evolution-of-wind-turbine-heights-and-output/. [Zugriff am 08 12 2019].

[2] G. S. Bir, „User's Guide to PreComp," National Renewable Energy Laboratory, 2005.

[3] W. Y. M. C. Hui Chen, „A critical assessment of computer tools for calculating composite wind turbine blade properties," 2009.

[4] L. Wang, „Nonlinear Aeroelastic Modelling of Large Wind Turbine Composite Blades," May 2015.

[5] G. S. S. László P. Kollár, Mechanics of Composite Structures, Cambridge University Press, 2003.

[6] Guideline for the Certification of Wind Turbines, Germanischer Lloyd, 2010.

[7] M. Knops, Analysis of Failure in Fiber Polymer Laminates - The Theory of Alfred Puck, 2008.

[8] G. B. a. P. Migliore, „Preliminary Structural Design of Composite Blades for Two- and Three-Blade Rotors," NREL National Renewable Energy Laboratory, 2004.

[9] H. Hertel, Leichtbau, Springer-Verlag , 1980.

[10] J. Wiedemann, Leichtbau Elemente und Konstruktion, Springer-Verlag Berlin Heidelberg, 2007.

[11] „Polyurethan-Klebstoffe sorgen für frischen Wind," [Online]. Available: https://www.henkel.de/spotlight/2014-08-27-news-polyurethan-klebstoffe-sorgen-fuer-frischen-wind-150300. [Zugriff am 27 11 2019].

[12] M. Z. G. v. B. G. v. K. Turaj Ashuri, „An Analytical Model to Extract Wind Turbine Blade Structural Properties for Optimization and Up-scaling Studies".

[13] H. Kossira, Grundlagen des Leichtbaus, Springer, 1996.

[14] V. N. K. S. B. A. F. Stoddard, „Determination of Elastic Twist in Horizontal Axis Wind Turbines (HAWTs)," National Renewable Energy Laboratory, Texas, August 1989.

[15] D. L. L. David J. Malcolm, „Modeling of blades as equivalent beams for aeroelastic analysis," *AIAA Reno,* 2003.

[16] VDI-2014, Entwicklung von Bauteilen aus Faser-Kunststoff-Verbund, Düsseldorf: Verein Deutscher Ingenieure, 1993.

[17] R. G. B. WARREN C. YOUNG, Roark's Formulas for Stress and Strain, McGraw-Hill, 2002.

[18] A. Nettles, Basic Mechanics of Laminated Composite Plates, Alabama: NASA Reference Publication 1351, 1994.

[19] L. M. S. Junior, „Stress Analysis on a Thin-Walled Composite Blade of a large Wind Turbine," Florianópolis, 2016.

Appendix A (Manual for VBA tools)

1. Create a excel workbook containing all the node coordinates “Node Coordinates”
    a. Separated worksheets: Suction shell, Pressure shell, SWLE, SWTE, Flat back

2. Workbook “Coordinate Input”
    a. Import coordinates (Enter the station Z value)
    b. Assign points (NE, TE, FBE, SWLE, SWTE)
        i. If the profile has no flat back, enter “0” for the FBE cell.
    c. Rearrange SW coordinates if necessary
        i. Shear webs coordinates always start with suction side (X) and end with pressure side (O)
        ii. The code helps to rearrange only if the imported coordinates start from pressure side (O) and end with suction side (X). Otherwise please arrange manually
    d. Rearrange the coordinates (LE-TE)
        i. Shell coordinates always start with LE=(0,0)
    e. Add FB coordinates below if necessary
    f. Coordinate transformation -> Chord coordinate system
        i. Click only one time, otherwise the profile with keep rotated with the twist angle)
    g. Create girder planes (Enter the parameter a-h)
    h. Find out the girder points (With the help of the button “Track node” by entering the node number)
    i. Enter the girder points
    j. Assign the girder points with label

3. Cross-sectional properties tool
   (The name of the worksheets should not be changed)
    a. Button: Import material table
    b. Button: Import coordinates
        i. Enter the number of shear webs 1 or 2
        ii. The coordinates from “Coordinate input” file are imported to the worksheet “O-Side_FB”, “X-Side_FB”, “ShearWeb_Nose”, and if applicable “ShearWeb_Tail” as well.
        iii. Distance and angle between two adjacent nodes are calculated
        iv. Node labels for layup tables are created (LE(+), MGLE(+), MGTE(+), TGLE, TE(-), FBE)
    c. Create layup tables for pressure, suction and shear web separately by using the available node labels (Last three worksheets: “Layup_O-Side_FB”, “Layup_X-Side_FB”, “Layup_ShearWeb”)
        i. Column A: Section number and description of the layer
        ii. Column B: Material name (Taken from the material table)
        iii. Column C, D: Starting point of the layer (Column D is empty, when the starting point is at LE, MGLE, MGTE, TGLE)
        iv. Column E, F: Ending point of the layer (Column F is empty, when the ending point is at MGLE, MGTE, TGLE, TE, FBE)
        v. A positive value in Column D and F is measured from LE towards the TE. A negative value is measured from the TE to the LE.
        vi. Column G: Layer orientation (The 0° layer orientation means that the layup is put parallel to the blade pitch axis; It is important to put “NA” for core material because the code reads “NA”, when the layer is core material)

vii. For shear web: first table is the layup table for shear web leading edge and the second table is the layup table for shear web trailing edge.
viii. Column C, K: Starting point of the layer (Always from X-Side)
ix. Column E, M: Ending point of the layer (Always at O-Side)

d. Button: Section layout design
   i. Worksheet "O-Side_FB", "X-Side_FB", "ShearWeb_Nose", and if applicable "ShearWeb_Tail":
      1. Row 1 starting from Column M: Description of the layer
      2. Row 2 starting from Column M: Material name and layer orientation
      3. "1" indicates the layer is covered from assigned node to the next adjacent node. For example: the layer is covered from MGLE to MGTE

MGLE		1
MGLE	51	1
MGLE	131	1
MGLE	173	1
MGLE	253	1
MGTE		

   ii. Worksheet "Element data ShearWeb", "Element data O_FB", "Element data X_FB":
      1. Elements are created using two adjacent nodes
      2. Number of layers is calculated for each element and the stack-up can be seen in the Column K

e. Button: Material properties analysis (Worksheet "Element data ShearWeb", "Element data O_FB", "Element data X_FB")
   i. Material properties are imported from the Workbook "Material table" (Column M:AG)
   ii. Layers are built towards the inside the cross section (Column AK:AL); for shear web: towards the leading edge
   iii. Mean engineering constants of each layer (Column AO:AS)
   iv. Stiffness and compliance matrices of each layer (Column BA:BP)
   v. Stiffness matrices with respect to the neutral plane of each element (Column CS:DJ)
   vi. Compliance matrices with respect to the neutral plane of each element (Column DM:EE)
   vii. Restriction: The module to calculate ABD Matrix of the Sandwich plate is only applicable to the situation that there is only one core/foam per element. Otherwise, the ABD module needs to be modified.

f. Enter the loads in Worksheet "Main": bending moments and shear forces in chord coordinate system

g. Button: Cross-sectional properties and axial strain (Worksheet "Complete data ABD")
   i. All elements are listed in one worksheet (From TE/FBE of pressure side to LE and then to TE/FBE of suction side, followed by the elements of shear web)
   ii. Elastic center is determined
   iii. Principal coordinate system is created
   iv. "Cross-sectional properties" table: Elastic center, axial and bending stiffnesses with respect to chord CS (EA, EIyy, EIxx, EIxy), principal axis angle, bending stiffnesses with respect to principal CS (EImax, EImin)
   v. Column Q: Axial strain at the neutral plane
   vi. Column R: Axial load at the neutral plane
   vii. Column S: Axial force at the neutral plane

viii. Column AM: Axial strain at the outermost layer of each element (for the purpose of more conservative calculation)

h. Button: Set boundary points for the cells (Worksheet "Shearflow_points")
   i. Node number is used instead of node label

i. Button: Shear flow and shear strain (Worksheet "Shearflow Cell1", "Shearflow Cell2", "Shearflow Cell3")
   i. Column AJ: Shear load (Constant shear load across the thickness of the element)
   ii. Column AO: Shear strain at the neutral plane
   iii. Shear center is determined

j. Worksheet "Matrix" is only for intermediate calculation

4. Structural analysis tool
   a. Import material table and cross sectional properties tool
   b. Create Element table (Worksheet)
   c. Laminate failure analysis (FF, IFF)
      i. Make sure that the ply strengths are available in the Standard Material Table (Using the name "Material name" + "-lamina")
      ii. The name in column (M:Q and AP:AW) cannot be changed because it refers to the material table
      iii. (ξ, ζ, η) Element coordinate system $\xrightarrow[Layup\ orientation\ (Column\ I)]{}$ (x, y, z) Layer coordinate system
      iv. (x, y, z) layer coordinate system $\xrightarrow[Layup\ (Column\ K)]{}$ $(1,2,3)$ Fiber coordinate system $(1 \Leftrightarrow 0°, 2 \Leftrightarrow 90°)$
      v. Clear all
      vi. Click on the button "Laminate failure analysis"
      vii. IFF: Cells in the column "fE,IFF" turns red if the value exceeds 1
      viii. FF: Cells in the column "fE,FF" turns red if the value exceeds 1
   d. Buckling analysis
      i. Choose the segment for analysis
      ii. Choose the first element and last element number of that segment by referring to the worksheet "Element table"
      iii. Choose the load
      iv. Choose isotropic or anisotropic condition
      v. Choose plate or shell
      vi. Click on the button "Get segment data" (Click on this whenever "Material" is changed, because different data will be imported for isotropic and anisotropic condition respectively)
      vii. Click on the button "Calculate properties"
      viii. Calculate buckling coefficient (Sometimes need to read it from the diagrams from the worksheet "Buckling coefficient diagrams" and enter manually)
      ix. Calculate critical load
   e. Bonding analysis
      i. Clear all
      ii. Enter the element number of the bonded join
      iii. Click on the button "Bonding analysis" to import the calculated shear flow from Cross-sectional properties tool and thus calculate the minimum width of the adhesive layer with the use of allowable shear stress (3.14 N/mm^2) given by GL.
   f. Worksheet "Matrix" is only for intermediate calculation

Appendix B (Buckling coefficient diagrams)

Isotropic laminate and sandwich plate

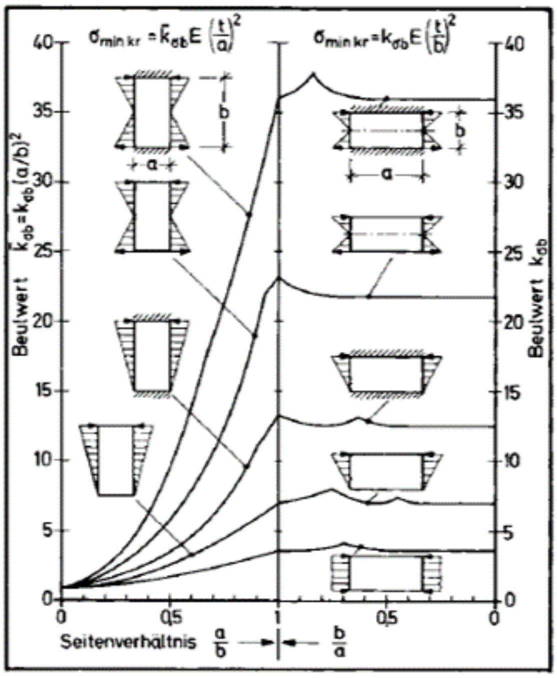

Bild 2.3/4. Isotrope Rechteckplatte, gelenkig gestützt. Beulwerte bei linear veränderlicher Randbelastung (Scheibenbiegung); nach [2.9]

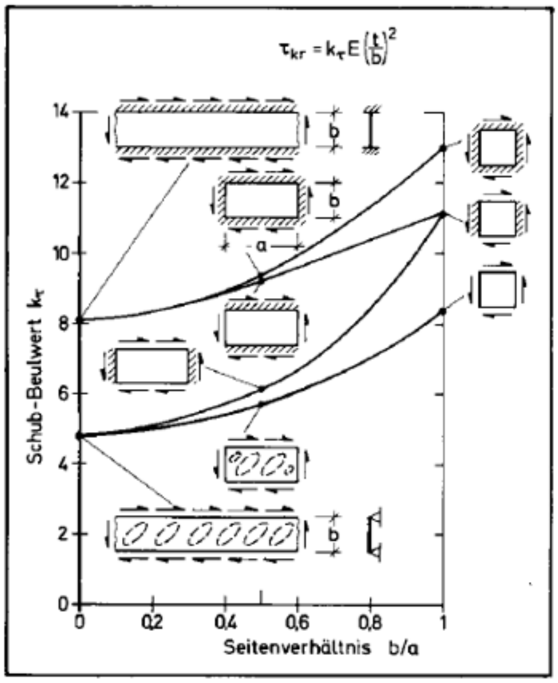

Bild 2.3/5. Isotrope Rechteckplatte. Schubbeulwerte, Einfluß des Seitenverhältnisses und der Randbedingungen; nach [2.9]

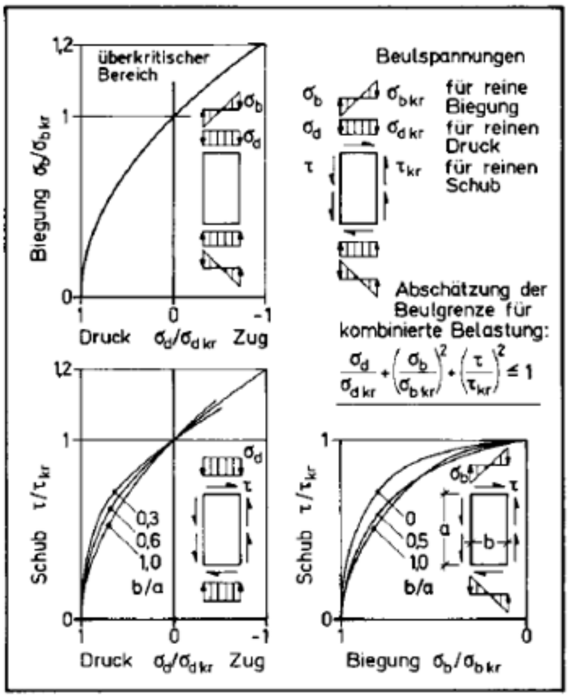

Bild 2.3/6. Isotrope Rechteckplatte. Beulgrenzen für kombinierte Belastung: Druck, Schub und Scheibenbiegung; nach [2.9]

Isotropic laminate shell

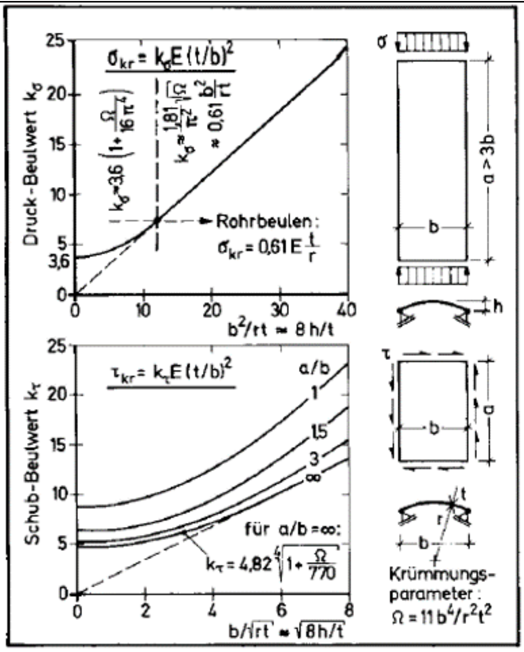

Bild 2.3/7. Kreiszylindrische Teilschale mit radial gestützten Rändern. Beulwerte für Längsdruck und Schub, Einfluß des Krümmungsmaßes; nach [2.13]

Isotropic sandwich shell

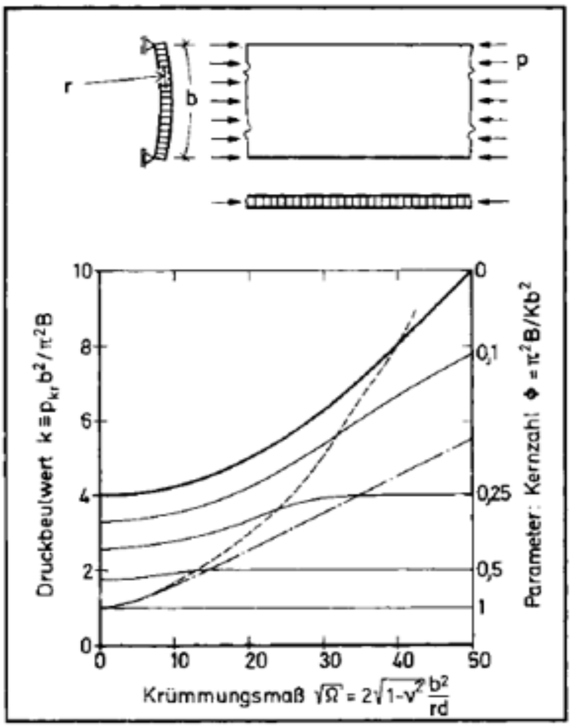

Bild 5.3/17. Sandwichschalenstreifen, isotrop; Längsränder radial gestützt. Druckbeulwert, abhängig von Krümmungsmaß und Kernzahl; nach [5.6, 10]

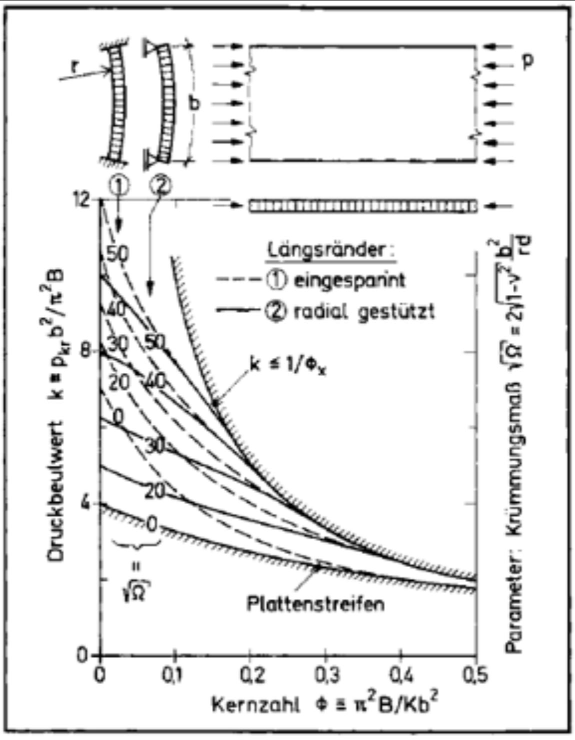

Bild 5.3/18. Sandwichschalenstreifen, isotrop; Längsränder eingespannt oder radial gestützt. Druckbeulwert über Kernzahl, Krümmungs- und Randeinfluß; nach [5.6]

Anisotropic laminate plate

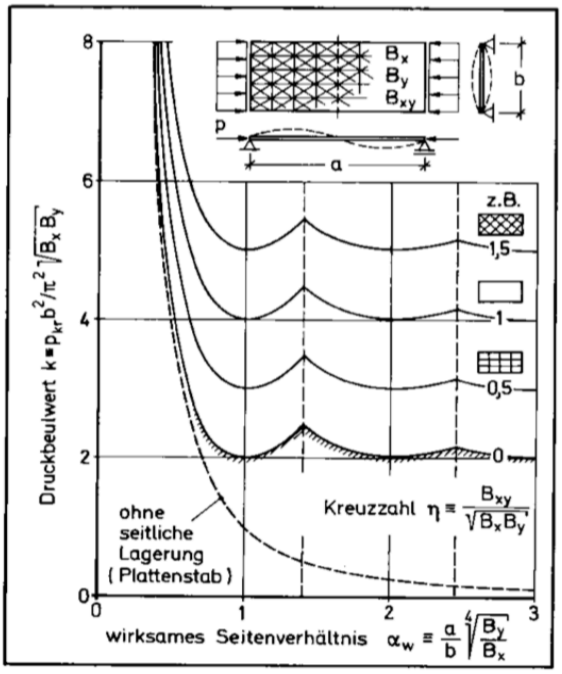

Bild 4.3/1. Orthotrope Rechteckplatte, allseitig gestützt. Druckbeulwert, abhängig von Seiten- und Steifigkeitsverhältnis. Einfluß der seitlichen Lagerung

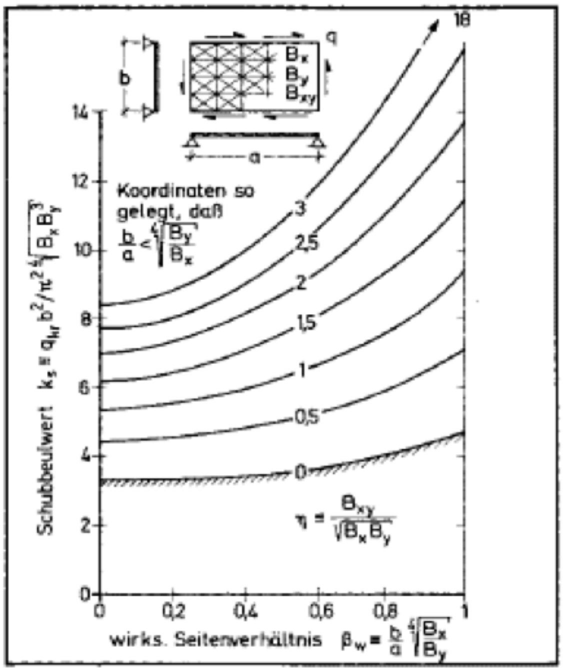

Bild 4.3/5. Orthotrope Rechteckplatte, allseitig gestützt. Schubbeulwert, abhängig von Seiten- und Steifigkeitsverhältnissen; nach [4.8]

Anisotropic laminate shell

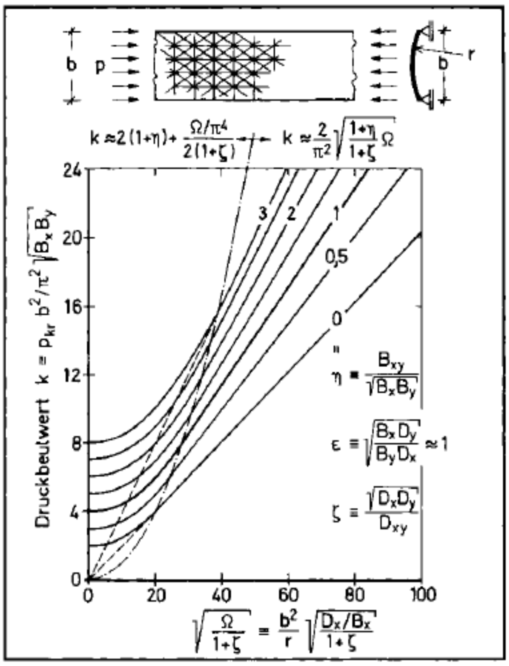

Bild 4.3/9. Orthotroper Schalenstreifen; Längsränder radial gestützt. Druckbeulwert, abhängig von Krümmungsmaß und Steifigkeitsparametern